ROBUST CONTROL
THROUGH
ROBUSTNESS ENHANCEMENT

Control Configurations And Two-Step Design Approaches

Carles Pedret i Ferré

Submitted in partial fulfillment of the
requirements for the degree of
Doctor Engineer
at Universitat Autònoma de Barcelona

May 5, 2003

Dr. Ramon Vilanova i Arbós, lecturer at the Universitat Autònoma de Barcelona,

CERTIFIES:

That the thesis entitled **Robust Control Through Robustness Enhancement** by **Carles Pedret i Ferré** presented in partial fulfillment of the requirements for the degree of Doctor Engineer, has been written under his supervision.

Dr. Ramon Vilanova i Arbós

Bellaterra, May 5, 2003

Preface

The main goal of a control system is that of causing a dynamic process to behave in a desired manner. The analysis and design of such a control system to provide a demanded behaviour is usually done by employing a *mathematical model* of the dynamic process. This model is chosen to represent the major dynamical features of the process. For the reason that the mathematical model is an idealization of the real process, it is imprecise and this inaccuracy entails the existence of *model uncertainty*. This fact, among others, complicates the analysis and design of a control system.

The choice of the control structure plays an essential role to allow the attainment of the demanded behaviour. Typically, some kind of specifications, for example, *open-loop* and *closed-loop* specifications, can not be fulfilled simultaneously and trade-offs between them have to be considered.

Therefore, it is important to distinguish between difficulties to the control problem (such as model uncertainty, disturbances that cause the output to deviate from its desired value, etc.) and difficulties due to the control structure. In this way, our research has been focused on attempting to find out new control structures to avoid traditional difficulties related with standard, well-established, feedback control configurations.

The common, distinguishing, feature of the control structures we work with is the so-called Observer-Controller configuration. Our work, previously focused on single-input single-output systems, shows the benefits of using such a configuration:

(Pedret *et al.*, 1999) In this work we present a two-step design procedure in which reference model specifications are tackled first as nominal requirements and second, the robustness properties of the resulting nominal design are enhanced. The reference model specifications are

achieved by means of an appropriate selection of the state feedback controller. The robustness considerations are taken into account by performing a Youla type parameterization of all possible observers for a given plant.

(Vilanova *et al.*, 1999) In this work, we suggest, for the first time, the actual Observer-Controller configuration for robustness enhancement. The consideration of robustness enhancement problem comes from the fact that the approach is based on improving the robustness properties of a previously existing controller instead of on the design of a robust controller.

(Pedret *et al.*, 2001) In this work, the design procedure for the robust enhancement approach is refined and illustrated with the control of an open-loop unstable process.

(Pedret, 2000) The above-referred publications are the basis of the Master Thesis.

All this favorable receptions motivated to go on with the extension of the research to multivariable systems. The establishment of the robustness properties proposed for scalar case were no longer applicable for the multivariable case. Nevertheless, the transfer function formulation, in which the SISO framework is based, allowed an straightforward generalization to MIMO systems. Then, an alternative, more systematic, design procedure had to be chosen and we fond that the design procedure could be suitable adjusted to fit the $\mathcal{H}_\infty$ / Structured Singular Value framework.

This work presents the above-mentioned generalization of the Observer-Controller configuration which has also accepted for publication **(Pedret *et al.*, 2003)**. In addition to the multivariable approach to robustness enhancement, this work presents a new two degrees-of-freedom control configuration, also based on the Observer-controller configuration.

This work was typeset using LaTeX. The simulations, numerical computations and figures where developed in MATLAB[1].

[1] MATLAB is a registered trademark of MathWorks, Inc.

Acknowledgements

Voldria mostrar el meu agraïment a totes aquelles persones que han estat el meu costat durant aquests anys a la Universitat Autònoma de Barcelona. Molt especialment al Dr. Ramon Vilanova, per haver-me marcat el camí que ha fet possible aquest treball.

Un agraïment, també molt especial, als meus pares, per tants anys d'esforços i renúncies. I a la Susana, per estar al meu costat, per ajudar-me i comprendre'm en tot.

Aquest treball s'ha realitzat en el marc dels projectes TAP97-1144 i DPI2000-0691 de la *Comisión Interministerial de Ciencia y Tecnología*.

Carles

Contents

Preface **v**

1 Introduction **1**

1.1 The control problem 1

1.2 Feedback configuration 3

1.3 Robustness and performance 5

1.4 A new controller architecture 7

1.5 Notation 8

1.6 Outline of this Thesis 9

2 Preliminaries for multivariable feedback control **11**

2.1 Introduction 11

2.2 General control problem formulation 12

2.3 Uncertainty and robustness 16

2.3.1 Uncertainty representation 17

2.3.2 Robust stability for unstructured uncertainty 20

2.3.3 Robust stability for structured uncertainty 21

2.3.4 Robust Performance 23

2.4 Controller synthesis 28

2.5 Summary 35

3 Factorization Approach **37**
3.1 Introduction . . . 37
3.2 Motivation for the fractional representation . . . 38
3.3 Coprime factorizations over $\mathcal{RH}_\infty$ . . . 40
3.3.1 RCF feedback control interpretation . . . 44
3.3.2 LCF feedback control interpretation . . . 47
3.4 Observer-Controller configuration . . . 49
3.4.1 Partial state feedback . . . 50
3.4.2 RHP-zeros . . . 51
3.4.3 Observed partial state feedback . . . 53
3.5 Summary . . . 56

4 The Observer-Controller configuration for Robustness Enhancement **57**
4.1 Introduction . . . 57
4.2 Problem description . . . 60
4.3 Configuration for robustness enhancement . . . 61
4.4 Design for robustness enhancement . . . 65
4.4.1 Design for robust stability . . . 66
4.4.2 Design for robust performance . . . 69
4.4.3 Design outline . . . 71
4.5 Application example . . . 72
4.5.1 Design of the nominal controller . . . 73
4.5.2 Design of the Robustness Enhancement Block . . . 77
4.6 Summary . . . 85

5 The 2-DOF Observer-Controller configuration **87**
5.1 Introduction . . . 87
5.2 Displaying the 2-DOF control configuration . . . 90
5.3 Feedback controller design . . . 94
5.3.1 Direct access to the partial state . . . 96
5.3.2 Observer-based access to the partial state . . . 99
5.3.3 Design procedure . . . 100

5.4 Reference controller design 107
5.4.1 Static controller 108
5.4.2 Dynamic controller 109
5.5 Application Example 116
5.6 Summary 121

6 Conclusions and Further Research 123
6.1 Conclusions 123
6.1.1 The Robustness Enhancement approach 124
6.1.2 The 2-DOF approach 125
6.2 Further research 126

A Background matrix theory 129
A.1 Eigenvalues and eigenvectors 129
A.2 Norms 130
A.2.1 Vector norms 130
A.2.2 Matrix norms 131
A.2.3 Signal norms 132
A.2.4 System norms 133
A.2.5 The spectral radius 135
A.3 Singular Value Decomposition 135
A.4 The condition number 138
A.5 Relative Gain Array 138
A.6 Useful matrix identities 139

B Distillation Column 141
B.1 Introduction 141
B.2 Idealized *LV*-configuration 143
B.3 Other configurations 145
B.4 The benchmark problem 145

C State-space solutions 149

List of Acronyms 155

Notation and Symbols **157**

List of Figures **162**

References **163**

Chapter 1

Introduction

In this Chapter we introduce the control problem with regards of the standard control structures used to address it. Such standard control configurations present well-known conflicting objectives which can be mitigated by using alternative control configurations.

1.1 The control problem

A primary objective of a control system is to make the output of a dynamic process behave in a certain manner. This desired behaviour for the output is pursued by means of manipulations on the input of the process. Nevertheless, hard constrains such as limits on the controls or states and conflicting performance objectives prevents the accomplishment of the desired behaviour for the controlled process.

The design procedure of a control system usually involves a mathematical model of the dynamic process, the *plant model* or nominal model. Consequently, many aspects of the real plant behaviour can not be captured in an accurate way with the plant model leading to uncertainties. Such plant model miss-matching should be characterized, albeit loosely, by means of *disturbances signals* and/or *plant parameter variations*, often characterized by probabilistic models, or *unmodeled dynamics*, commonly characterized in the frequency domain.

Usually, high performance specifications are given in terms of the plant model. For this reason, model uncertainties characterization should be in-

corporated to the design procedure in order to provide a reliable control system capable to deal with the real process and to assure the fulfillment of the performance requirements. The term *robustness* is used to denote the ability of a control system to cope with the uncertain scenario.

The performance specifications are usually given accordingly for the *regulation* problem or for the *tracking* problem. The former is to manipulate the input of the plant to counteract the effect of output disturbances. The later is to handle the input of the plant to keep the controlled variables close to the given reference signal.

The key point is the way the controller generates the control signal in a suitable manner. There exist a lot of different strategies and methodologies to cope with this problem, say the controller design problem. However, any possible choice can be classified as belonging to *open-loop control* or *closed-loop control*.

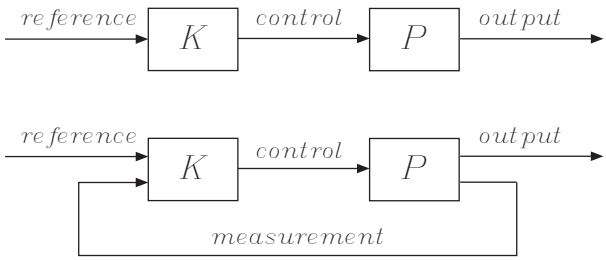

Figure 1.1: Open-loop and closed-loop control configurations.

Although the two options are available, when bearing in mind a control system, closed-loop configurations automatically appears. This is because open-loop control, as depicted in Figure 1.1, is effective only in some, relatively simple, situations in which plant variations and output disturbances do not cause the actual output to deviate significantly from the specified reference input. Thereupon, with this scheme there is no way of knowing if the output variables deviates from it desired value. This is the reason of introducing feedback: without feedback, there is no means of comparing the actual behaviour of the process with its desired behaviour to automatically correct its performance. Feedback control may therefore be used to counteract potential effects of plant variations and output disturbances. On the other hand, the presence of feedback signal implies the need for a physical measurement. A sensor is needed to monitorize the output variable and in,

many cases, the measurements are corrupted with noise, which also complicates the design process.

In order for a control system to achieve the specified performance requirements in the presence of external disturbances and model uncertainties it is necessary to resort to feedback control. Another fundamental reason for making use of feedback is that unstable plants can only be stabilized by feedback. Therefore, the ability of feedback to mitigate the effect of external disturbances, to reduce the effect of model uncertainties and to stabilize unstable plants is of crucial importance in controller design.

Of course, there is also the opposite situation, in which the plant is stable and the used of feedback (if not done properly) can drive the system to the instability. This is not the case with an open-loop control scheme, where the stability of the system is always guaranteed as long as the plant, and the controller, are stable. The only thing that concerns open-loop control is performance in terms of tracking.

The failure of open-loop control is due to the lack of information, being feedback a way of providing such information. Moreover, with a feedback controller we are not only accessing to this information but establishing a way of using it. Thus, if a feedback compensator is to be used to achieve the desired performance in terms of tracking, the additional cost of the stability constraint must be paid. The performance specification is now relegated to play a secondary role and the primary concern is now stability, even if the plant is open loop-stable.

1.2 Feedback configuration

It is well known that standard feedback control is based on generating a control signal u by processing the error signal, $e = r - y$, that is, the difference between the reference inputs and the output controlled signals. Therefore, the input to the plant is

$$u = K(r - y) \tag{1.1}$$

In such a case the associated design problem has one degree of freedom (1-DOF).

The errors signal in the 1-DOF control structure shown in Figure 1.2 is related to the external inputs r and d by means of the sensitivity function

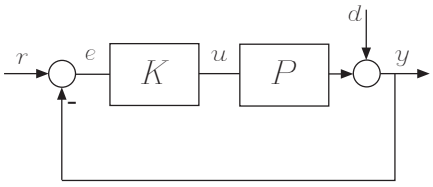

Figure 1.2: Standard one degree-of-freedom feedback control system.

$S \doteq (I + PK)^{-1}$, i.e., $e = S(r - d)$. Apart from the sign, the reference r and the disturbance d have the same effect on the error e. Therefore, if r and d vary in a similar manner the controller K can be chosen to minimize e in some sense. Alternatively, if r and d have different nature, the controller has to be chosen either for good step responses for r or good ramp attenuation for d or else some compromise have to be found. If there are strict requirements on both command response (tracking problem) and disturbance rejection (regulation problem), an acceptable compromise might not exist.

Different design strategies can be considered to design the controller K but the trade-off between disturbance rejection and command tracking is inherent in the nature of 1-DOF feedback control scheme. To allow independent controller adjustments for both r and d, additional controller blocks have to be introduced into the system as in Figure 1.3.

Two degrees-of-freedom (2-DOF) control configuration are characterized by allowing a separate processing of the reference inputs and the controlled outputs. The 2-DOF compensators present the advantage of a complete separation between feedback and reference tracking properties: the feedback properties of the control system are assured by a feedback controller, i.e., the first degree of freedom; the reference tracking specifications are addressed by a prefilter controller, i.e., the second degree of freedom, which determines the open-loop processing of the reference commands.

In the 2-DOF control configuration shown in Figure 1.3 the references, r, and the measurements, y, enter the controller separately and are independently processed, i.e.,

$$u = K \begin{bmatrix} r \\ y \end{bmatrix} = K_2\, r - K_1\, y \tag{1.2}$$

In such control configuration, the feedback controller K_1 and the prefilter K_2 are selected arbitrarily with internal stability the only restriction.

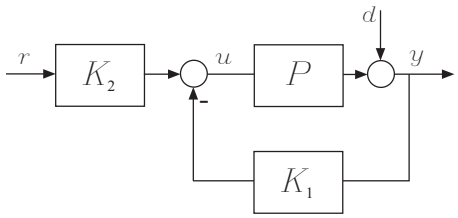

Figure 1.3: Standard two degrees-of-freedom control configuration.

Many design procedures for both the 1-DOF and 2-DOF feedback control configuration are based on the characterization of the class of stabilizing controllers for a plant in term of a parameter denoted, in a widespread way, Q. This theory appeared in (Youla *et al.*, 1976*b*) and (Youla *et al.*, 1976*a*) for the continuous-time. More precisely, the term Q is a stable, proper, filter build into a stabilizing controller. Consequently, the relevant transfer matrix functions of the associated closed-loop system turn out to be linear in the operator Q which allows optimization over Q (Vidyasagar, 1985), (Boyd and Barratt, 1991).

1.3 Robustness and performance

It is well known that there is an intrinsic conflict between performance and robustness in the standard feedback framework, see (Doyle and Stein, 1981), (Chen, 1995) for a detailed analysis and discussions. We have argued that the system responses to commands is an open-loop property while robustness properties are associated with the feedback. Therefore, one must make a tradeoff between achievable performance (in terms command tracking) and robustness (against external disturbances and model uncertainties). In this way, a high performance controller designed for a nominal model may have very little robustness against the model uncertainties and the external disturbances.

For this reason, worst-case robust control design techniques such as $\mathcal{H}_\infty$ control, ℓ_1 control, (Francis, 1987), (Green and Limebeer, 1995), (Morari and Zafirou, 1989), (Stoorvogel, 1992), among many others and μ synthesis (Zhou *et al.*, 1996), have gained popularity in the last twenty years, or so. Unfortunately, it is well recognized in the robust control community that a robust controller design is usually achieved at the expense of performance.

This is not hard to understand since all these robust control design techniques are based on the worst possible scenario which may never occur in a particular control system.

It is well-known that 2-DOF compensators offers the advantage of the separation principle between *performance* and *robustness* (Youla and Bongiorno, 1985), (Vilanova, 1996). In this case, performance should be understood in terms of command tracking. Then, the closed-loop properties can be shaped independently of the reference tracking transfer function. As is pointed out in (Safonov *et al.*, 1981), classical approaches to controller design tend to stress the use of feedback either for robustness and for modify the systems' response to commands. Hence, it would seem so natural to choose a 2-DOF to tackle the control design problem. In this way, the feedback controller could be used to give robustness to the control system and the prefilter controller could be used to define the command's response.

Why are 2-DOF compensators not used as expected? As it is suggested in (Vilanova and Serra, 1998), one possible reason may be the lack of methodologies to design the two compensators. Since the best way to allocate the gain between the two compensators is not so clear, the approaches found in the literature are mainly based on optimization problems over a Youla parametrisation to get the final, robust, compensator (Youla and Bongiorno, 1985), (Vidyasagar, 1985), (Limebeer *et al.*, 1993).

In recent years, several approaches have appeared as explicit two-step design procedures to take into account the robustness properties of a controller (Hrissagis and Crisalle, 1997), (Ansay *et al.*, 1998), (Zhou, 2000). Commonly, the initial controller is reformulated as the central controller in the Youla parametrisation of the stabilizing controllers from a nominal plant and an optimization problem is performed over the Youla parameter to get the final, *robustified*, controller. The controller architectures works in such a way that the feedback control system will be solely controlled by the performance controller when there is no model uncertainties and external disturbances and the robustification controller will only be active when there are model uncertainties or external disturbances.

The approaches based on a reformulation of a control system as the central controller in the Youla parametrisation allows the Youla parameter to be made adaptive (Tay *et al.*, 1998).

1.4 A new controller architecture

In this Thesis, we shall propose a new controller architecture to try to completely overcome the conflict between performance and robustness in the traditional feedback framework. The proposed control configuration comes from the coprime factorization approach and, in such a context, a somewhat uncommon observer-based control configuration is derived. It is the Observer-Controller configuration and it is used in different arrangements.

The first proposal, deals with the robustness enhancement problem as an alternative to the design of a robust control system. With the lofty goal of achieving high performance in the face of disturbances and uncertainties we proceed as follows: first, an initial feedback control system is set for the nominal plant to satisfy tracking requirements and second, the resulting robustness properties are conveniently enhanced while leaving unaltered the tracking responses provided by the initial controller. The approach is based on the generation of a complement for the nominal control system by means of an structure based on the Observer-Controller configuration. The final control system works in such a way that the plant will be solely controlled by the initial nominal feedback controller when there is neither model uncertainties nor external disturbances and the robustification controller will only be active when there is model uncertainties and/or external disturbances.

The second proposal also addresses the goal of high performance in the face of disturbances and uncertainties. In this case, a two degrees-of-freedom control configuration is developed. We proceed as follows: first, an observer-based feedback control scheme is designed to guarantee some levels of stability robustness and second, a prefilter controller is computed to guarantee robust open-loop processing of the reference commands.

Despite both proposals are not based on a reformulation in terms of the Youla parameter, it is possible to perform a Youla parametrization to characterize the set of all observers for the nominal plant. Such approach is not considered here. See (Pedret *et al.*, 1999) or (Pedret, 2000) for more details.

Essentially, this thesis proposes two 2-DOF control configurations for high performance and robustness properties. The first presented proposal do not fit the standard 2-DOF control scheme made up with a feedback controller and a prefilter controller. Nevertheless, it can also be seen to lie in the 2-DOF control configuration in the sense that a complete separation of

properties is achieved. In such case, the tracking properties of the nominal plant are attained by a controller and the robustness properties are considered and enhanced if necessary by the Observer-Controller configuration. The design procedures involves μ and constrained $\mathcal{H}_\infty$ optimization, respectively.

1.5 Notation

The most important notation is summarized in the List of Acronyms and in the Notation and Symbols, at the end of this Thesis. We have used lower-case letters for vectors and signals, e.g., u, y, r and capital letters for matrices, transfer functions and systems, e.g., P, K. Matrix elements are usually denoted by lower-case letters, so p_{ij} is the ij'th element in the matrix P. However, upper-case letters are sometimes used to denote partitions in a matrix, i.e., P is partitioned so that P_{ij} is itself a matrix.

An abuse of notation is usually performed with the Laplace variable s, which is often omitted for simplicity. So we often write P when we mean $P(s)$.

Let $M \in \mathcal{C}^{n\times m}$. Then $\bar{\sigma}(M)$ denotes the largest singular value of M. $\mathcal{H}_\infty$ denotes the Banach space of bounded analytic functions with the ∞-norm defined as

$$\|F\|_\infty \doteq \sup_\omega \bar{\sigma}(F(j\omega)) \tag{1.3}$$

for any $F \in \mathcal{H}_\infty$. A state space realization of a rational proper transfer (matrix) function $G(s)$ is denoted by

$$G(s) = \left[\begin{array}{c|c} A & B \\ \hline C & D \end{array}\right] = C(sI - A)^{-1}B + D. \tag{1.4}$$

Let P be a block matrix

$$P = \left[\begin{array}{c|c} P_{11} & P_{12} \\ \hline P_{21} & P_{22} \end{array}\right]. \tag{1.5}$$

Then, the liner fraction transformation (LFT) of P over F is defined as

$$\mathcal{F}(P, F) = P_{11} + P_{12}F(I - P_{22}F)^{-1}P_{21} \tag{1.6}$$

where F is assumed to have appropriate dimensions and $(I - P_{22}F)^{-1}$ is well-defined.

1.6 Outline of this Thesis

This thesis has not been written to offer a completed-in-itself reading. Well-known background theory has been sacrificed for the shake of simplicity and only the fundamental issues to frame the work have been provided. Some important issues for multivariable control have been reported but appended at the back of this thesis. So, we have organized the work as follows:

Chapter 2: In this Chapter the concept of model uncertainty is presented, assuming that the real plant is unknown but belonging to a class of models built around the nominal model. The General Control Configuration is introduced as long as the general framework for the μ analysis and synthesis of controllers for multivariable systems.

Chapter3: In this Chapter we give a short introduction to the factorization approach which consist on factorize a transfer (matrix) function of a system, not necessarily stable, as a ratio of two stable transfer (matrix) functions. Within the factorization framework, the *Observer-Controller* configuration is introduced to be used in the different control configurations proposed in this thesis.

Chapter 4: In this Chapter we present a new configuration to improve the robustness properties of a nominal high performance control system. The robustness enhancement approach is based on the generation of a complement for a nominal control system by means of an Observer-Controller structure. The resulting two-step design procedure allows an enhancement of the robustness properties without modifying the nominal controller. The design procedure is systematized by a translation into the $\mathcal{H}_\infty$ / Structured Singular Value framework and evaluated on a high purity distillation column example.

Chapter 5: In this Chapter we present a new 2-DOF control configuration based on an observer-based feedback control scheme to guarantee some levels of stability robustness and a prefilter controller computed to guarantee robust open-loop processing of the reference commands. The feedback control scheme is configured by solving a constrained $\mathcal{H}_\infty$ optimization problem

using the right coprime factorization of the plant in an active way. The prefilter controller is designed by assuming a Reference Model with the desired relations from the reference signals and by solving a Model Matching Problem imposed on the prefilter controller such that the response of the overall close-loop system match that of the Reference Model. The design procedure is also evaluated on a high purity distillation column example.

Chapter 6: This Chapter provides the concluding remarks and proposals for further research.

Appendix A: This Appendix reviews some basic topics of matrix theory and has been are included as background material for this thesis.

Appendix B: This Appendix introduces a typical high-purity distillation process of the type used in the literature as a benchmark problem for comparing methods for robust controller design.

Appendix C: This Appendix provides the state-space solutions of several examples carried out along this thesis.

Chapter 2

Preliminaries for multivariable feedback control

In this Chapter the concept of model uncertainty is presented, assuming that the real plant is unknown but belonging to a class of models built around the nominal plant. The general configuration to formulate control problems is introduced. The structured singular value framework is used to get necessary and sufficient conditions for robust stability and robust performance. A μ-"optimal" controller is synthesized for the control of a high purity distillation column.

2.1 Introduction

In this Chapter we review the general method of formulating control problems introduced by (Doyle, 1983). Within this framework, we recall the general method for representing uncertainty for multivariable systems. We deal with the *structured singular value*, μ, a powerful tool introduced by (Doyle, 1982) which provides a generalization of the singular value, $\bar{\sigma}$, and the spectral radius, ρ. We see that, by using μ, it is possible to get necessary and sufficient conditions for robust stability and also for robust performance. We also show how the "optimal" robust controller, in terms of minimizing μ, can be designed using DK-iteration (also called μ synthesis). We show this ad-hoc method that involves solving a sequence of scaled $\mathcal{H}_\infty$ problems.

The original high purity distillation column benchmark problem introduced by (Skogestad *et al.*, 1988) is considered since it has been used in the literature as a test for robust controller designs. In the original benchmark problem a μ-"optimal" one degree-of-freedom robust controller is presented as the optimal solution. So, the μ-"optimal" controller for the distillation process is reproduced here to be used as a guide for the different control configurations presented in this work.

The Chapter is organized as follows: Section 2.2 review the general control problem formulation. Section 2.3 present the general framework for the analysis and synthesis of controllers for robust stability and robust performance with MIMO systems. In Section 2.4 we see how the structured singular value can be used to synthesize a μ-"optimal" robust controller.

2.2 General control problem formulation

In this Section the general control configuration to formulate control problems is presented (Doyle, 1983). Within this framework, the scheme in Figure 2.1 is considered, where G is the generalized plant and K is the generalized controller. Four types of external variables are dealt: exogenous inputs, w, i.e., commands, disturbances and noise; exogenous outputs, z, e.g., error signals to be minimized; controller inputs, v, e.g., commands, measured plant outputs, measured disturbances; control signals, u.

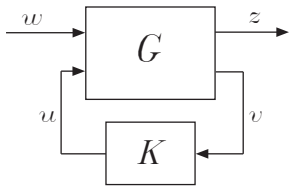

Figure 2.1: General control problem formulation with no model uncertainty.

The controller design problem is divided into the *analysis* and the *synthesis* phases. The controller K is synthesized such that some measure, in fact a norm, of the transfer function from w to z is minimized, e.g. the $\mathcal{H}_\infty$ norm. Then the controller design problem is to find a controller K —that generates a signal u considering the information from v to mitigate the effects of w on z— minimizing the closed-loop norm from w to z. For the analysis phase,

the scheme in Figure 2.1 is to be modified to group the generalized plant G and the resulting synthesized controller K in order to test the closed-loop performance achieved with K. How to group G and K is treated further on.

To get meaningful controller synthesis problems, weights on the exogenous inputs w and outputs z are incorporated. The weighting matrices are usually frequency dependent and typically selected such that the weighed signals are of magnitude 1, i.e. the norm from w to z should be less than 1.

Example 2.2.1. The feed-back control system shown in Figure 2.2 is considered to illustrate how to find the weighted generalized plant G.

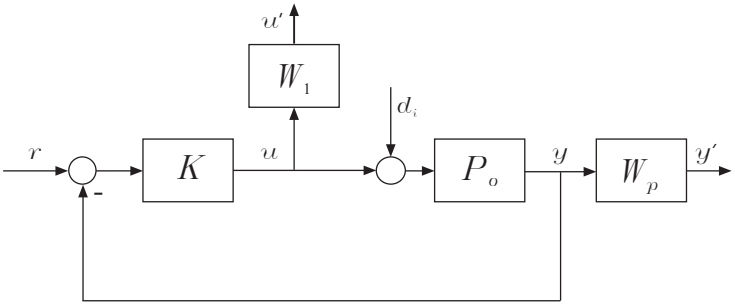

Figure 2.2: One degree-of-freedom control configuration.

First, the feed-back control system we are dealing with is to be rearranged as in Figure 2.1 with

$$w \doteq \begin{bmatrix} d_i \\ r \end{bmatrix}, \quad z \doteq \begin{bmatrix} u' \\ y' \end{bmatrix} \quad \text{and} \quad v \doteq r - y \tag{2.1}$$

Therefore, the generalized plant G is transfer matrix function that relates the input signals $[w\ u]^T$ and the output signals $[z\ v]^T$. It can be written as

$$G = \left[\begin{array}{cc:c} 0 & 0 & W_1 \\ W_pP_o & 0 & W_pP_o \\ \hdashline -P_o & -I & -P_o \end{array}\right] \tag{2.2}$$

△

In the above example, a weighted generalized plant G has been derived to allow synthesizing the controller K. If the generalized plant G is partitioned as

$$G = \begin{bmatrix} G_{11} & G_{12} \\ G_{21} & G_{22} \end{bmatrix} \tag{2.3}$$

such that its parts are compatible with the signals w, z, u and v in the generalized control configuration, then

$$\begin{aligned} z &= G_{11}w + G_{12}u \\ v &= G_{21}w + G_{22}u \end{aligned} \tag{2.4}$$

From the Example 2.2.1 we have

$$\begin{aligned} G_{11} &= \begin{bmatrix} 0 & 0 \\ W_pP_o & 0 \end{bmatrix}, \; G_{12} = \begin{bmatrix} W_1 \\ W_pP_o \end{bmatrix} \\ G_{21} &= \begin{bmatrix} -P_o & I \end{bmatrix}, \; G_{22} = -P_o \end{aligned} \tag{2.5}$$

Usually, a state-space realization for G is required in order to apply standard control strategies. In such a case, a state-space realization for G can be obtained by directly realizing the transfer matrix G using any standard multivariable realization techniques (Zhou and Doyle, 1998), (Green and Limebeer, 1995).

Once the stabilizing controller K is synthesized, it rests to analyze the closed-loop performance that it provides. In this phase, the controller for the configuration in Figure 2.1 is incorporated into the generalized plant G to form the system $\mathcal{N}$, as it is shown in Figure 2.3.

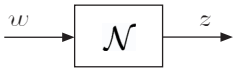

Figure 2.3: General block diagram for analysis with no uncertainty.

Straightforward algebra shows that, by substituting $z = \mathcal{N}w$ and $u = Kv$ into equations (2.4), the expression for $\mathcal{N}$ is given by

$$\mathcal{N} = G_{11} + G_{12}K(I - G_{22}K)^{-1}G_{21} \doteq \mathcal{F}_\ell(G, K) \tag{2.6}$$

where $\mathcal{F}_\ell(G, K)$ denotes the lower Linear Fractional Transformation (LFT) of G and K.

In order to obtain a good design for K, a precise knowledge of the plant is required. The dynamics of interest are modeled but this model may be inaccurate and may not reflect the changes suffered by the plant with time. To deal with this problem, the concept of model uncertainty comes out. The plant P is assumed to be unknown but belonging to a class of models, $\mathcal{P}$, built around a nominal model P_o. The set of models $\mathcal{P}$ is characterized by a matrix Δ, which can be either a full matrix or a block diagonal matrix, that includes all possible perturbations representing uncertainty to the system. Weighting matrices $W_1(s)$ and $W_2(s)$ are usually employed to express the uncertainty in terms of normalized perturbations in such a way that $\|\Delta\|_\infty \leq 1$. A detailed treatment of model uncertainty is dealt in Section 2.3.

The general control configuration in Figure 2.1 may be extended to include model uncertainty as it is shown in Figure 2.4.

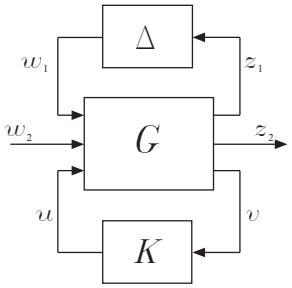

Figure 2.4: General control configuration with model uncertainty.

The block diagram in Figure 2.4 is used to synthesize a controller K. To transform it for analysis, the lower loop around G is closed by the controller K and it is incorporated into the generalized plant G to form the system $\mathcal{N}$ as it is shown in Figure 2.5. The same lower LFT is obtained as in (2.6) where no uncertainty where considered.

To evaluate the relation form $w = [w_1\ w_2]^T$ to $z = [z_1\ z_2]^T$ for a given controller K in the uncertain system, the upper loop around $\mathcal{N}$ is closed with the perturbation matrix Δ. This results in the following upper LFT:

$$\mathcal{F}_u(\mathcal{N}, \Delta) \doteq \mathcal{N}_{22} + \mathcal{N}_{21}\Delta(I - \mathcal{N}_{11}\Delta)^{-1}\mathcal{N}_{12} \tag{2.7}$$

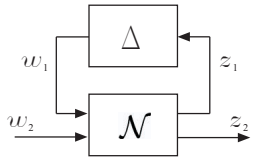

Figure 2.5: General block diagram for analysis with uncertainty.

To represent any control problem with uncertainty by the general control configuration in Figure 2.4 it is necessary to represent each source of uncertainty by a single perturbation block Δ, normalized such that $\|\Delta\|_\infty \leq 1$. The perturbations can represent parametric uncertainty, non modeled, etc. as will be seen in Section 2.3.

For numerical calculations purposes, the generalized plant G can be obtained using available software (Balas *et al.*, 1998).

2.3 Uncertainty and robustness

The concept of model uncertainty has just been introduced in Section 2.2. We know that precise knowledge of the plant is required for a proper design of K, otherwise the controller is bound to fail when driving the real system. Nevertheless, an exact knowledge of the plant is not always possible: models may be inaccurate and may not reflect the changes suffered by the plant with time. Therefore, it is often assumed that the real plant, denoted by P, is unknown but belonging to a class of models, $\mathcal{P}$, built around a nominal model, P_o. The set of models $\mathcal{P}$ is characterized by a matrix Δ which can be either a full matrix or a block diagonal matrix including all possible perturbations representing uncertainty to the system.

In this Section we present the general framework for the analysis and synthesis of controllers for robust stability and robust performance with MIMO systems. The following terminology is used:

Definition 2.3.1. The closed-loop system has Nominal Stability (NS) if the controller K internally stabilizes the nominal model P_o, i.e., the four transfer matrices $\mathcal{N}_{11}$, $\mathcal{N}_{12}$, $\mathcal{N}_{21}$ and $\mathcal{N}_{22}$ in the closed-loop transfer matrix $\mathcal{N}$ shown in Figure 2.3 are stable.

$\diamond$

Definition 2.3.2. The closed-loop system has Nominal Performance (NP) if the performance objectives are satisfied for the nominal model P_o, i.e., $\|\mathcal{N}_{22}\|_\infty < 1$ in Figure 2.3.

$\diamond$

Definition 2.3.3. The closed-loop system has Robust Stability (RS) if the controller K internally stabilizes every plant $P \in \mathcal{P}$, i.e., in Figure 2.5, $\mathcal{F}_u(\mathcal{N}, \Delta)$ is stable $\forall \Delta,\ \|\Delta\|_\infty \leq 1$.

$\diamond$

Definition 2.3.4. The closed-loop feedback system has Robust Performance (RP) if the performance objectives are satisfied for $P \in \mathcal{P}$, i.e., in Figure 2.5, $\|\mathcal{F}_u(\mathcal{N}, \Delta)\|_\infty < 1\ \forall \Delta,\ \|\Delta\|_\infty \leq 1$.

$\diamond$

The nominal stability and nominal performance can be checked using standard techniques. The conditions to satisfy robust stability and robust performance are considered next.

2.3.1 Uncertainty representation

Two ways of representing model uncertainty are considered next: *unstructured* and *structured* uncertainty. With unstructured uncertainty, the individual sources of uncertainty are described with a single perturbation which is a full matrix compatible with the plant P. With a structured uncertainty description, the individual sources of uncertainty are not linked together in one full matrix. Instead, the sources of uncertainty are represented separately.

Unstructured uncertainty

Unstructured uncertainty is a kind of uncertainty description which is often used to get simple models. Uncertainty is expressed in terms of a specific single perturbation matrix Δ, usually with dimensions compatible with those of the plant and normalized such that $\bar{\sigma}(\Delta) \leq 1$.

Let $P \in \mathcal{P}$ be any member of the set of possible plants $\mathcal{P}$ and let $P_o \in \mathcal{P}$ denote the nominal model of the plant. Then, unstructured uncertainty are commonly expressed in terms of the following four single perturbations as shown in Figure 2.6:

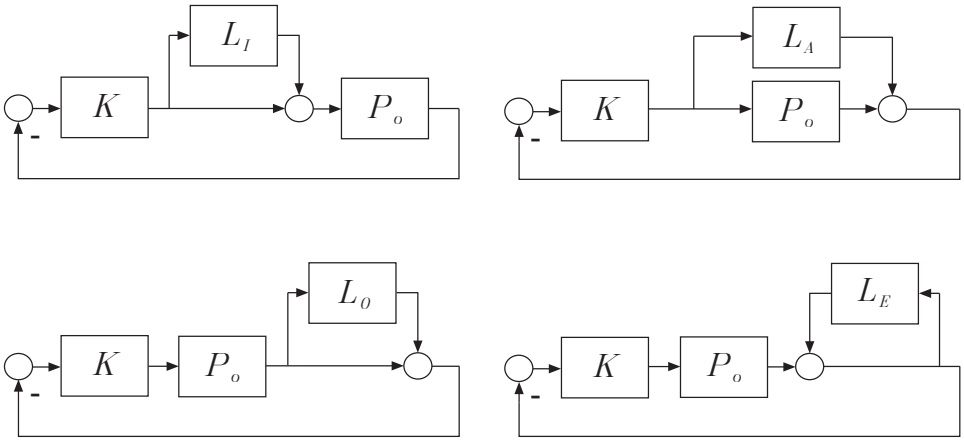

Figure 2.6: Common uncertainty representations involving single perturbations: multiplicative input uncertainty (L_I); additive uncertainty (L_A); multiplicative output uncertainty (L_O); inverse multiplicative output uncertainty (L_E).

$$\mathcal{P}_A = \{P : P = P_o + L_A\}, \quad L_A = w_A\Delta \tag{2.8}$$

$$\mathcal{P}_O = \{P : P = (I + L_O)P_o\}, \quad L_O = w_O\Delta \tag{2.9}$$

$$\mathcal{P}_I = \{P : P = P_o(I + L_I\}, \quad L_I = w_I\Delta \tag{2.10}$$

$$\mathcal{P}_E = \left\{P : P = (I - L_E)^{-1}P_o\right\}, \quad L_E = w_E\Delta \tag{2.11}$$

where L_A stands for additive perturbation, L_O multiplicative output perturbation, L_I multiplicative input perturbation and L_E inverse multiplicative output perturbation.

In all cases the magnitude of the perturbation L may be measured in terms of a bound on $\bar{\sigma}(L)$,

$$\bar{\sigma}(L) \leq w(\omega) \quad \forall\omega \tag{2.12}$$

where

$$w(\omega) = \max_{P \in \mathcal{P}} \bar{\sigma}(L) \tag{2.13}$$

The bound $w(\omega)$ can also be interpreted as a scalar weigh on a normalized perturbation $\Delta(s)$,

$$L(s) = w(s)\Delta(s), \;\; \bar{\sigma}(\Delta(j\omega)) \leq 1 \;\; \forall\omega \tag{2.14}$$

Sometimes, matrix weighs are used to describe the uncertainty, $L = W_1\Delta W_2$. Nevertheless, neither the scalar weigh $w(s)$ nor the transfer function matrices W_1 and W_2 do not generally constitute an exact description of the uncertainty. This leads to a conservative uncertainty description in which the set of plants satisfying (2.14) are larger than the original set $\mathcal{P}$.

Structured uncertainty

To avoid the conservatism, inherent in the unstructured uncertainty description, the individual sources of uncertainty are represented separately. This uncertainty description involves multiple norm-bounded perturbations,

$$\bar{\sigma}(\Delta_i) \leq 1 \quad \forall\omega \tag{2.15}$$

and weighting matrices W_1 and W_2 are used to describe the actual perturbation L_i

$$L_i = W_2\Delta_i W_1 \tag{2.16}$$

The individual uncertainties Δ_i are combined into one large block diagonal perturbation matrix

$$\Delta = \text{diag}\{\Delta_1, ..., \Delta_m\} \tag{2.17}$$

satisfying

$$\bar{\sigma}(\Delta) \leq 1 \quad \forall\omega \tag{2.18}$$

Structured uncertainty representation considers the individual uncertainty present on each input channel and combines them into one large diagonal block (2.17). This representation avoids the non-physical couplings at the input of the plant that appears with the full perturbation matrix Δ in an unstructured uncertainty description. Consequently, the resulting set of plants is not so large as with an unstructured uncertainty description and the resulting robustness analysis is not so conservative.

2.3.2 Robust stability for unstructured uncertainty

Let us consider the unstructured uncertainty description characterized by a full complex transfer function matrix $\Delta(s)$ satisfying $\bar{\sigma}(\Delta) \leq 1$. In such a situation, each one of the block diagrams in Figure 2.6 can be arranged to fit in the general control configuration shown in Figure 2.4 in order to synthesize the controller K.

We saw in Section 2.2 that to transform each one of the diagrams in Figure 2.6 for analysis, the lower loop around G has to be closed by the controller K and incorporated into the generalized plant G to form the system $\mathcal{N}$, shown in Figure 2.5. The following lower LFT was obtained

$$\mathcal{N} = G_{11} + G_{12}K(I - G_{22}K)^{-1}G_{21} \tag{2.19}$$

We also saw that the uncertain closed-loop transfer function from w to z in Figure 2.5 was related by the upper LFT

$$\mathcal{F}_u(\mathcal{N}, \Delta) \doteq \mathcal{N}_{22} + \mathcal{N}_{21}\Delta(I - \mathcal{N}_{11}\Delta)^{-1}\mathcal{N}_{12} \tag{2.20}$$

Assuming that the system is nominally stable, the only source of instability in the upper LFT (2.20) is the term $(I - \mathcal{N}_{11}\Delta)^{-1}$. Therefore, the stability of the system in Figure 2.5 is equivalent to the stability of the structure shown in Figure 2.7, where $\mathcal{M} \doteq \mathcal{N}_{11}$, i.e. the portion of the transfer matrix function $\mathcal{N}$ seen by the perturbation block Δ.

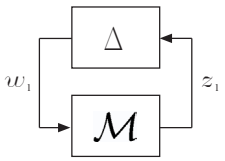

Figure 2.7: General $\mathcal{M}\Delta$ structure for robust stability analysis.

The system shown in Figure 2.7 is stable if and only if $\det(I - \mathcal{M}\Delta)$ does not encircle the origin as s crosses the Nyquist D contour for all possible Δ. Because the perturbations are norm bounded, i.e., $\bar{\sigma}(\Delta) \leq 1$, this is equivalent to (Morari and Zafirou, 1989)

$$\det(I - \mathcal{M}\Delta) \neq 0 \;\; \forall\omega, \; \forall\Delta, \; \bar{\sigma}(\Delta) \leq 1 \tag{2.21}$$

$$\Updownarrow$$

$$\rho(\mathcal{M}\Delta) \leq 1 \;\; \forall\omega, \; \forall\Delta, \; \bar{\sigma}(\Delta) \leq 1 \tag{2.22}$$

This condition is not itself useful to check the stability of the $\mathcal{M}\Delta$ structure since it must be tested for all possible perturbations Δ. What is desired is a condition on the matrix $\mathcal{M}$, preferably on some norm of $\mathcal{M}$.

The following theorem establishes a condition on $\mathcal{M}$ so that it can not be destabilized by Δ.

Theorem 2.3.1. (Small Gain Theorem) *Assume that $\mathcal{M}$ is stable. Then the interconnected $\mathcal{M}\Delta$ system shown in Figure 2.7 is well-posed and internally stable for all perturbations Δ with $\bar{\sigma}(\Delta) \leq 1$ if and only if*

$$\|\mathcal{M}\|_\infty < 1 \tag{2.23}$$

Proof. *See (Morari and Zafirou, 1989) or (Zhou* et al.*, 1996).*

□

Robust stability conditions for the different uncertainty representations shown in Figure 2.6 can be derived from Theorem 2.3.1. See (Morari and Zafirou, 1989) for more details.

2.3.3 Robust stability for structured uncertainty

Let us consider an structured uncertainty description characterized by a diagonal transfer function matrix $\Delta(s) = \text{diag}\{\Delta_1, ..., \Delta_m\}$. In general, Δ_i may be any stable rational transfer matrix satisfying $\bar{\sigma}(\Delta_i) \leq 1 \; \forall\omega$. In such a situation, each one of the block diagrams in Figure 2.6 can be arranged to fit in the general control configuration shown in Figure 2.4 to synthesize the controller K and also arranged to form the system $\mathcal{N}$ shown in Figure 2.5. The uncertain closed loop transfer function from w to z in this figure is related, as with an unstructured uncertainty description, by the upper LFT (2.20). As we saw above, the stability of the $\mathcal{N}\Delta$ structure is determined by the term $(1 - \mathcal{N}_{11}\Delta)^{-1}$. Therefore, to test the stability of the structure in Figure 2.5 is equivalent to test the stability of the $\mathcal{M}\Delta$ structure shown in Figure 2.7, where $\mathcal{M} \doteq \mathcal{N}_{11}$.

By assuming norm bounds on each individual uncertainty, e.g., $\bar{\sigma}(\Delta_i) \leq 1$, it is possible to derive a necessary and sufficient non-conservative condition on $\mathcal{M}$ so that it can not be destabilized by Δ. This is pursued by the structured singular value.

Structured Singular Value

The Structured Singular Values (denoted SSV or μ) was introduced in (Doyle, 1982). At the same time, the Multivariable Stability Margin, k_m, for a diagonal perturbed system was presented in (Safonov, 1982) as the inverse of μ. Despite the later represents a more natural definition of robustness margins, the former offers a number of other advantages such as providing a generalization of the singular values, $\bar{\sigma}$, and the spectral radius, ρ. The SSV is used to get necessary and sufficient, non-conservative, conditions for robust stability and also for robust performance in presence of structured perturbations.

The SSV is defined to obtain the tightest possible bound on $\mathcal{M}$ such that $\det(I - \mathcal{M}\Delta) \neq 0$. The problem is to find the smallest structured Δ, measured in terms of $\bar{\sigma}(\Delta)$, which makes $\det(I - \mathcal{M}\Delta)$ singular. Then, $\mu(\mathcal{M}) = 1/\bar{\sigma}(\Delta)$. The definition of $\mu(\mathcal{M})$ adopted form (Doyle, 1982) reads as follows.

Definition 2.3.5. For a square complex matrix $\mathcal{M}$, the Structured Singular Value, $\mu_\Delta(\mathcal{M})$, is defined at each frequency such that

$$\mu_\Delta(\mathcal{M}) \doteq \frac{1}{\min_\Delta \{\bar{\sigma}(\Delta) | \det(I - \mathcal{M}\Delta) = 0 \text{ for some structured } \Delta\}} \tag{2.24}$$

If no Δ exist such that $\det(I - \mathcal{M}\Delta) = 0$, then $\mu_\Delta(\mathcal{M}) \doteq 0$

$\diamond$

It should be noted that the structured singular values, μ, depends on the matrix $\mathcal{M}$ and the structure of the perturbation Δ, therefore the notation $\mu_\Delta(\mathcal{M})$. For the unstructured uncertainty case, i.e. where Δ is a full matrix, the smallest Δ which yields singularity has $\bar{\sigma}(\mathcal{M}) = 1/\bar{\sigma}(\Delta)$. For the structured uncertainty case we have $\mu(\mathcal{M}) = 1/\bar{\sigma}(\Delta)$.

A necessary and sufficient condition on matrix $\mathcal{M}$ for robust stability is provided by the following theorem.

Theorem 2.3.2. *Assume the nominal system ($\Delta = 0$) is stable. Then the $\mathcal{M}\Delta$ system shown in Figure 2.7 is stable for all Δ, $\bar{\sigma}(\Delta) \leq 1$ if and only if*

$$\mu_{\Delta}(\mathcal{M}) < 1, \ \forall \omega \tag{2.25}$$

Proof. *(Doyle, 1982).*

□

Theorem 2.3.2 may be interpreted as a Generalized Small Gain theorem applied to equation (A.29), which also takes the structure of Δ into account. $\mu_{\Delta}(\mathcal{M})$ is seen as a generalization of the spectral radius, $\rho(\mathcal{M})$, and the maximum singular value, $\bar{\sigma}(\mathcal{M})$. It can be shown (Doyle, 1982) that $\mu_{\Delta}(\mathcal{M}) = \rho(\mathcal{M})$ when the perturbation Δ is totally structured, i.e., $\Delta = \delta_i I, \ |\delta_i| \leq 1$ and that $\mu_{\Delta}(\mathcal{M}) = \bar{\sigma}(\mathcal{M})$ when the perturbation Δ is unstructured, e.g., Δ is a full matrix.

Definition 2.3.5 is not itself useful for computing $\mu_{\Delta}(\cdot)$: currently, no simple computational method exists for exactly calculating μ in general and an efficient exact method is most likely not possible (Braatz *et al.*, 1994). This motivated to approximate $\mu_{\Delta}(\mathcal{M})$ by computing upper and lower bounds. The upper bound is derived by the computation of non-negative scaling matrices D_{ℓ} and D_r defined within a set $\mathcal{D}$ that commutes with the structure Δ. For a detailed discussion on the specification of such a set $\mathcal{D}$ of scaling matrices see, for instance, (Packard and Doyle, 1993). The commutation of $\mathcal{D}$ with Δ implies that $D_r \Delta = \Delta D_{\ell}$ and $\mu_{\Delta}(\mathcal{M}) = \mu_{\Delta}(D_{\ell} \mathcal{M} D_r^{-1})$ for all D_{ℓ}, $D_r \in \mathcal{D}$. Then, the upper bound of $\mu_{\Delta}(\mathcal{M})$ can be computed from

$$\mu_{\Delta}(\mathcal{M}) \leq \inf_{D_{\ell}, D_r \in \mathcal{D}} \bar{\sigma}(D_{\ell} \mathcal{M} D_r^{-1}) \tag{2.26}$$

Optimization problem (2.26) is convex in D (Packard and Doyle, 1993), i.e. it has only one minimum. It has been shown (Doyle, 1982) that the inequality is, in fact, an equality if the number of blocks in Δ are less than 4. Otherwise, the bound has evidenced to be tight in a few percent (Balas *et al.*, 1998).

2.3.4 Robust Performance

Often, stability is not the only property of a closed loop system that must be guaranteed for all possible plants in the uncertainty set $\mathcal{P}$. In most cases,

the performance objectives are desired to be kept even for the worst-case plant in the uncertainty set.

According to Definition 2.3.4, robust performance is achieved if

$$\|\mathcal{F}_u(\mathcal{N}, \Delta)\|_\infty < 1, \ \forall \Delta, \ \bar{\sigma}(\Delta) \leq 1 \tag{2.27}$$

where $\mathcal{F}_u(\mathcal{N}, \Delta)$ is the upper LFT derived from the general block diagram for analysis with uncertainty in Figure 2.5.

In order to evaluate robust performance using the structured singular value function, let us compare the condition in equation (2.23) for robust stability and the formally identical condition in equation (2.27) for robust performance. From Theorem 2.3.1 we know that stability of the $\mathcal{M}\Delta$ structure in Figure 2.7, with Δ a full complex matrix, is equivalent to $\|\mathcal{M}\|_\infty < 1$. From this theorem we can conclude that the condition for robust performance $\|\mathcal{F}_u\|_\infty < 1$ is equivalent to the stability of the $\mathcal{F}_u\Delta_P$ structure, with Δ_P being a full complex matrix of appropriate dimensions.

The structure of $\mathbf{\Delta}$ is now given by

$$\mathbf{\Delta} \doteq \left\{ \begin{bmatrix} \Delta & 0 \\ 0 & \Delta_P \end{bmatrix} : \Delta, \Delta_P \in \mathcal{RH}_\infty, \ \bar{\sigma}(\Delta) \leq 1, \ \bar{\sigma}(\Delta_P) \leq 1 \right\} \tag{2.28}$$

Figure 2.8 shows the equivalence between RP and RS. Condition (2.27) for RP is satisfied iff the system $\mathcal{N}$ is robustly stable with respect to the block diagonal perturbation $\mathbf{\Delta}$ defined in (2.28).

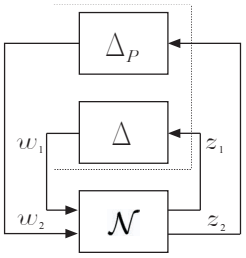

Figure 2.8: Block diagram for testing robust performance.

The following theorem can be stated:

Theorem 2.3.3. *The nominally stable system $\mathcal{N}$ in Figure 2.8 subjected to the block diagonal uncertainty Δ ($\bar{\sigma}(\Delta) \leq 1$) satisfies the robust performance condition $\|\mathcal{F}_u(\mathcal{N}, \Delta)\|_\infty < 1$ if and only if*

$$\mu_{\mathbf{\Delta}}(\mathcal{N}) < 1, \ \forall \omega \tag{2.29}$$

where μ is computed with respect to the structure $\mathbf{\Delta}$ in (2.28) and Δ_P is a full complex perturbation with appropriate dimensions.

Proof. *(Packard and Doyle, 1993), (Zhou* et al.*, 1996).*

□

Remark 2.3.1. *The robust performance condition (2.29) based on the SSV involves the enlarged perturbation set $\mathbf{\Delta} = \text{diag}\{\Delta, \Delta_P\}$ and allows to test robust performance in a non-conservative way. Δ represents the true uncertainty and may be a full matrix, i.e., unstructured uncertainty, or a block diagonal matrix, i.e., structured uncertainty; Δ_P is a full complex matrix arising from a $\mathcal{H}_\infty$ norm performance specification. Since $\mathbf{\Delta}$ always has structure, the use of the $\mathcal{H}_\infty$ norm, $\|\mathcal{N}\|_\infty < 1$, is generally conservative for robust performance.*

As long as Definition 2.3.5 is not itself useful for computing $\mu_\Delta(\cdot)$, the value of $\mu_{\mathbf{\Delta}}(\mathcal{N})$ is to be approximated by it upper bound computed from

$$\mu_{\mathbf{\Delta}}(\mathcal{N}) \leq \inf_{D_\ell, D_r \in \mathcal{D}} \bar{\sigma}(D_\ell \mathcal{N} D_r^{-1}) \tag{2.30}$$

This approximation was argued in Section 2.3.3, when the μ-condition for robust stability (2.25) is computed by means of its upper bound (2.26).

Example 2.3.1. Let us find the matrix $\mathcal{N}$ for the one degree-of-freedom control configuration with a multiplicative input uncertainty representation and performance defined in terms of weighted sensitivity as shown in Figure 2.9.

The proposed control scheme is to be rearranged into the $\mathcal{N}\Delta$ structure in Figure 2.8 with

$$w_1 \doteq d_i, \quad z_1 \doteq u', \quad w_2 \doteq d_o \quad \text{and} \quad z_2 \doteq y' \tag{2.31}$$

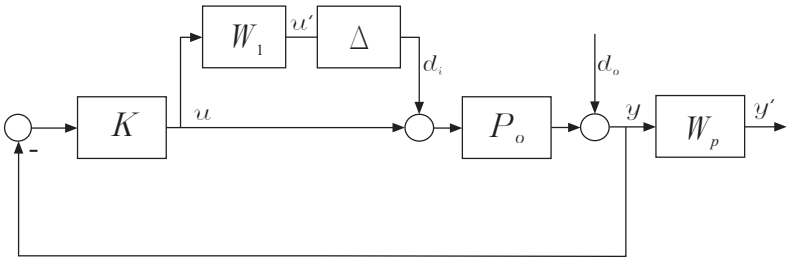

Figure 2.9: One degree-of-freedom control configuration with a multiplicative input uncertainty representation.

Therefore, the interconnection matrix $\mathcal{N}$ can be written, after some straightforward algebra, as

$$\mathcal{N} = \begin{bmatrix} -W_1 T_o & -W_1 S_o K \\ W_p S_o P_o & W_p S_o \end{bmatrix} \tag{2.32}$$

where

$$S_o = (I + P_o K)^{-1} \tag{2.33}$$

and

$$T_o = (I + P_o K)^{-1} P_o K \tag{2.34}$$

are the output sensitivity transfer function and the complementary sensitivity transfer function, respectively.

△

Example 2.3.2. Let us consider the nominal model of a distillation process given by (B.8). Appendix B.4 also describes the uncertainty and the performance weights. A diagonal PI controller from (Skogestad *et al.*, 1988) is employed to illustrate the usage of the SSV to test for NP, RS and RP:

$$K(s) = k\frac{(75s+1)}{s}\begin{bmatrix} 1 & 0 \\ 0 & -1 \end{bmatrix}, \quad k = 0.024 \tag{2.35}$$

Figure 2.10 illustrates the μ-plots for distillation process with the diagonal PI controller. It should be noted that neither NP nor RS are satisfied.

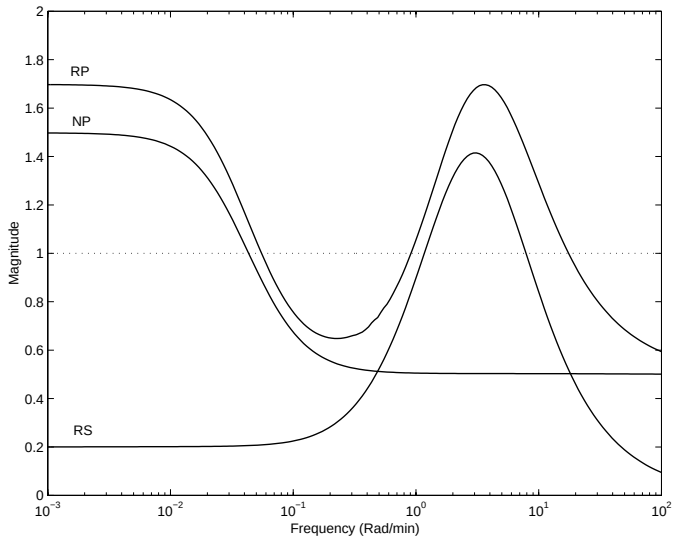

Figure 2.10: μ-plots for diagonal PI controller.

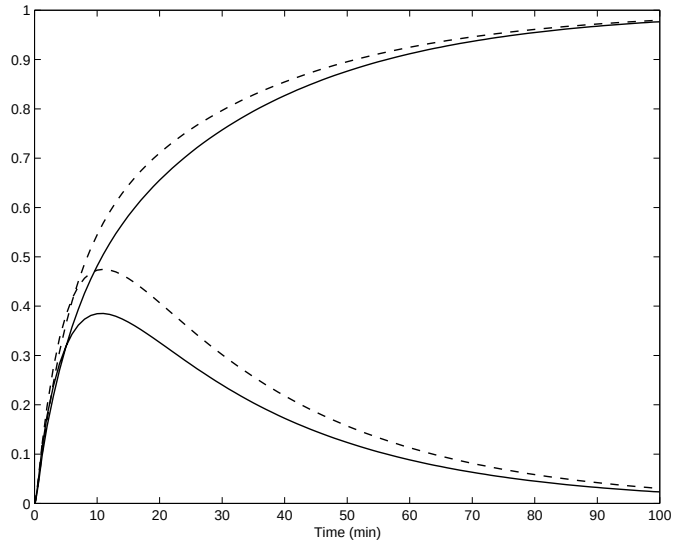

Figure 2.11: Closed loop response with diagonal PI controller to reference input. Nominal plant (solid) and the perturbed plant $P_3(s)$ (dashed).

In fact, no choice of k is able to satisfy both requirements (Skogestad *et al.*, 1988). As it is expected, RP is not fulfilled either.

Time response of y_1 and y_2 to a filtered setpoint change in y_1, $r_1 = 1/(5s+1)$, is shown in Figure 2.11. They confirm the poor performance offered by the diagonal PI controller either for the nominal plant model and for the uncertain plant $P_3(s)$ in (B.11). Despite the uncertain plant $P_3(s)$ is one of the worst plants in $\mathcal{P}$, it does not destabilize the closed loop system. Nevertheless, there exists a plant in the set $\mathcal{P}$ for which the controller does not guarantee closed loop stability. For instance, the plants $P_5(s)$ and $P_6(s)$ defined in (B.15) can not be stabilized by the diagonal PI controller.

△

2.4 Controller synthesis

We have seen that the structured singular value provides a systematic way to test for both robust stability (2.25) and for robust performance (2.29) with a given controller K. In addition to this analysis tool, the structured singular value can be used to synthesize the controller K.

The robust performance condition (2.29) implies robust stability (2.25), since

$$\sup_{\omega} \mu_{\Delta}(\mathcal{N}) \geq \sup_{\omega} \mu_{\Delta}(\mathcal{M}) \tag{2.36}$$

Therefore, a controller designed to guarantee robust performance will also guarantee robust stability.

Provided that the interconnection matrix $\mathcal{N}$ is a function of the controller K, as seen from equation (2.19), the μ-"optimal" controller K can be found by minimizing

$$\sup_{\omega} \mu_{\Delta}(\mathcal{N}) \tag{2.37}$$

At the present moment, there is no direct method to find the controller K by minimizing (2.37). However, the procedure known as DK-iteration (also called μ synthesis) (Zhou *et al.*, 1996) is an ad-hoc method that attempts to minimize the upper bound (2.30) of μ. Thus, the objective function (2.37) is transformed into

$$\min_{K} \inf_{D_\ell,\, D_r \in \mathcal{D}} \sup_{\omega} \bar{\sigma}(D_\ell \mathcal{N} D_r^{-1}) \tag{2.38}$$

The DK-iteration approach involves to alternatively minimize

$$\sup_{\omega} \bar{\sigma}(D_\ell \mathcal{N} D_r^{-1}) \tag{2.39}$$

for either K or D_ℓ and D_r while holding the other constant. For fixed D_ℓ and D_r, the controller is solved via $\mathcal{H}_\infty$ optimization; for fixed K, a convex optimization problem is solved at each frequency. The magnitude of each element of $D_\ell(j\omega)$ and $D_r(j\omega)$ is fitted with an stable and minimum phase transfer function and wrapped back into the nominal interconnection structure. The procedure is carried out until $\sup_\omega \bar{\sigma}(D_\ell \mathcal{N} D_r^{-1}) < 1$.

Although convergence in each step is assured, joint convergence is not guaranteed. However, DK-iteration works well in most cases (Balas *et al.*, 1998), (Packard and Doyle, 1993), (Zhou *et al.*, 1996), (Skogestad and Postlethwaite, 1997). The optimal solutions in each step are of supreme importance to success with the DK-iteration. Moreover, when K is fixed, the fitting procedure plays an important role in the overall approach. Low order transfer function fits are preferable since the order of the $\mathcal{H}_\infty$ problem in the following step is reduced yielding controllers of lower dimension. Nevertheless, the method is characterized by giving controllers of very high order that must be reduced applying model reduction techniques (Glover, 1984).

The synthesis procedure can be summarized as follows:

1. **K-step**: Scale the interconnection matrix $\mathcal{N}$ with $D_\ell(s)$ and $D_r(s)$, and synthesize an $\mathcal{H}_\infty$ controller for the scaled design problem, i.e., minimize $\left\| D_\ell \mathcal{N} D_r^{-1} \right\|$ for K with fixed $D_\ell(s)$ and $D_r(s)$.

2. **D-step**: Find $D_\ell(j\omega)$ and $D_r(j\omega)$ to minimize frequency-by-frequency the upper bound, $\bar{\sigma}(D_\ell \mathcal{N} D_r^{-1}(j\omega))$, with fixed $\mathcal{N}(s)$. Fit the magnitude of each element of $D_\ell(j\omega)$ and $D_r(j\omega)$ to stables and minimum phase transfer functions $D_\ell(s)$ and $D_r(s)$. Go to step 1 until $\left\| D_\ell \mathcal{N}(K) D_r^{-1} \right\|_\infty < 1$ or the ∞-norm no longer decreases.

Remark 2.4.1. *In some cases, it may be desirable simply to design a controller for the plant model P_o to satisfy certain nominal performance specifications and only guaranteeing robust stability. This may occur in cases such as plants operating most of the time close to its nominal point, with occasional plant perturbations. In such cases, performance may not be of primary importance when perturbations occur provided that the system remains stable. The loosing of performance may be treated in a second stage of the design. Then, if the controller K is to be designed just for robust stability, the μ-"optimal" controller K can be found by minimizing*

$$\sup_{\omega} \mu_{\Delta}(\mathcal{M}) \tag{2.40}$$

Now, the objective function (2.40) if transformed into

$$\min_{K} \inf_{D_\ell,\, D_r \in \mathcal{D}} \sup_{\omega} \bar{\sigma}(D_\ell \mathcal{M} D_r^{-1}) \tag{2.41}$$

The next example illustrates the above iterative controller design procedure on a distillation process.

Example 2.4.1. Let us consider the distillation process described in Appendix B.2. The linear model of the plant is

$$P_o(s) = \frac{1}{75s+1} \begin{bmatrix} 87.8 & -86.4 \\ 108.2 & -109.6 \end{bmatrix} \tag{2.42}$$

As in Example 2.3.2, a diagonal block input uncertainty is considered with weigh

$$W_1(s) = 0.2 \frac{5s+1}{0.5s+1} I \tag{2.43}$$

The performance requirement is just

$$\bar{\sigma}(S_o) < |W_p|^{-1} \tag{2.44}$$

where $S_o = (I + P_o K)^{-1}$ is the output sensitivity and

$$W_p(s) = 0.5 \frac{10s+1}{10s} I \tag{2.45}$$

The control objective is to minimize the peak value of $\mu_{\mathbf{\Delta}}(\mathcal{N})$, where $\mathbf{\Delta} = \text{diag}\{\Delta, \Delta_P\}$ is defined as in (2.28). The transfer matrix function $\mathcal{N}$ was given in (2.32). First, the generalized plant G has to be found, as in (2.2). It includes the plant model, P_o, the performance weigh, W_p, and the uncertainty weigh, W_1, but not the controller. The controller to be designed, K, appears into $\mathcal{N}$ since $\mathcal{N} = \mathcal{F}_\ell(G, K)$. Once the generalized plant G is found, the structure of $\mathbf{\Delta}$ has to be defined: Δ consists on two 1×1 blocks and Δ_P consists on one 2×2 blocks. The scaling matrices D_ℓ and D_r have the structure $D_\ell = D_r = \text{diag}\{d_1, d_2, d_3 I_2\}$ with I_2 being a 2×2 identity matrix. We may chose $d_3 = 1$ since we do not want to scale the controller. As initial scalings we select $d_1^0 = d_2^0 = 1$ to scale G with the matrices $\text{diag}\{D_\ell,\ I_2\}$ and $\text{diag}\{D_r,\ I_2\}$. The design procedure is detailed next.

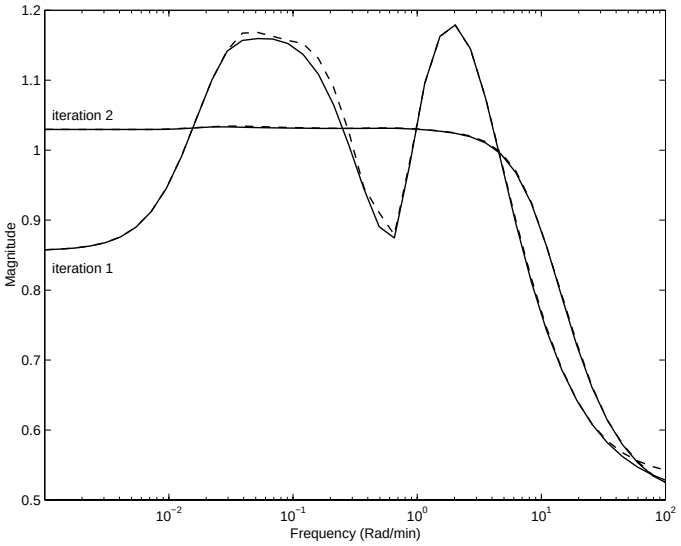

Figure 2.12: Upper μ-bound (solid) and scaled upper μ-bound (dashed).

Iteration 1

K-step: The $\mathcal{H}_\infty$ controller for the scaled plant, with $D_\ell = D_r = I$, has six states (2 from P_o, 2 from W_1 and 2 from W_p). The achieved ∞-norm is $\left\| D_\ell \mathcal{N} D_r^{-1} \right\|_\infty = 1.1798$.

D-step: The upper μ-bound has a peak value of $\mu = 1.1714$. The curve is illustrated in Figure 2.12. The frequency-dependent

$d_1^1(\omega)$ and $d_2^1(\omega)$ are each fitted using 3th order transfer functions $D_\ell(s)$ and $D_r(s)$. Figure 2.13 shows the frequency-dependent scaling $d_1^1(\omega)$ in solid line and the fitted transfer functions $D_\ell(s)$ and $D_r(s)$ in dashed line. The scaling $d_2^1(\omega)$ is very closed to $d_1(\omega)$ and therefore, it is not shown. This indicates that the worst case full block Δ is in fact diagonal.

Iteration 2

K-step: With the 6 state scaling $D_\ell(s)$ and $D_r(s)$ we obtain a 18 state $\mathcal{H}_\infty$ controller. The ∞-norm is $\left\|D_\ell \mathcal{N} D_r^{-1}\right\|_\infty = 1.0329$

D-step: The upper μ-bound has a peak value of $\mu = 1.0329$. The curve is illustrated in Figure 2.12. The frequency-dependent $d_1^2(\omega)$ and $d_2^2(\omega)$ are each fitted using 2th order transfer functions $D_\ell(s)$ and $D_r(s)$. Figure 2.13 shows the frequency-dependent scaling $d_1^2(\omega)$ in solid line and the fitted transfer functions $D_\ell(s)$ and $D_r(s)$ in dashed line.

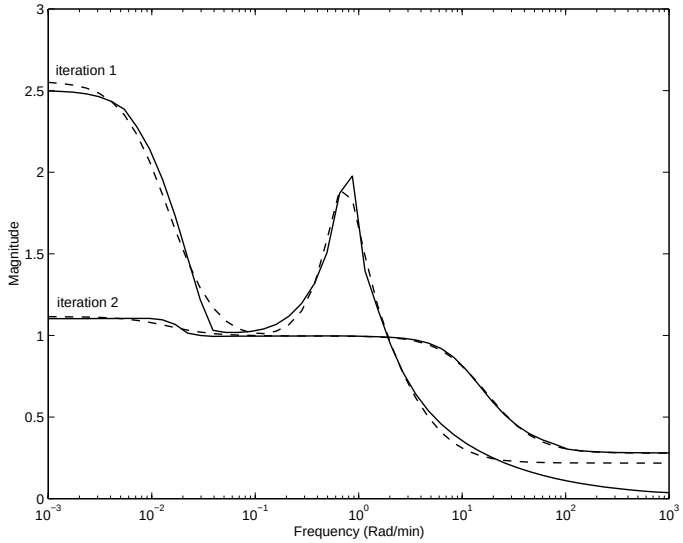

Figure 2.13: Frequency-dependent scaling $d_1(\omega)$ (solid) and the fitted transfer functions (dashed).

The DK-iteration procedure is stopped after two iterations. With the the 6 state scalings $D_\ell(s)$ and $D_r(s)$ the ∞- norm is no longer reduced from the previous iteration.

Figure 2.14 shows the μ-curves for the nominal performance (NP), robust stability (RS) and robust performance (RP) with the achieved μ-"optimal" controller, K_{opt}. The state-space realization of such an optimal controller is given in Table C.1. The objectives of RS and NP are easily fulfilled. Nevertheless, the peak μ-value is 1.0329 which means that the performance specification $\bar{\sigma}(S_o) < |W_p|^{-1}$ is almost fulfilled for all possible plants.

The μ-"optimal" controller in (Skogestad *et al.*, 1988) has a peak μ-value of 1.06. By trial and error, a μ-"optimal" controller with a peak μ-value of 0.974 was found in (Lundström, 1994).

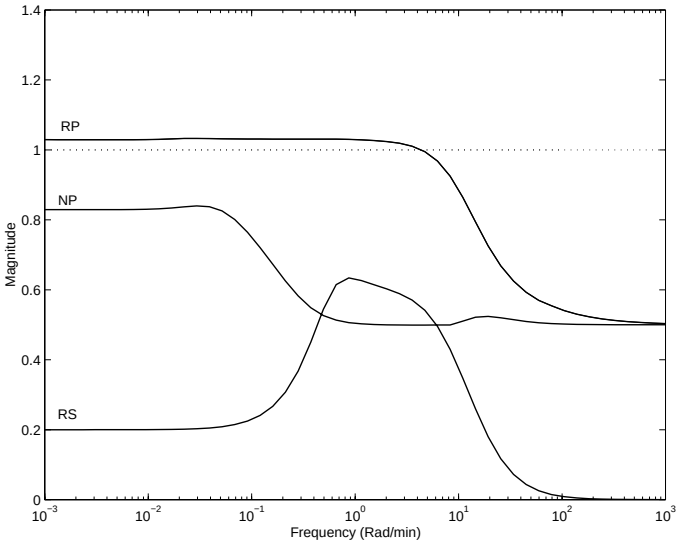

Figure 2.14: μ-plots for K_{opt}.

The time response of both y_1 and y_2 to a filtered setpoint change in y_1, $r_1 = 1/(5s+1)$, is shown in Figure 2.15. The solid lines represents the responses for the nominal plant, P_o; the dashed lines represents the responses for the uncertain plants, $P_i = P_o E_{I_i}$ for $i = 1, \ldots, 6$ as in (B.15). The predictions from the μ-curves in Figure 2.14 are fulfilled and the responses show no strong sensitivity to input uncertainty.

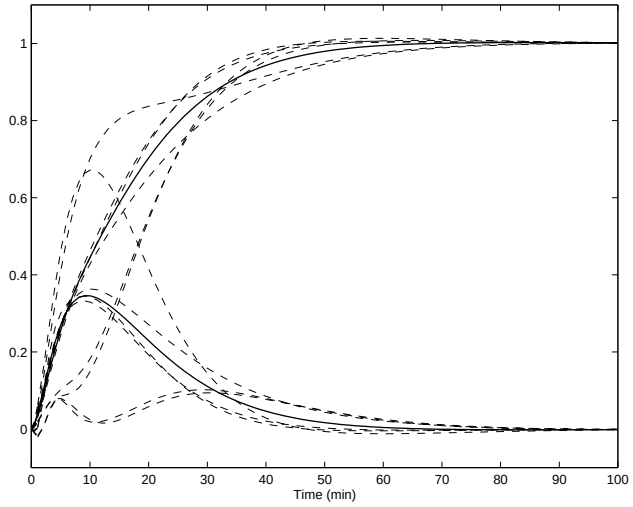

Figure 2.15: Closed-loop setpoint change with the μ-"optimal" controller K_{opt}: response for the nominal plant P_o (solid) and for the uncertain plants $P_i = P_o E_{I_i}$, $i = 1, \ldots, 6$ (dashed).

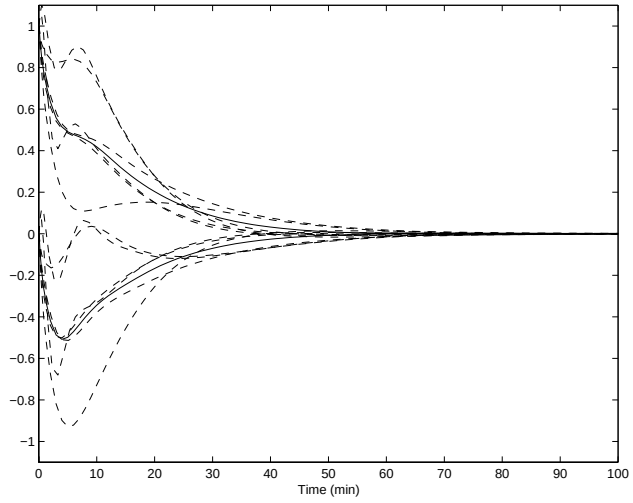

Figure 2.16: Closed-loop response with the μ-"optimal" controller K_{opt} to a disturbance in the output signal y_1: response for the nominal plant P_o (solid) and for the uncertain plants $P_i = P_o E_{I_i}$, $i = 1, \ldots, 6$ (dashed).

Figure 2.16 shows the response to a unitary step disturbance at the output with the μ-"optimal" controller K_{opt}. The response for the nominal plant P_o is illustrated in solid and the responses for the uncertain plants $P_i = P_o E_{I_i}$, $i = 1, \ldots, 6$ in equation (B.15) are illustrated in dashed lines.

△

2.5 Summary

The general method of formulating control problems has been introduced and the general approach for representing uncertainty for multivariable systems has been presented. We have recalled how the *structured singular value*, μ, allows to get necessary and sufficient conditions for robust stability and also for robust performance. In addition, we have reviewed the DK-iteration procedure, which has been applied to the control a high purity distillation column. Such a distillation process has also been controlled by means of a PI control strategy, showing unacceptable responses.

Chapter 3

Factorization Approach

In this Chapter we give a short introduction to the so-called factorization or fractional approach *which is to be used along this work. The central idea is to factor a transfer (matrix) function of a system, not necessarily stable, as a ratio of two stable transfer (matrix) functions. Within the factorization framework, the* Observer-Controller *configuration is introduced to be used in the different control configurations proposed in this work.*

3.1 Introduction

A short introduction to the so called *factorization or fractional approach* is provided in this Chapter. The central idea is to factor a transfer (matrix) function of a system, not necessarily stable, as a ratio of two stable transfer (matrix) functions. This idea provides a methodology for the resolution of several control problems, i.e., the stabilization of a non necessary stable system, and the analysis of feedback control systems. The factorization approach will constitute the framework for the analysis and design in subsequent Chapters. The treatment in this Chapter is fairly standard and follows (Vilanova, 1996), (Vidyasagar, 1985), (Nett *et al.*, 1984), (Francis, 1987) or (Maciejowski, 1989). Although the idea of coprime factorizations is mainly based on ring theory[1] and a rigorous algebraic approach exist to the stabilization problem from the factorization approach (Desoer *et al.*, 1980), (Desoer

[1] In fact, the set of stable transfer functions is a ring.

and Gustafson, 1984), (Vidyasagar *et al.*, 1982), (Vidyasagar, 1985), the presentation here will not be on the algebraic side since, to make it properly, we should need to introduce a lot of, sometimes messy, notation.

Within the factorization approach we present the *Observer-Controller* configuration, a somewhat uncommon configuration which is based on a king of state feedback (Vidyasagar, 1985) (Kailath, 1980). The Observer-Control configuration constitutes the basis for the different control structures proposed in this work.

The Chapter is organized as follows: Section 3.2 introduces a condition for internal stability in terms of the plant and the controller factors and it is shown how every plant has associated a stabilizing controller. This controller is determined by the components of a *Bezout* equation that provides coprime plant factors. Section 3.3 deals with the factorization of transfer (matrix) functions. Finally, Section 3.4 presents the Observer-Controller configuration, the somewhat uncommon configuration, that will constitute the basic structure for the different control configurations in this work.

3.2 Motivation for the fractional representation

The specifications on a control system can be seen as given by some criterion to be optimized or by specifying some set of desirable transfer functions that the compensated system should belong to. The typical and the most important example is that of stabilizing an unstable plant. This specification may, of course, include stabilization in the sense of requiring the poles of the compensated system to belong to some stability region $\mathcal{D}$. The introduction of the factorization approach for representing a system comes from the following observation (Vidyasagar, 1985): the set of desired transfer functions for the compensated system is easily specified, but it rests to specify the class of transfer functions within the plant transfer function may lie. This class will be determined by choosing the compensation scheme to be used. Therefore, the classical feedback configuration of Figure 3.1 has to be considered.

The transfer matrix from the external inputs $[r\ d_i]^T$ to the outputs $[u\ y]^T$ is:

$$\mathcal{H}(P_o, K) = \begin{bmatrix} K(I + P_oK)^{-1} & P_oK(I + P_oK)^{-1} \\ KP_o(I + KP_o)^{-1} & P_o(I + KP_o)^{-1} \end{bmatrix} \tag{3.1}$$

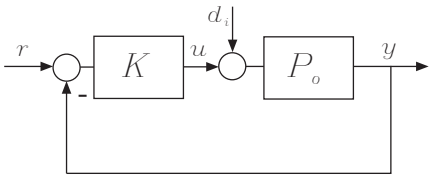

Figure 3.1: Classical unity feedback configuration.

By defining

$$\mathcal{G} = \begin{bmatrix} K & 0 \\ 0 & P_o \end{bmatrix} \qquad \mathcal{F} = \begin{bmatrix} 0 & I \\ -I & 0 \end{bmatrix} \tag{3.2}$$

the transfer matrix (3.1) can be rewritten as:

$$\mathcal{H}(P_o, K) = \mathcal{G}(I + \mathcal{F}\mathcal{G})^{-1} \tag{3.3}$$

Therefore, the system of Figure 3.1 is *internally stable* if every element of $\mathcal{H}(P_o, K)$ is stable. If we solve (3.3) for $\mathcal{G}$

$$\mathcal{G} = \mathcal{H}(I - \mathcal{F}\mathcal{H})^{-1} = \mathcal{H}\,\mathrm{Adj}(I - \mathcal{F}\mathcal{H})/\det(I - \mathcal{F}\mathcal{H}) \tag{3.4}$$

Expression (3.4) shows that every element of the matrix $\mathcal{G}$ can be expressed as the ratio of two stable transfer functions. Recall that the elements of $\mathcal{G}$ are the controller and the plant to be controlled. Thus,

> *once the set of stable transfer functions has been established, the class of all transfer functions that can be encompassed within the theory of stabilization consist on those transfer functions that can be expressed as a ratio of two stable transfer functions.*

These observations suggest a way of addressing the stabilization problem, say the one where both the plant and the controller are represented as the ratio of stable transfer functions. This is the *Factorization Approach*. It may be shown, that the set of all stabilizing compensators for a given plant can be expressed in a parameterized factorization manner from the factors of the plant. This is the celebrated Youla parametrisation of all the stabilizing controllers presented in (Youla *et al.*, 1976*b*; Youla *et al.*, 1976*a*).

3.3 Coprime factorizations over $\mathcal{RH}_\infty$

A usual way of representing a scalar system is as a rational transfer function of the form

$$P_o(s) = \frac{n(s)}{m(s)} \tag{3.5}$$

where $n(s)$ and $m(s)$ are polynomials and (3.5) is called *polynomial fraction representation* of $P_o(s)$. Another way of representing $P_o(s)$ is as the product of a stable (matrix) transfer function and a (matrix) transfer function with stable inverse, i.e.,

$$P_o(s) = N(s)M^{-1}(s) \tag{3.6}$$

where $N(s),\ M(s)\ \in\ \mathcal{RH}_\infty$.

In the Single-Input Single-Output (SISO) case, it is easy to get a fractional representation in the polynomial form (3.5). Let $\zeta(s)$ be a Hurwitz polynomial such that $\deg\zeta(s) = \deg m(s)$ and set

$$N(s) = \frac{n(s)}{\zeta(s)} \qquad M(s) = \frac{m(s)}{\zeta(s)} \tag{3.7}$$

The factorizations to be used will be a special one called *Coprime Factorizations*. Two polynomials $n(s)$ and $m(s)$ are said to be coprime if their greatest common divisor is 1 (no common zeros). It follows from Euclid's algorithm — see for example (Kailath, 1980) — that $n(s)$ and $m(s)$ are coprime iff there exists polynomials $x(s)$ and $y(s)$ such that the following Bezout identity is satisfied:

$$x(s)m(s) + y(s)n(s) = 1 \tag{3.8}$$

Note that if z is a common zero of $n(s)$ and $m(s)$ then $x(z)m(z)+y(z)n(z) = 0$ and therefore, $n(s)$ and $m(s)$ are not coprime.

This concept is automatically generalized to transfer functions $N(s)$, $M(s)$, $X(s)$ and $Y(s)$. Two transfer function are coprime when any possible common factor, say $U(s)$, between $N(s)$ and $M(s)$ is minimum phase. Thus, if $N(s) = W(s)U(s)$ and $M(s) = Z(s)U(s)$, then U^{-1} is stable. This way, the common factor can be absorbed into $X(s)$ and $Y(s)$. Now, let us move to the general situation of a multivariable system. In this case, distinction on right and left factorizations has to be done.

Example 3.3.1. Finding a coprime factorization for a scalar transfer function is fairly easy. Let us consider the scalar system

$$P_o(s) = \frac{(s+1)(s-2)}{(s+3)(s-4)} \tag{3.9}$$

We first make all the RHP-poles of P_o zeros of M, and all the RHP-zeros of P_o zeros of N. We then allocate the poles of N and M so that N and M are both proper and the identity $P_o = NM^{-1}$ holds. Then,

$$N(s) = \frac{(s-2)}{(s+3)}, \qquad M(s) = \frac{(s-4)}{(s+1)} \tag{3.10}$$

is the simplest coprime factorization. Usually, $N(s)$ and $M(s)$ are selected to have the same poles as each other and the same order as $P_o(s)$. Then, taking $\zeta(s) = (s+p_1)(s+p_2)$,

$$N(s) = \frac{(s+1)(s-2)}{(s+p_1)(s+p_2)}, \qquad M(s) = \frac{(s+3)(s-4)}{(s+p_1)(s+p_2)} \tag{3.11}$$

is a coprime factorization of $P_o(s)$ for any $p_1,\ p_2 > 0$.

△

Remark 3.3.1. *The above example shows that a coprime factorization for a system $P_o(s)$ is not unique and can be achieved for any Hurwitz polynomial $\zeta(s)$ satisfying* $\deg\zeta(s) = \deg m(s)$. *It is clear that the polynomial $\zeta(s)$ is canceled and the frequency response of NM^{-1} is that of P_o. Nevertheless, the allocation of the poles p_1, p_2 determines the shape of $N(j\omega)$ and $M(j\omega)$.*

The relevance of Remark 3.3.1 will be seen further on.

Assuming that $M(s)$ be squared and nonsingular, the following definitions can be written:

Definition 3.3.1. (Bezout identity) Two transfer functions N_r and M_r are *right coprime* if and only if there exists stable matrix transfer functions X_r and Y_r such that

$$\begin{bmatrix} X_r & Y_r \end{bmatrix} \begin{bmatrix} M_r \\ N_r \end{bmatrix} = X_r M_r + Y_r N_r = I \tag{3.12}$$

Similarly, two transfer functions N_ℓ and M_ℓ are *left coprime* if and only if there exists stable matrix transfer functions X_ℓ and Y_ℓ such that

$$\begin{bmatrix} M_\ell & N_\ell \end{bmatrix} \begin{bmatrix} X_\ell \\ Y_\ell \end{bmatrix} = M_\ell X_\ell + N_\ell Y_\ell = I \tag{3.13}$$

◇

The stable matrix transfer functions X_r, Y_r, (X_ℓ, Y_ℓ) are called right (left) Bezout complements.

Now, let $P_o(s)$ be a proper real rational matrix. Then,

Definition 3.3.2. A *right coprime factorization* (RCF) of $P_o(s)$ is a factorization $P_o = N_r M_r^{-1}$, where N_r and M_r are right coprime over $\mathcal{RH}_\infty$.

◇

Definition 3.3.3. A *left coprime factorization* (LCF) of $P_o(s)$ is a factorization $P_o = M_\ell^{-1} N_\ell$, where N_ℓ and M_ℓ are left coprime over $\mathcal{RH}_\infty$.

◇

Finally,

Definition 3.3.4. P_o has *doubly coprime factorization* if there exist a RCF $P_o = N_r M_r^{-1}$, a LCF $P_o = M_\ell^{-1} N_\ell$ and X_r, Y_r, X_ℓ, Y_ℓ $\in \mathcal{RH}_\infty$ such that

$$\begin{bmatrix} X_r & Y_r \\ -N_\ell & M_\ell \end{bmatrix} \begin{bmatrix} M_r & -Y_\ell \\ N_r & X_\ell \end{bmatrix} = I \tag{3.14}$$

◇

Transfer functions are a good way of representing systems because they give more immediate insight into a systems behaviour. However, for numerical calculations a state-space realization is usually desired.

With the above definitions, the following theorem arises to provide right and left coprime factorizations for the proper real rational matrix $P_o(s)$, where

$$P_o(s) = \left[\begin{array}{c|c} A & B \\ \hline C & D \end{array}\right] \tag{3.15}$$

is a minimal stabilisable and detectable state-space realization.

Theorem 3.3.1. *Define*

$$\begin{bmatrix} M_r & -Y_\ell \\ N_r & X_\ell \end{bmatrix} \doteq \left[\begin{array}{c|cc} A+BF & B & -L \\ \hline F & I & 0 \\ C+DF & D & I \end{array}\right] \tag{3.16}$$

$$\begin{bmatrix} X_r & Y_r \\ -N_\ell & M_\ell \end{bmatrix} \doteq \left[\begin{array}{c|cc} A+LC & -(B+LD) & L \\ \hline F & I & 0 \\ C & -D & I \end{array}\right] \tag{3.17}$$

where F and L are such that $A+BF$ and $A+LC$ are stable. Then, $P_o = N_r M_r^{-1}$ ($P_o = M_\ell^{-1} N_\ell$) is a RCF (LCF).

Proof. *The theorem is demonstrated by substituting (3.16) and (3.17) in to equation (3.14).*

□

Standard packages can be used to compute appropriate F and L matrices numerically. Given $A \in \mathcal{R}^{n\times n}$, $B \in \mathcal{R}^{n\times m}$ and $C \in \mathcal{R}^{p\times n}$ a matrix F such that the eigenvalues of $A+BF$ are those specified in vector

$$p_F = [p_{F_1} \cdots p_{F_n}]^T \tag{3.18}$$

can be computed with the restriction that no eigenvalue should have a multiplicity greater than the number of inputs. Similarly, a matrix H such that the eigenvalues of $A+LC$ are those specified in vector

$$p_L = [p_{L_1} \cdots p_{L_n}]^T \tag{3.19}$$

can be computed with the same restriction associated with the multiplicity of the eigenvalues.

We next exemplify the computation of a coprime factorization for a given system $P_o(s)$ provided a minimal stabilisable and detectable state-space realization (3.15). For illustrative purposes we have tried a single-input single-output plant case.

Example 3.3.2. Let us calculate a coprime factorization for a scalar system

$$P_o(s) = \frac{(s-1)}{s(s+5)} \tag{3.20}$$

with eigenvalues for $A + BF$ allocated to form the polynomial $\zeta(s) = (s + 2)(s + 5)$, i.e., $p_F = [2 \;\; 5]^T$, and with eigenvalues for $A + LC$ allocated to form the polynomial $(s + 3)(s + 4)$, i.e., $p_L = [3 \;\; 4]^T$.

Then, $P_o(s) = N(s)M^{-1}(s)$,

$$N(s) = \frac{s-1}{(s+2)(s+5)}, \qquad M(s) = \frac{s}{(s+2)} \tag{3.21}$$

form a coprime factorization with

$$X(s) = \frac{s + 4.5 \pm j5.45}{(s+3)(s+4)}, \qquad Y(s) = \frac{-24(s+5)}{(s+3)(s+4)} \tag{3.22}$$

the associate Bezout complements.

△

Either the right coprime factorization and the left coprime factorization provided by Theorem 3.3.1 can be given a feedback control interpretation.

3.3.1 RCF feedback control interpretation

A feedback control interpretation for the mathematical *right* coprime factorization stated above is to be provided here. Let us consider the system $P_o(s)$ with the realization (3.15). Under *stabilizability* assumption on the pain (A, B), it is possible using standard methods to construct a constant *stabilizing state-feedback gain (matrix)* F, in that $A + BF$ has all eigenvalues within the RHP. It can be shown in Figure 3.2. The gain F can be obtained from various methodologies from linear controller designs. Optimal state-feedback gain matrix F can be found by means of the Linear Quadratic Regulator (LQR) problem approach. It is based on finding a unique positive semi-definite solution of an algebraic Riccati equation (Stein and Athans, 1987). Eigenvalues assignment approaches can be found in (Ogata, 1990).

The realization of P_o (3.15) affected by state-variable feedback is shown in Figure 3.2. From such diagram block, the following equations are derived:

$$\begin{cases} \dot{x}(t) &= Ax(t) + Bu(t) \\ y(t) &= Cx(t) + Du(t) \\ u(t) &= Fx(t) \end{cases} \tag{3.23}$$

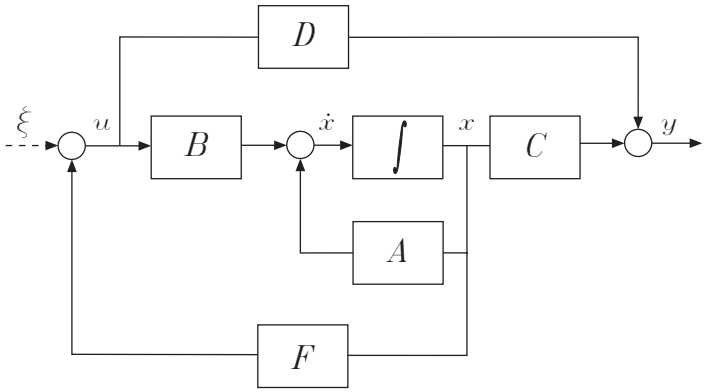

Figure 3.2: Realization of P_o (3.15) affected by state-variable feedback and the artificial signal ξ.

We can define the artificial signal $\xi(t) = u(t) - Fx(t)$. Then

$$\begin{cases} \dot{x}(t) &= (A + BF)x(t) + B\xi(t) \\ y(t) &= (C + DF)x(t) + D\xi(t) \\ u(t) &= Fx(t) + \xi(t) \end{cases} \tag{3.24}$$

Taking Laplace transforms,

$$\frac{u(s)}{\xi(s)} = F(sI - (A + BF))^{-1}B + I \doteq M_r(s) \tag{3.25}$$

$$\frac{y(s)}{\xi(s)} = (C + DF)(sI - (A + BF))^{-1}B + D \doteq N_r(s) \tag{3.26}$$

so that

$$y(s) = N_r(s)\xi(s) = N_r(s)M_r^{-1}(s)u(s) = P_o(s)u(s) \tag{3.27}$$

The relation between the input signal u and the output signal y in equation (3.27) is illustrated in Figure 3.3.

Equations (3.25) and (3.26) can be expressed in a more compact form as

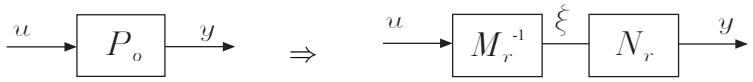

Figure 3.3: Diagram block representation of *right coprime factorization* $P_o = N_r M_r^{-1}$.

$$M_r(s) = \left[\begin{array}{c|c} A+BF & B \\ \hline F & I \end{array}\right] \tag{3.28}$$

and

$$N_r(s) = \left[\begin{array}{c|c} A+BF & B \\ \hline C+DF & D \end{array}\right] \tag{3.29}$$

We have seen that a coprime factorization for a system $P_o(s)$ provided a minimal stabilisable and detectable state-space realization (3.15) with $A \in \mathcal{R}^{n\times n}$, $B \in \mathcal{R}^{n\times m}$ and $C \in \mathcal{R}^{p\times n}$ is not unique. We have also seen that such coprime factorization can be found by numerical computation of matrices F and L such that the eigenvalues of $A+BF$ and $A+LC$ are those specified in vector (3.18) and (3.18), respectively. As is was pointed out in Remark (3.3.1), the allocated nodes for N_r and M_r are cancelled for the identity $P_o = N_r M_r^{-1}$ to be satisfied. Nevertheless, the allocation of the eigenvalues of $A+BF$ determines the shape of N_r and M_r^{-1}. It is illustrated next.

Example 3.3.3. Let us calculate right coprime factorizations for the plant

$$P_o(s) = \frac{1}{(0.2s+1)(s+1)} \left[\begin{array}{cc} 1 & 1 \\ 2s+1 & 2 \end{array}\right] \tag{3.30}$$

provided a minimal stabilisable and detectable state-space realization (3.15) with $A \in \mathcal{R}^{4\times 4}$, $B \in \mathcal{R}^{2\times 1}$. Figure 3.4 a) shows the frequency response of right coprime factors N_r and M_r^{-1} achieved with eigenvalues for $A+BF$ allocated at $p_F = [0.1 \;\; 0.2 \;\; 0.3 \;\; 0.4]^T$. Figure 3.4 b) shows the frequency response of right coprime factors N_r and M_r^{-1} achieved with eigenvalues for $A+BF$ allocated at $p_F = [10 \;\; 20 \;\; 30 \;\; 40]^T$.

The identity $P_o = N_r M^{-1}$ is obviously fulfilled in both right coprime factorizations. Nevertheless the different pole placement has repercussions

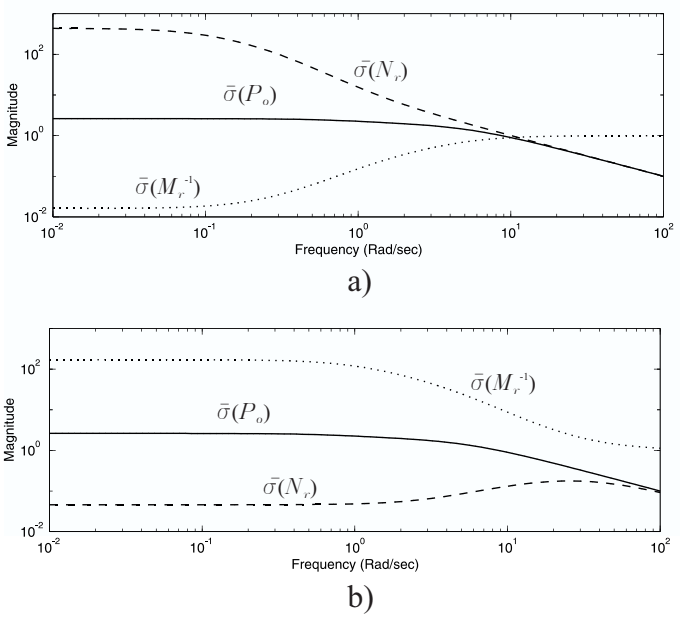

Figure 3.4: Right coprime factorizations $P_o = N_r M_r^{-1}$ for two different p_F: a) high-pass shape for $M_r^{-1}(j\omega)$ b) low-pass shape for $M_r^{-1}(j\omega)$.

on the frequency response of the resulting right coprime factors. For instance, a high-pass shape for $M_r^{-1}(j\omega)$ is shown in Figure 3.4 a) while a low-pass shape for $M_r^{-1}(j\omega)$ is shown in Figure 3.4 b).

△

The above example has illustrated how different p_F for the pole placement of $A + BF$ results in different frequency responses for the achieved right coprime factors N_r and M_r. Analogously, it may also be shown that different p_L for the pole placement of $A + LC$ results in different frequency responses for the achieved right coprime Bezout complements X_r and Y_r.

3.3.2 LCF feedback control interpretation

A feedback control interpretation for the mathematical *left* coprime factorization is to be provided here. Let us consider the system $P_o(s)$ with the realization (3.15).

Under *observability* assumption on the pain (A, C), state estimates $\hat{x}(t)$ are to be obtained by means of an observer structure driven by the difference between the system output $y(t)$ and its estimation $\hat{y}(t)$. The state-space Observer-Controller configuration is shown in Figure 3.5. It is possible using standard methods to construct a constant *stabilizing output injection gain (matrix)* L, in that $A + LC$ has all eigenvalues within the RHP. The gains L and F can be obtained from various methodologies from linear controller designs (Stein and Athans, 1987), (Ogata, 1990).

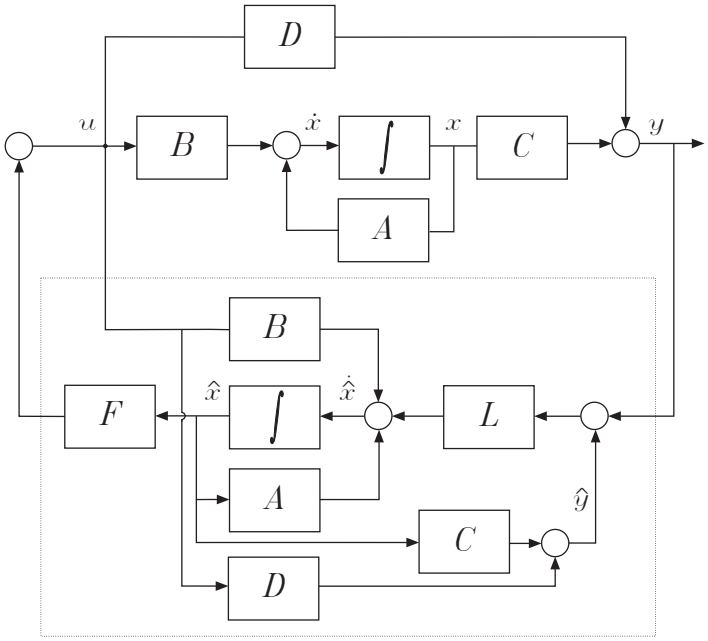

Figure 3.5: Realization of P_o (3.15) affected by state-variable observer and controller.

The following observation equations are obtained:

$$\begin{cases} \dot{\hat{x}}(t) &= A\hat{x}(t) + Bu(t) + L(\hat{y}(t) - y(t)) \\ \hat{y}(t) &= C\hat{x}(t) + Du(t) \end{cases} \tag{3.31}$$

Let us define the "observation error" signal ν as

$$\nu = \hat{y} - y = C\hat{x} + Du - y$$

Then,

$$\begin{cases} \dot{\hat{x}}(t) &= (A+LC)\hat{x}(t) - Ly(t) + (B+LD)u(t) \\ \hat{y}(t) &= C\hat{x}(t) + Du(t) \end{cases} \tag{3.32}$$

Taking Laplace Transforms,

$$\frac{\nu(s)}{y(s)} = -[C(sI-(A+LC))^{-1}L + I] \doteq M_\ell(s) \tag{3.33}$$

$$\frac{\nu(s)}{u(s)} = C(sI-(A+LC))^{-1}(B+LD) + D \doteq N_\ell(s) \tag{3.34}$$

so that

$$y(s) = M_\ell^{-1}(s)\nu(s) = M_\ell^{-1}(s)N_\ell(s)u(s) = P_o(s)u(s) \tag{3.35}$$

Equations (3.33) and (3.34) can be expressed in a more compact form as

$$M_\ell(s) = -\left[\begin{array}{c|c} A+HC & H \\ \hline C & I \end{array}\right] \tag{3.36}$$

and

$$N_\ell(s) = \left[\begin{array}{c|c} A+LC & B+LD \\ \hline C & D \end{array}\right] \tag{3.37}$$

3.4 Observer-Controller configuration

This Section presents the Observer-Controller configuration. This somewhat uncommon configuration is based on the usage of the partial state ξ that appears on the context of *right* coprime factorizations.

3.4.1 Partial state feedback

In Section 3.3.1, a state feedback control interpretation of the right coprime factorization of P_o is provided. A controller-form realization of the RCF $P_o = N_r M_r^{-1}$ shall demonstrate that the state variables of any minimal realization of P_o are completely determined by $\xi(\cdot)$ and its derivatives — see (Kailath, 1980) for more details. Therefore $\xi(\cdot)$ is often called the *partial state*[1] of a system. In this context, the state feedback through a gain matrix K can be schematically represented as in Figure 3.6.

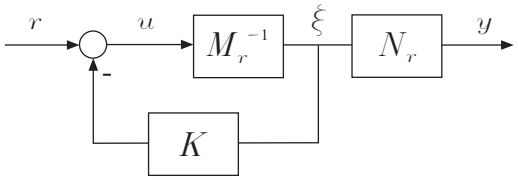

Figure 3.6: Representation of partial state feedback from a right coprime factorization $P_o = N_r M_r^{-1}$.

Given a controllable and observable system with the strictly proper transfer function

$$P_o(s) = N_r(s) M_r^{-1}(s) \tag{3.38}$$

with $N_r(s)$ and $M_r(s)$ right coprime, it is possible to design a compensator $K(s)$ to make the overall relation from the input r to the output y have a strictly proper transfer function, say

$$T_{ref}(s) = N_r(s) Z^{-1}(s) \tag{3.39}$$

with all nodes freely assignable.

What is required in order to achieve such a *desired* input/output transfer function (3.39) is to first access the partial state ξ,

$$\xi(s) = M_r^{-1}(s) u(s) \tag{3.40}$$

[1] It should noted that to observe the *partial state* will not be the same as to perform a partial observation of the state variables, usual in the state-space control context.

and then feed it back to the input through an appropriate compensator, say $K(s)\xi(s)$.

If there are no disturbances acting on the system shown in Figure 3.6, the relations from the reference command r to the output u and control signal y are, respectively,

$$T_{ur} = (I + KM_r^{-1})^{-1} = (M_r + K)^{-1}M_r \doteq Z_r^{-1}M_r \tag{3.41}$$

and

$$T_{yr} = N_r(I + M_r^{-1}K)^{-1}M_r^{-1} = N_r(M_r + K)^{-1} \doteq N_r Z_r^{-1} \tag{3.42}$$

Theorem 3.4.1. *Provided that $N_r(s)$ and $M_r(s)$ are stable, the nominal control system shown in Figure 3.6, with input output transfer matrix function (3.39), will be stable if and only if $Z_r^{-1}(s)$ is stable and $Z_r(s) = M_r(s) + K(s)$ is unimodular.*

Proof. *The fact that $Z_r^{-1}(s)$ must be stable is obvious. Then, if $Z_r(s)$ is unimodular it must occur that* $\det Z_r(s)$ *is a nonzero scalar and its inverse $Z_r^{-1}(s) = \mathrm{Adj}Z_r(s)/\det Z_r(s)$ is clearly a polynomial. Conversely, if $Z_r(s)$ and $Z_r^{-1}(s)$ are both polynomial matrices, let* $\det Z_r(s) = \alpha_1(s)$ *and* $\det Z_r^{-1}(s) = \alpha_2(s)$*. Clearly, $\alpha_1(s)$ and $\alpha_2(s)$ will also be polynomials, and moreover $\alpha_1(s)\alpha_2(s) = 1$. This can only happen if $\alpha_1(s)$ and $\alpha_2(s)$ are both scalars. Therefore $Z_r(s)$ must be unimodular.* □

Finally, to obtain the *desired* transfer function $T_{ref}(s)$ (3.39) we choose

$$K(s) = Z_r(s) - M_r(s) \tag{3.43}$$

Remark 3.4.1. *This way, the set of stabilizing Observer-Controller compensators are characterized by a free, unimodular, parameter $Z_r(s)$.*

3.4.2 RHP-zeros

The partial state feedback control configuration shown in Figure 3.6 allows to design a controller $K(s)$ to make the closed-loop relation from the reference r to the output y have a strictly proper transfer function $T_{ref} = N_r Z_r^{-1}$ having all nodes freely assignable and characterized by a free, unimodular, parameter $Z_r(s)$.

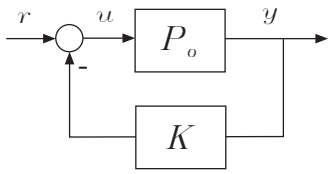

Figure 3.7: Output feedback control configuration.

The scheme in Figure 3.6 presents an important advantage with respect to the a standard output feedback control configuration shown in Figure 3.7.

A plant having a right-half plane zero, z, is subjected to serious performance limitations. It may be proven (Hold and Morari, 1985) that stable plants with RHP-zeros have inverse response. Moreover, RHP-zeros located close to the origin cause control problems to arise (Skogestad and Postlethwaite, 1997). It is well-known from classical root-locus analysis (Kuo, 1982), (Dorf, 1990), (Ogata, 1990) that as the feedback gain increases towards infinity, the closed-loop poles move to the positions of the open-loop zeros. Thus, the presence of RHP-zeros implies high-gain instability. In theory, any linear plant may be stabilized without regard of the location of its RHP-poles and RHP-zeros, provided the plant does not contain unstable hidden nodes. However, this may require an unstable controller and, for practical purposes, it is sometimes undesirable.

Let us consider a SISO system $P_o(s) = n(s)/m(s)$ affected by a negative output feedback controller $K(s) = k$ as shown in Figure 3.7. The closed loop response from the reference r to the output y is

$$T(s) = \frac{KP_o}{1 + KP_o} = \frac{n(s)}{m(s) + kn(s)} = \frac{n_{cl}(s)}{m_{cl}(s)} \tag{3.44}$$

Remark 3.4.2. *It is seen from (3.44) that the zero polynomial is* $n_{cl}(s) = n(s)$*, so the zero locations are unchanged by output feedback.*

Remark 3.4.3. *The pole locations from (3.44) are changed by output feedback. That is, as the feedback gain* k *is increased, the closed loop poles move from open-loop poles to the open-loop zeros, i.e.,*

$$k \to 0 \quad \Rightarrow \quad \text{roots}\{m_{cl}(s)\} = \text{roots}(m(s)\} \tag{3.45}$$

$$k \to \infty \quad \Rightarrow \quad \text{roots}\{m_{cl}(s)\} = \text{roots}\{kn(s)\} \tag{3.46}$$

Therefore, RHP-zeros implies high gain instability.

On the other hand, let us also consider a SISO system with a coprime factorization $P_o(s) = N(s)M^{-1}(s)$ with $N(s) = n(s)/\zeta(s)$ and $M(s) = m(s)/\zeta(s)$ affected by a partial state feedback controller $K(s) = k$ as shown in Figure 3.6. The closed loop response from the reference r to the output y is

$$T(s) = \frac{NM^{-1}}{1 + KM^{-1}} = \frac{n(s)}{m(s) + k\zeta(s)} = \frac{n_{cl}(s)}{m_{cl}(s)} \tag{3.47}$$

Remark 3.4.4. *We can see from (3.47) that the pole locations are still changed by partial state feedback. Nevertheless, as the feedback gain k is increased, the closed loop poles move from open-loop poles to the open-loop nodes of $k\zeta(s)$, i.e.,*

$$k \to 0 \quad \Rightarrow \quad \text{roots}\{m_{cl}(s)\} = \text{roots}\{m(s)\} \tag{3.48}$$

$$k \to \infty \quad \Rightarrow \quad \text{roots}\{m_{cl}(s)\} = \text{roots}\{k\zeta(s)\} \tag{3.49}$$

As long as $\zeta(s)$ is assumed to be any Hurwitz polynomial such that $\deg\zeta(s) = \deg m(s)$*, we conclude that partial state feedback control configuration as that shown in Figure 3.6 avoids RHP-zeros to commit instability.*

Remark 3.4.5. *The fact that partial state feedback control configuration avoids RHP-zeros to cause instability is an important result. In such a way, the methodology used to design the controller $K(s)$ does not have to be constrained with the requirement that the resulting controller $K(s)$ be stable.*

The directions associated with MIMO systems makes more difficult to consider how RHP-zeros in a separately manner, as in the SISO case. It is well-known that a multivariable plant may have a RHP-zero and a RHP-pole at the same location, but their effect may not interact if they are in completely different parts of a system.

3.4.3 Observed partial state feedback

In Section 3.4.1 we dealt with the assumption that the partial state could be directly accessed. Now, such ideal scenario is transformed in order to provide an observation of the partial state.

The somewhat uncommon configuration (Vidyasagar, 1985), (Kailath, 1980) presented in this Section is based on the reconstruction ξ^o of the partial state ξ. The *Observer-Controller* configuration is illustrated in Figure 3.8.

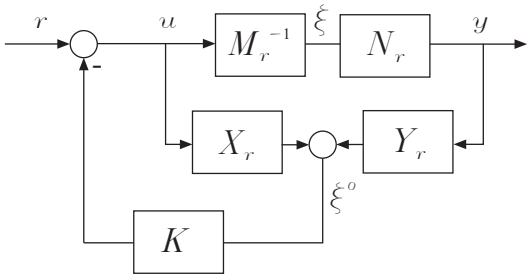

Figure 3.8: The Observer-Controller configuration.

To reconstruct the partial state we make use of the Bezout identity relating the right coprime transfer matrices, $N_r(s)$ and $M_r(s)$,

$$X_r(s)M_r(s) + Y_r(s)N_r(s) = I \tag{3.50}$$

which immediately yields the configuration of Figure 3.8.

We will show that the observer scheme allows the exact reconstruction ξ^o of the partial state if and only if the two components $X_r(s)$ and $Y_r(s)$ satisfy the Bezout identity (3.50). The following relations are got form Figure 3.8:

$$\xi(s) = M_r^{-1}(s)u(s) \ , \qquad y(s) = N_r(s)\xi(s) \tag{3.51}$$

The observed signal ξ^o can be expressed as

$$\xi^o(s) = X_r(s)u(s) + Y_r(s)y(s) \ , \tag{3.52}$$

and, by substituting (3.51) into equation (3.52), we have

$$\xi^o(s) = [X_r(s)M_r(s) + Y_r(s)N_r(s)]\xi(s) \tag{3.53}$$

Hence, as long as the Bezout identity (3.50) holds, it is possible the exact reconstruction of the partial state, $\xi^o = \xi$.

The case in which disturbances affect the control system is illustrated in Figure 3.9. In case of disturbances at the input of the plant, $d_o = 0$, the reconstruction is affected by the perturbation. We have that

$$\xi(s) = M_r^{-1}(s)[u(s) + d_i(s)] \tag{3.54}$$

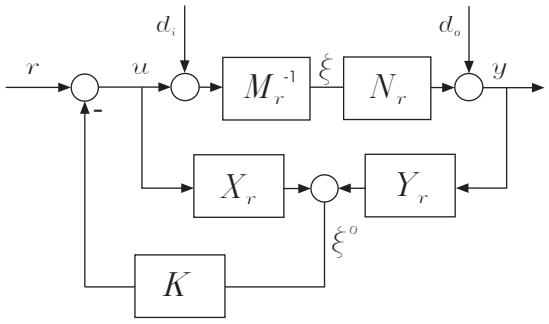

Figure 3.9: The Observer-Controller configuration with external perturbations.

and

$$\xi^o(s) = \xi(s) - X_r(s)d_i(s) \tag{3.55}$$

In case of disturbances affecting at the output of the plant, $d_i = 0$, we have that

$$\xi(s) = N_r^{-1}(s)[y(s) - d_o(s)] \tag{3.56}$$

and

$$\xi^o(s) = \xi(s) + Y_r(s)d_o(s) \tag{3.57}$$

Therefore, the Bezout identity (3.50) allows the exact reconstruction of the partial state, ξ, if no disturbances enter the control system. If disturbances affect the control system, the observed partial state ξ^o is no longer equal to the partial state ξ. This, in principle, unforeseen situation can be used in a constructive manner since the observed partial state ξ includes a measure of the disturbances. With an appropriate feedback of (3.55) and/or (3.57) through the matrix transfer function $K(s)$ the effect that the disturbances cause to the controlled variable can be minimized in some sense.

As it has been shown, the key equation for the reconstruction of the partial state is the Bezout identity (3.50). By application of a Youla type parametrization, it is possible to write the set of observers that gives the partial state ξ as the set of solutions to the Bezout identity. If X_r^* and Y_r^*

are solutions of the Bezout identity and Q is a stable, but otherwise free, parameter, the set

$$\{X_r,\, Y_r \;:\; X_r = X_r^* - N_r Q,\;\; Y_r = Y_r^* + M_r Q\} \tag{3.58}$$

characterizes all linear observers for ξ (Ding *et al.*, 1994). The Q parameter may be selected on the bases of some robustness criterion.

In (Pedret *et al.*, 1999) we dealt with the design of the state feedback compensator $K(s)$ considering reference model specifications. The methodology is presented as a two-step design procedure in which the reference model specifications are tackled first as nominal requirements and second, the robustness properties of the resultant nominal design are enhanced. The reference model specifications are achieved by means of an appropriate selection of the partial state feedback controller $K(s)$. The robustness considerations are taken into account by performing a Youla type parameterization of all solutions of the Bezout identity as that in the set (3.58).

3.5 Summary

In this Chapter we have presented the coprime factorization framework for multivariable linear systems. The condition for internal stability in terms of the plant and the controller factors has been given and it is been shown how every plant has associated a stabilizing controller determined by the components of a *Bezout* equation that provides coprime plant factors. State-space realizations for the coprime factorization of a given system have been obtained.

Within the right coprime factorization approach, the Observer-Controller configuration has been introduced. We have seen that this control configuration avoids one of the inherent control problem caused by RHP-zeros, i.e., the structure prevent the system to be unstable with high gain feedback control. Such control configuration will constitute the basis for all the control structures designed in this work.

Chapter 4

The Observer-Controller configuration for Robustness Enhancement

In this Chapter we present a new approach to improve the robustness properties of a nominal control system. It can be seen as an alternative to the design of robust controllers. The method is based on the generation of a complement for a nominal control system by means of an Observer-Controller structure. The resulting two-step design procedure allows an enhancement of the robustness properties without modifying the nominal controller. The design procedure is systematized by a translation into the $\mathcal{H}_\infty$ / Structured Singular Value framework and evaluated on a high purity distillation column example.

4.1 Introduction

The design of robust controllers has been one of the great deals of Linear Control Theory over the last decades. Some, now well established, approaches have been developed: (Ackerman, 1993), (Grimble, 1994), (Green and Limebeer, 1995), (Zhou *et al.*, 1996), among others. A common feature of most of the advanced robust control algorithms is that of setting an optimization problem posed in terms of the uncertainty description. This optimization problem is usually solved in terms of the *Youla*-parameter

(Vidyasagar, 1985), (Boyd and Barratt, 1991). The problem with that kind of approaches is that of mixing the performance measures for the nominal controller and the robustness properties in the overall design process.

A different approach is that of the Internal Model Control (IMC) (Morari and Zafirou, 1989). This approach is based on computing an optimal controller, the IMC controller, as the first stage of the design. In the second stage of the design procedure, the IMC controller is detuned to cope with robustness. This approach has the advantage that complete different measures can be used for both nominal performance properties and the robustness characteristics.

Some other works that could be considered to deal with the robustness enhancement problem appeared in the literature as explicitly two-step design approaches: (Hrissagis *et al.*, 1996), (Hrissagis and Crisalle, 1997), (Ansay and Wertz, 1997). Such approaches consist on an enhancement of the robustness properties of the initial controller at the second step of the design procedure. The robustness enhancement problem proceeds as follows:

1) The initial controller is reformulated as the central controller in the Youla parametrisation of the stabilizing controllers from a nominal plant.

2) An optimization problem is performed for the Youla parameter to get the final, *robustified*, controller

The approach presented in (Ansay and Wertz, 1997) uses a special form of the Youla parameterization. This special form of the Youla parametrization allows to get all controllers yielding the same closed-loop characteristic polynomial provided by an initial controller. The initial controller is a Generalized Predictive Controller (Clarke *et al.*, 1987). The problem with this approach is that the extension to the unstable plant case is not straightforward as it can be seen in (Ansay *et al.*, 1998). Also, the extension to the multivariable plant case looks difficult.

The extension to the unstable plant case is not a problem with the approach presented in (Hrissagis *et al.*, 1996) and (Hrissagis and Crisalle, 1997). In such cases, a complete Youla parametrization is used and the general problem is posed as an optimization problem with respect to the Youla parameter and some norm that depends on the specifications. However, all the referred approaches for robustness enhancement lies on the polynomial description of

the plant and the controller. Therefore, the generalization to multivariable systems is difficult.

In (Vilanova *et al.*, 1999) we suggested a way of using the Observer-Controller structure that overcomes the above mentioned difficulties. The approach is not based on setting the controller to be robustified as the central controller of the stabilizing controller family. Instead,

1) An initial feedback control system is set for the nominal plant to satisfy some step response requirements[1].

2) The resulting robustness properties are conveniently enhanced while leaving unaltered the step responses provided by the initial controller.

The approach is based on the generation of a complement for the nominal control system by means of the Observer-Controller configuration. That is, a correcting control action to the initial feedback loop that compensates the presence of uncertainty not, necessarily, considered by the initial controller. Within this approach, the structure of the initial controller is not taken into account and the resulting control configuration does not modify the initial controller. This constitutes the main difference, and advantage, with respect to the above referred approaches.

The Observer-Controller configuration approach to enhance the robustness properties of an initial controller allows an unified treatment for both stable and unstable systems. The approach was successfully applied to the control of the temperature in an open-loop unstable batch chemical reactor (Pedret *et al.*, 2001).

The approach can also be seen to lie in the two degrees-of-freedom control configuration in the sense that a complete separation of properties is achieved: in the first stage of the design, step responses of the nominal system are attained by a controller set up to satisfy the requirements in an "optimal" manner; in the second stage, model uncertainties are considered and the robustness properties given by the nominal control system are enhanced.

The Chapter is organized as follows: Section 4.2 introduces the feedback control system and presents the proposal to design a feedback controller just for the nominal plant. Section 4.3 gives what we call *Robustness Enhancement Block* to allow robust stability to be guaranteed. In Section 4.4.1,

[1] This fact does not imply any restriction on the structure of the initial controller.

the Robustness Enhancement Block is designed in a systematic way by a translation into the $\mathcal{H}_\infty$ / Structured Singular Value framework. Finally, the proposed configuration is evaluated on a high purity distillation column example, in Section 4.5

4.2 Problem description

Let us consider the feedback control system shown in Figure 4.1 in which P_o is the model of the plant P and K_1 is the nominal feedback controller.

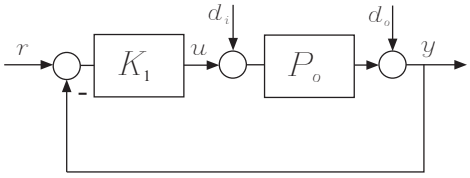

Figure 4.1: Nominal feedback control system.

From the scheme in Figure 4.1, the transfer matrix function that relates the input signals and the output signals, $[u\, y]^T$, is:

$$\begin{bmatrix} u \\ y \end{bmatrix} = \begin{bmatrix} -T_o & -S_oK_1 & S_oK_1 \\ S_oP_o & S_o & T_o \end{bmatrix} \begin{bmatrix} d_i \\ d_o \\ r \end{bmatrix} \tag{4.1}$$

where

$$S_o = (I + P_oK_1)^{-1} \tag{4.2}$$

and

$$T_o = (I + P_oK_1)^{-1}P_oK_1 \tag{4.3}$$

are the output sensitivity transfer function and the complementary sensitivity transfer function, respectively.

The feedback controller K_1 can be designed such that, when applied to the nominal plant P_o, provides desired specifications, e.g., design in terms of reference tracking and/or disturbance rejection. In practice, the knowledge

of the model uncertainty must be incorporated into the controller design procedure. Otherwise the controller K_1 designed just for the nominal plant P_o is bound to fail when it is faced with the real plant $P \in \mathcal{P}$. In fact, we must demand the control system to provide, at least, closed-loop stability with all the plants in the set $\mathcal{P}$, i.e., robust stability. The requirement that the performance achieved with the nominal plant P_o be met for all the plants in $\mathcal{P}$, i.e., robust performance, could be considered as the ultimate goal for the controller design. In some cases, it may be desirable simply to design a controller for the plant model P_o to satisfy certain nominal performance specifications and only guaranteeing robust stability. This may occur in cases such as plants operating most of the time close to its nominal operating point, with occasional plant perturbations. So, performance may not be of primary importance when perturbations occur provided that the system remains stable.

The presented approach proposes to deal with the design of the feedback controller K_1 just for step response requirements with the nominal plant P_o. This controller can be designed by any technique from feedback control theory. For instance, a PID control law could be a suitable choice for some systems. Also, an $\mathcal{H}_\infty$ weighted model reference optimization problem of the form,

$$\|W_p(T_{ref} - T_o)\|_\infty \tag{4.4}$$

could be solved, where T_{ref} if the reference model which specifies the desired closed-loop step responses. Since the system response to commands is an open-loop property (Safonov *et al.*, 1981), no stability margins are necessarily guaranteed when the desired closed-loop behaviour is achieved. Therefore, the Observer-Controller structure can be used to incorporate a second degree of freedom to enhance the robustness properties provided by the nominal control system. Next Section presents the Observer-Controller configuration.

4.3 Configuration for robustness enhancement

Let us assume that the feedback controller K_1 has been given or previously designed just to provide the desired step response requirements with the nominal plant, P_o. The controller set up with the latter assumptions could give rise to poor stability margins: since the it has been designed just for

the nominal step response requirements no stability margins are necessarily guaranteed.

The Observer-Controller configuration detailed in Section 3.4 is used in such a way that a second degree of freedom is offered. This extra degree of freedom can be utilized to consider the, possibly, lack of robustness provided by the nominal controller K_1. The proposed method is based on the generation of a complement, δu, to the nominal feedback control system. This is carried out by means of what we call a *Robustness Enhancement Block*. The resulting overall control system is shown in Figure 4.2.

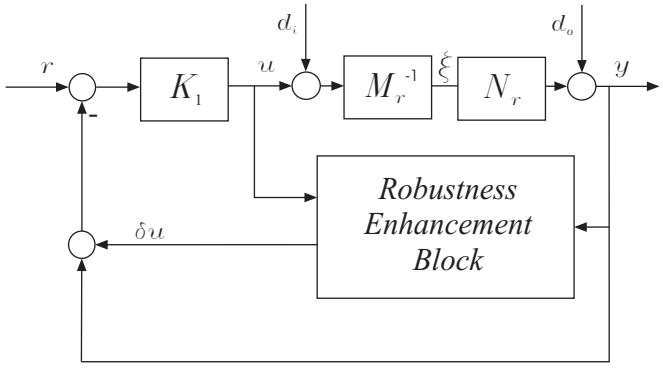

Figure 4.2: Overall control configuration for robustness enhancement.

The Robustness Enhancement Block is added to the nominal feedback control system shown in Figure 4.1. Such structure is based on the fractional representation framework addressed in Chapter 3. Within that formulation, we know that a a right coprime factorization of a matrix transfer function P_o reads as

$$P_o = N_r M_r^{-1} \tag{4.5}$$

where N_r and M_r^{-1} are said to be right coprime over $\mathcal{RH}_\infty$ if they have the same number of columns and if there exist stable matrices X_r and Y_r satisfying the Bezout identity

$$X_r M_r + Y_r N_r = I \tag{4.6}$$

Figure 4.2 shows the so-called partial state ξ, i.e., the fictitious signal that appears after the factorization of P_o. The key idea of the Robustness Enhancement Block is the use of such an artificial signal, ξ, as the control variable. Now, it is possible to write

$$y = N_r\xi + d_o, \;\; u = M_r\xi - d_i \tag{4.7}$$

The above definitions are useful to present the feedback interconnection we will work with. It is based on the reconstruction of the partial state, ξ. Equations (4.6) and (4.7) show immediately how to recover the partial state:

$$\begin{aligned} \xi^o &= X_r u + Y_r y = & (4.8)\\ &= (X_r M_r + Y_r N_r)\xi - X_r d_i + Y_r d_o & (4.9) \end{aligned}$$

As long as the two observer transfer matrix functions X_r, Y_r, make the Bezout identity (4.6) to be satisfied, the scheme allows the reconstruction, i.e.,

$$\xi^o = \xi - X_r d_i + Y_r d_o \tag{4.10}$$

The reconstructed signal ξ^o in (4.10) incorporates a measure of the disturbance signals that can affect the plant, P_o. Therefore, it can serve in the specific function of compensating the possibly poor robustness bounds of the nominal feedback control scheme in Figure 4.1.

In Section 3.4 we saw that the observed partial state, ξ^o, could be feedback through and arbitrary transfer function to constitute a state feedback controller. The design of this transfer function for the SISO case and based on model reference specifications was presented in (Pedret *et al.*, 1999).

Now, the estimated partial state, ξ^o, is used to compute an estimation of the output signals. Figure 4.3 reveals what is inside the Robustness Enhancement Block.

The estimated output signal, $N_r\xi^o$, is used to generate a residues[1] signal, $\chi = N_r\xi^o - y$, which is feed back through a transfer matrix function K_2 to

[1] In absence of uncertainty and disturbances the value of χ is zero. Therefore, χ is called the residues signals

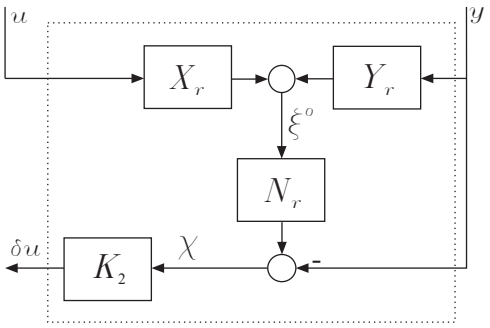

Figure 4.3: Detail of the Robustness Enhancement Block.

complement the nominal control system. This provides an IMC-*like* control scheme (Morari and Zafirou, 1989): the inner loop is closed *only when necessary* by a correcting control action δu.

It should be noted that, under a nominal situation, i.e., $P = P_o$ and also $d = 0$, the residues signal, χ, is zero and the performance is that of the nominal controller K_1. In a more realistic situation, i.e. $P \neq P_o$ and possibly $d \neq 0$, the residues signal, χ, through the matrix transfer function K_2, complements the nominal feedback control system in order to prevent unmodelled dynamics and disturbances from altering the behaviour provided by the nominal controller K_1.

From the control schemes in Figure 4.2 and Figure 4.3 we can compute the new relations between the input signals and the output signals,

$$\begin{bmatrix} u \\ y \end{bmatrix} = \begin{bmatrix} -T_o(I + P_o^{-1}K_2N_rX_r) & -S_oK_1(I + K_2(I - N_rY_r)) & S_oK_1 \\ S_oP_o(I - K_1K_2N_rX_r) & S_o(I - P_oK_1K_2(I - N_rY_r)) & T_o \end{bmatrix} \begin{bmatrix} d_i \\ d_o \\ r \end{bmatrix} \tag{4.11}$$

where S_o is the nominal output sensitivity (4.2) and T_o is the nominal complementary sensitivity (4.3).

It should be noted from the new input/output relations (4.11) that the inclusion of the Robustness Enhancement Block alters the nominal input/output relations (4.1). Nevertheless, such modifications only affects the transfer matrix functions from the disturbances signals, $[d_i\ d_o]^T$, to the outputs. The relations form the reference signals, r, remain unaltered. Such modifications to the nominal relations from the disturbances are likely to

be of benefit with an appropriate design of the free, stable, transfer matrix function K_2. This is done in next Section.

4.4 Design for robustness enhancement

We have seen how the Robustness Enhancement Block modifies the nominal transfer matrix functions from the disturbances, $[d_i\ d_o]^T$, while leaving the relations from the references, r, unaltered. As it is known (see Section 2.3 for details), Robust Stability impose bounds on the frequency response of the transfer matrix functions from the disturbance signals, $[d_i\ d_o]^T$, e.g., a multiplicative input uncertainty description bounds the frequency response of the transfer matrix function from d_i to u. This property is to be used to perform a two-step design procedure. First, the nominal controller K_1 is designed just for the nominal plant P_o to provide the desired step responses. Then, in a second stage, the controller K_2 is designed to guarantee closed-loop stability for all possible plant P in the set $\mathcal{P}$ to guarantee the performance in terms of disturbances for all $P \in \mathcal{P}$.

Let us assume, without lost of generality, that multiplicative input uncertainty is considered. In such an uncertainty description, the plant P is unknown but belonging to a set of plants, $\mathcal{P}$, built around a nominal model P_o,

$$\mathcal{P} = \{P : P = P_o(I + W_2 \Delta W_1)\}\,,\ \ \bar{\sigma}(\Delta) \leq 1\ \forall\omega \tag{4.12}$$

where $W_1 = w_I I$, $W_2 = I$.

The uncertainty description assumed above allows us to redraw the control configuration for robustness enhancement. Figure 4.4 shows the overall weighted control scheme.

From the overall control scheme in Figure 4.4 we can compute the transfer matrix function $\mathcal{N}$ that relates the input signals, $[d_i\ d_o\ r]^T$, and the weighted output signals, $[u'\ y']^T$,

$$\mathcal{N} = \begin{bmatrix} -W_1 T_o (I + P_o^{-1} K_2 N_r X_r) & -W_1 S_o K_1 (I + K_2 (I - N_r Y_r)) & S_o K_1 \\ W_p S_o P_o (I - K_1 K_2 N_r X_r) & W_p S_o (I - P_o K_1 K_2 (I - N_r Y_r)) & T_o \end{bmatrix} \tag{4.13}$$

where S_o is the nominal output sensitivity (4.2) and T_o is the nominal complementary sensitivity (4.3).

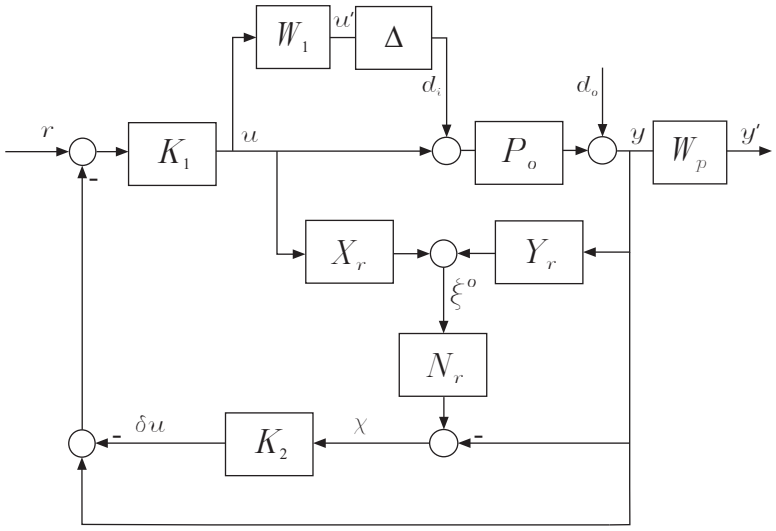

Figure 4.4: Overall control configuration for robustness enhancement.

4.4.1 Design for robust stability

Considering unstructured uncertainty, e.g., Δ is a full complex matrix of appropriate dimensions, Theorem 2.3.1 imposes a condition on the ∞-norm of the transfer matrix function from the input disturbance, d_i, to the weighted control signal, u', i.e., $\mathcal{N}_{11} \doteq \mathcal{M}$, in order for robust stability to be guaranteed. From (4.13) we have that

$$\|\mathcal{M}\|_\infty = \left\|-W_1 T_o (I + P_o^{-1} K_2 N_r X_r)\right\|_\infty \tag{4.14}$$

Therefore, from (4.14) and condition (2.23) we have,

$$\left\|-W_1 T_o (I + P_o^{-1} K_2 N_r X_r)\right\|_\infty < 1 \tag{4.15}$$

The left hand side of (4.15) can be seen as formed by two terms: the first one, $-W_1 T_o$, determines the robustness margins with the nominal feedback control system; the second one, $(I + P_o^{-1} K_2 N_r X_r)$, includes the free stable transfer matrix K_2. If the nominal feedback controller K_1 does not provide robust stability, i.e., $\bar{\sigma}(T_o) \geq |W_1|^{-1}$, the controller K_2 is designed to force the second term, $(I + P_o^{-1} K_2 N_r X_r)$, to supply the extra compensation needed in order to carry out with constraint (4.15).

The design procedure could be based on compelling the second term in the robust stability condition (4.15), to match a desired shape, i.e.,

$$I + P_o^{-1} K_2 N_r X_r \approx F \tag{4.16}$$

where F is a low-pass filter of fixed structure. This approach was successfully applied to the control of the temperature in an open-loop unstable batch chemical reactor (Pedret *et al.*, 2001).

The Structured Singular Value allows, as we saw in Section 2.3, to derive necessary and sufficient, non-conservative, conditions for robust stability. Within this framework, uncertainty is modeled in terms of norm-bounded perturbations on the nominal system and weighting matrices are used such that each perturbation is normalized to have magnitude one,

$$\bar{\sigma}(\Delta_i) \leq 1, \forall \omega \tag{4.17}$$

The individual uncertainties Δ_i are combined into one large block diagonal perturbation matrix

$$\Delta = \text{diag}\{\Delta_1, ..., \Delta_n\}, \ \bar{\sigma}(\Delta) \leq 1, \ \forall \omega \tag{4.18}$$

and the system is arranged to fit in the general control problem formulation (see Section 2.2) as it is shown in Figure 4.5.

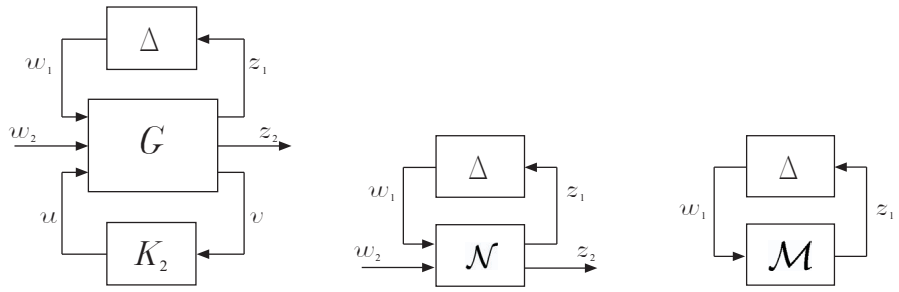

(a) (b) (c)

Figure 4.5: General interconnection of system with uncertainty.

For our approach, the interconnection matrix G in Figure 4.5(a) is a function of the nominal plant model $P_o = N_r M_r^{-1}$, the controller K_1, the right coprime factors, X_r, Y_r, the uncertainty weights W_1, W_2 and the performance weight W_p. We have that $w_1 = d_i$, $w_2 = [d_o \; r]^T$, $z_1 = u'$, $z_2 = y'$ and $v = \chi$. The augmented plant G and the controller K_2 are related by the following lower linear fractional transformation:

$$\mathcal{F}_\ell(G, K_2) \doteq G_{11} + G_{12}K_2(I - G_{22}K_2)^{-1}G_{21} \tag{4.19}$$

The lower LFT (4.19) is represented in Figure 4.5(b) by the matrix transfer function $\mathcal{N}$, in which the diagonal matrix Δ maps the signals z_1 and w_1 closing the upper loop around $\mathcal{M}$. It results in the following upper linear fractional transformation:

$$\mathcal{F}_u(\mathcal{N}, \Delta) \doteq \mathcal{N}_{22} + \mathcal{N}_{21}\Delta(I - \mathcal{N}_{11}\Delta)^{-1}\mathcal{N}_{12} \tag{4.20}$$

In order to check the stability of the closed loop structure in Figure 4.5(a), the Structured Singular Value, μ, pursues the tightest possible bound on $\mathcal{M}$ such that $\det(I - \mathcal{M}\Delta) \neq 0$. The problem is to find the smallest structured Δ, measured in terms of $\bar{\sigma}(\Delta)$, which makes $\det(I - \mathcal{M}\Delta)$ singular. Then, $\mu(\mathcal{M}) = 1/\bar{\sigma}(\Delta)$. Definition 2.3.5 of $\mu(\mathcal{M})$ is adopted from (Doyle, 1982).

It should be noted that the structured singular value, μ, depends on the matrix $\mathcal{M}$ and the structure of the perturbation Δ, therefore the notation $\mu_\Delta(\mathcal{M})$. For the unstructured uncertainty case, i.e., Δ is a full matrix, the smallest Δ which yields singularity has $\bar{\sigma}(\mathcal{M}) = 1/\bar{\sigma}(\Delta)$. For the structured uncertainty case we have $\mu(\mathcal{M}) = 1/\bar{\sigma}(\Delta)$.

Theorem 2.3.2 provides a necessary and sufficient condition for robust stability. Nevertheless, Definition 2.3.5 is not itself useful for computing $\mu_\Delta(\mathcal{M})$ and, currently, no simple computational method exists for exactly calculating μ in general and an efficient exact method is most likely not possible (Braatz *et al.*, 1994). This motivated to approximate $\mu_\Delta(\mathcal{M})$ by computing the upper bound,

$$\mu_\Delta(\mathcal{M}) \leq \inf_{D_\ell,\, D_r \,\in\, \mathcal{D}} \bar{\sigma}(D_\ell \mathcal{M} D_r^{-1}) \tag{4.21}$$

where D_ℓ and D_r are non-negative scaling matrices defined within a set $\mathcal{D}$ that commutes with the structure Δ.

We have seen that the structured singular value provides a systematic way to test for robust stability (2.25) for a given controller K_2. We will see next how to synthesize a controller K_2 for Robust Stability.

Controller synthesis: $\mathcal{H}_\infty$ controller K_2

To cope with robust stability, an $\mathcal{H}_\infty$ controller K_2 can be easily computed by means of the following optimization problem.

$$\min_{K_2} \sup_{\omega} \bar{\sigma}(\mathcal{M}) \tag{4.22}$$

The minimization problem (4.22) can be solved by using standard algorithms (Balas *et al.*, 1998), (Chiang and Safonov, 1992).

Therefore, a feedback controller K_1 can be designed to cope with nominal tracking performance and then, robust stability is assured by the Robustness Enhancement Block with an $\mathcal{H}_\infty$ controller K_2.

4.4.2 Design for robust performance

In the nominal feedback controller K_1, without the Robustness Enhancement Block, performance in terms of disturbance rejection is linked with performance in terms of tracking by the identity $T_o + S_o = I$. In such a way, a design for disturbance rejection specifications considers, indirectly, a design for tracking properties. On the other hand, the inclusion of the Robustness Enhancement Block breaks such identity, i.e.,

$$T_o + S_o(I - P_o K_1 K_2 (I - N_r Y_r)) \neq I \tag{4.23}$$

Therefore, with the proposed robustness enhancement structure we must specify that the design for performance is done in terms of disturbance rejection, i.e.,

$$\|W_p S_o (I - P_o K_1 K_2 (I - N_r Y_r)\|_\infty < 1 \tag{4.24}$$

The performance condition (4.24) can be checked, for all the set of plants $P \in \mathcal{P}$, by utilizing a RP test on the transfer matrix function $\mathcal{N}$ shown in Figure 4.6.

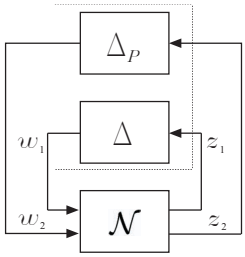

Figure 4.6: Block diagram for testing robust performance

Theorem 2.3.3 provides a test for robust performance computed with respect to an augmented uncertainty structure of the perturbation matrix $\mathbf{\Delta} = \text{diag}\{\Delta, \Delta_p\}$. The performance block Δ_p is a full square complex perturbation with appropriate dimension (see Section 2.3 for details).

Remark 4.4.1. *The robust performance condition (2.29) implies robust stability (2.25), since*

$$\sup_{\omega} \mu_{\mathbf{\Delta}}(\mathcal{N}) \geq \sup_{\omega} \mu_{\Delta}(\mathcal{M}) \tag{4.25}$$

As it is known from the robust stability analysis, Definition 2.3.5 is not itself useful for computing $\mu_{\Delta}(\mathcal{N})$ and this fact motivates to approximate $\mu_{\Delta}(\mathcal{N})$ by computing upper and lower bounds. This gives rise to the computation of the following upper bound:

$$\mu_{\Delta}(\mathcal{N}) \leq \inf_{D_\ell,\, D_r \in \mathcal{D}} \bar{\sigma}(D_\ell \mathcal{N} D_r^{-1}) \tag{4.26}$$

As well as for the computation of the robust stability bound in (4.21), the robust performance bound is also convex in D (Packard and Doyle, 1993).

We have seen that the structured singular value provides a systematic way to test for robust stability and also for robust performance in terms of disturbance rejection for a given controller K_2. In addition to the analysis tool, the structured singular value can be used to synthesize a μ-"optimal" controller K_2.

Controller synthesis: μ-"optimal" controller K_2

A μ-"optimal" controller K_2 can be designed within the structured singular value framework to cope with robust performance in terms of disturbance

rejection and, at the same time, as is is stated by Remark 4.4.1, designed for robust stability. Therefore, a μ-"optimal" controller K_2 can be found by minimizing

$$\sup_{\omega} \mu_{\Delta}(\mathcal{N}) \tag{4.27}$$

It is known that, at the present moment, there is no direct method to find the controller K_2 by minimizing (4.27). However, in Section 2.4 we dealt with the procedure known as DK-iteration (also called μ synthesis) (Zhou *et al.*, 1996). Is an ad-hoc method that attempts to minimize the upper bound (4.21) of μ and, thus, the objective function (4.27) is transformed into

$$\min_{K_2} \inf_{D_\ell,\, D_r \in \mathcal{D}} \sup_{\omega} \bar{\sigma}(D_\ell \mathcal{N} D_r^{-1}) \tag{4.28}$$

The DK-iteration approach involves to alternatively minimize

$$\sup_{\omega} \bar{\sigma}(D_\ell \mathcal{N} D_r^{-1}) \tag{4.29}$$

for either K_2 or D_ℓ and D_r while holding the other constant. For fixed D_ℓ and D_r, the controller is solved via $\mathcal{H}_\infty$ optimization; for fixed K_2, a convex optimization problem is solved at each frequency. The magnitude of each element of $D_\ell(j\omega)$ and $D_r(j\omega)$ is fitted with an stable and minimum phase transfer function and wrapped back into the nominal interconnection structure.

The procedure is carried out until $\sup_\omega \bar{\sigma}(D_\ell \mathcal{M} D_r^{-1}) < 1$. The DK-iteration approach is explained in more detail in Section 2.4.

The optimal solutions in each step are of supreme importance to success with the DK-iteration. Moreover, when K_2 is fixed, the fitting procedure plays an important role in the overall approach. Low order transfer function fits are preferable since the order of the $\mathcal{H}_\infty$ problem in the following step is reduced yielding controllers of lower dimension. Nevertheless, the method is characterized by giving controllers of very high order that must be reduced applying model reduction techniques (Glover, 1984).

4.4.3 Design outline

Here, we briefly describe the important points in the design procedure.

1. **Design of K_1:** Design a feedback controller K_1 to achieve tracking specifications for the nominal model of the plant, P_o.

2. **Uncertainty description:** Assume that the plant P to be controlled is unknown but belonging to a set of plants $\mathcal{P}$ build around the nominal model P_o, as in (4.12).

3. **Coprime Factorization:** Find a right coprime factorization of the nominal model of the plant, $P_o = M_r^{-1}N_r$. This gives rise to the associated Bezout components X_r and Y_r.

4. **Design of K_2:** Rearrange the scheme in Figure 4.4 to fit the general interconnection with uncertainty shown in Figures 4.5(a) and 4.6. Solve the optimization problem (4.22) to find a $\mathcal{H}_\infty$ controller K_2. Solve the optimization problem (4.28) to find a μ-"optimal" controller K_2.

5. **Implementation:** Implement the controller scheme shown in Figure 4.4 with the nominal feedback controller K_1 and the elements of the Robustness Enhancement Block, X_r, Y_r, N_r and the controller K_2.

We next present an example to illustrate the above design procedure.

4.5 Application example

The proposed approach is applied to the control of a high purity distillation system to illustrate the design procedure. The original control problem was formulated by (Skogestad *et al.*, 1988) as a bound on the weighted sensitivity with frequency bounded input uncertainty. The optimal solution to this problem was provided by (Skogestad *et al.*, 1988) considering a one degree-of-freedom $\mu-$optimal controller like that discussed in Example 2.4.1 and denoted K_{opt} — the state-space realization of K_{opt} is given in Table C.1. Nevertheless, our aim is not to design a robust control system but to show how the Observer-Controller configuration can be used to enhance the robustness properties of a controller, K_1, designed just for the nominal model of the plant, P_o, and to compare the performance of the resulting control configuration with that of the μ-"optimal" controller, K_{opt}.

The following is an idealized dynamic model of the distillation column (See Appendix B.2 for more details),

$$P_o = \frac{1}{75s+1}\begin{bmatrix} 87.8 & -86.4 \\ 108.2 & -109.6 \end{bmatrix} \tag{4.30}$$

A complex multiplicative uncertainty is assumed in each manipulated input of magnitude

$$W_1 = 0.2\frac{5s+1}{0.5s+1}I_2 \tag{4.31}$$

This implies a relative uncertainty up to 20% in the low frequency range which increases at high frequencies, reaching a value of 1 at about 1 Rad/min. The increase with frequency allows for various neglected dynamics associated with the actuator and the valve.

The nominal performance specification is stated by the weight

$$W_p = 0.5\frac{10s+1}{10s}I_2 \tag{4.32}$$

which implies integral action and allows an amplification of disturbances at high frequencies by a factor of two at most.

4.5.1 Design of the nominal controller

The nominal controller, K_1, is chosen as a simple diagonal (decentralized) feedback control system with two PI controllers,

$$K_1 = k\frac{75s+1}{s}\begin{bmatrix} 1 & 0 \\ 0 & -1 \end{bmatrix}, \quad k = 0.040 \tag{4.33}$$

In Example 2.3.2 we studied this controller with $k = 0.024$ for distillation process. The nominal performance specification of the original control problem is not fulfilled with K_1, i.e., $\bar{\sigma}(S_o) > |W_p|^{-1}$. As it is seen in Figure 2.10, the μ-plots with such PI controller reflects that neither NP nor RS are satisfied. As it is expected, RP is not fulfilled either.

In fact, no choice of k is able to satisfy both requirements (Skogestad *et al.*, 1988). Nevertheless, with the proposed robustness enhancement procedure, we can perform a two-step design to account for nominal performance and, in a second stage, to cope with robustness requirements.

With the concern of choosing the nominal controller just for nominal tracking performance, we chose the diagonal PI (4.33) with $k = 0.040$. This controller results in a nominally stable system and provides a nominal closed-loop step response *similar* to that of the $\mu-$optimal controller shown in Figure 2.15 in solid line. The nominal performance specification of the original control problem is fulfilled with K_1, i.e., $\bar{\sigma}(S_o) < |W_p|^{-1}$, as is is shown in Figure 4.7.

Since the knowledge of the model uncertainty has not been taken into account to design K_1, stability margins are not, necessarily, guaranteed. This can be tested from the transfer matrix function that relates d_i with the weighed control signal, u', i.e., $W_1 T_o$. From Theorem 2.3.2, we can write that robust stability is guaranteed iff $\bar{\sigma}(T_o) < |W_1|^{-1}$, $\forall\omega$. This condition is shown graphically in Figure 4.8 and is seen not to be satisfied for all frequencies.

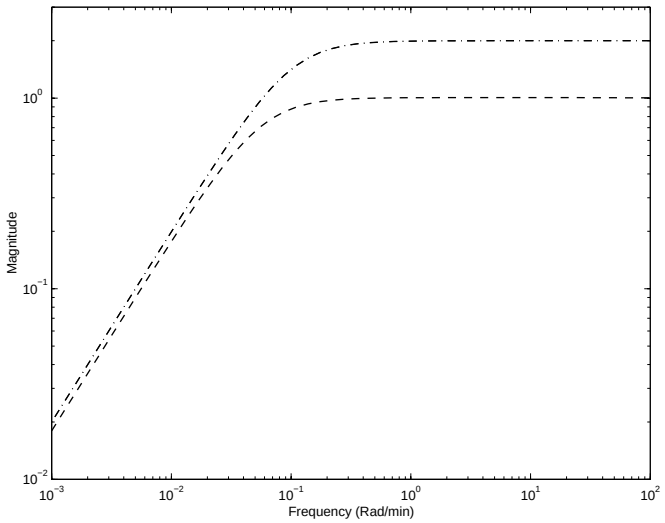

Figure 4.7: Nominal Performance bound for K_1, $\bar{\sigma}(S_o)$ (dashed). $|W_p|^{-1}$ (dash-dotted).

Figure 4.8 tells us that the system would be unstable for some plants in the set $\mathcal{P}$. Therefore, the nominal feedback controller K_1 does not provide robust stability.

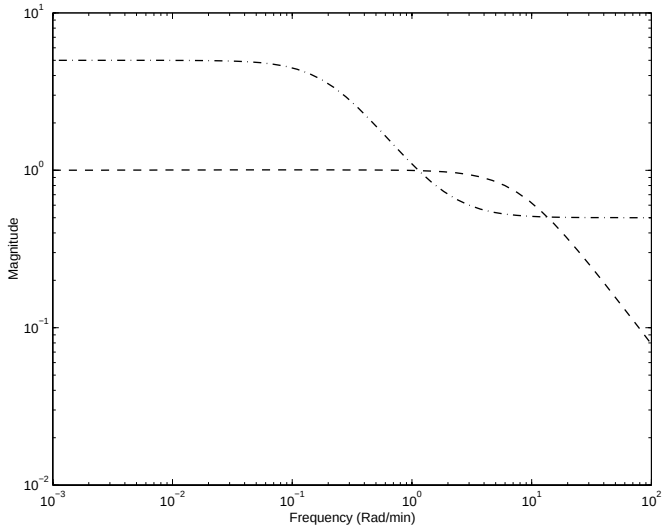

Figure 4.8: Robust Stability bound with K_1, $\bar{\sigma}(T_o)$ (dashed). $|W_1|^{-1}$ (dash-dotted).

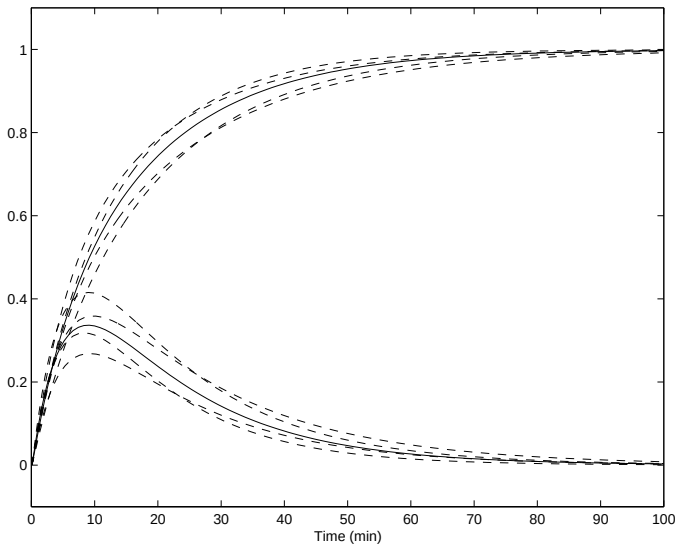

Figure 4.9: Stable closed-loop setpoint responses for K_1. Nominal plant (solid) and uncertain plants $P_i(s)$, $i = 1, \ldots, 4$ (dashed).

We have performed the first stage of the Observer-Controller configuration approach to robustness enhancement. A controller K_1 has been designed just for nominal tracking performance without regards of model uncertainty. Effectively, stability for the set of plants $\mathcal{P}$ is not guaranteed since it has not explicitly considered in the design procedure. Step response simulations for the nominal controller K_1 in (4.33) with the six perturbed plants $P_i(s) = P_o(s)E_{I_i}(s)$, with $E_{I_i} = I + W_1\Delta$ given in Equations (B.11) and (B.12), shows that the stability is fulfilled with $P_i(s)$, $i = 1, \ldots, 4$. On the contrary, the perturbed plants $P_i(s)$, $i = 5, \ldots, 6$ are no longer stabilized by K_1.

The time responses of y_1 and y_2 to a filtered setpoint change in y_1, $r_1 = 1/(5s + 1)$, are shown in Figure 4.9. The solid line represents the response for the controller K_1 with the nominal plant. The dashed lines represent the responses with the controller K_1 with the four perturbed plants $P_i(s)$, $i = 1, \ldots, 4$. The unstable responses for $P_i(s)$, $i = 5, \ldots, 6$ are not shown.

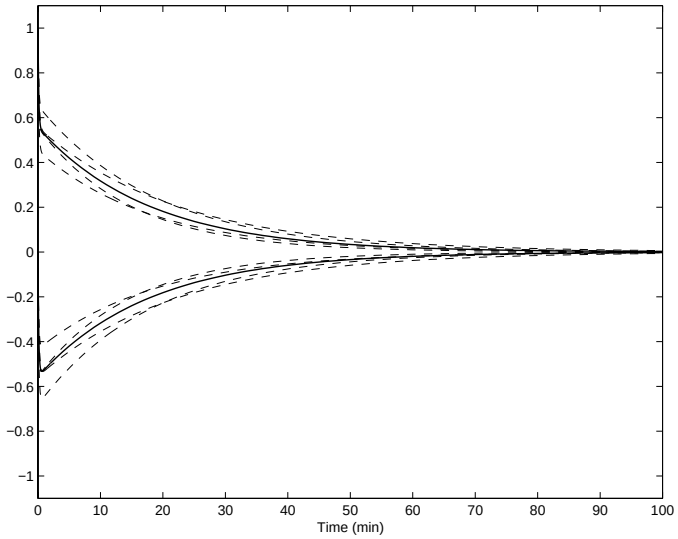

Figure 4.10: Closed-loop response to output disturbance for K_1. Nominal plant (solid) and uncertain plants $P_i(s)$, $i = 1, \ldots, 4$ (dashed).

Figure 4.10 shows the closed-loop response to output disturbance for K_1. Solid lines represent the disturbance rejection for the nominal plant

and dashed lines represent the disturbance rejection for the uncertain plants $P_i(s)$, $i = 1, \ldots, 4$. It can be shown that the perturbed plants offer a disturbance response very closed to that of the nominal plant. Nevertheless, we know that the stability for the set of plant $P_i(s), i = 1, \ldots, 6, \in \mathcal{P}$ with the nominal controller K_1 is not guaranteed. It is evidenced by means of the unstable responses for $P_i(s)$, $i = 5, \ldots, 6$, which are not shown.

We have seen that the nominal controller K_1 provides nominal performance but the requirement of robust stability is not satisfied. Then, the second stage of the design procedure is used next to extend the stability to the set of plants $\mathcal{P}$ while leaving the nominal tracking performance unaltered.

4.5.2 Design of the Robustness Enhancement Block

Recalling equation (4.13) we know that the Robustness Enhancement Block provides an extra term to the transfer matrix function from d_i to the weighted control signal, u', i.e., $I + P_o^{-1}K_2N_rX_r$. This term is to be designed to add the extra compensation needed to guarantee robust stability. First, we will design K_2 as an $\mathcal{H}_\infty$ controller. Second, we will design K_2 as a μ-"optimal" controller.

Design of K_2 as an $\mathcal{H}_\infty$ controller.

Given a right coprime factorization $P_o = N_rM_r^{-1}$, the nominal controller designed in the first stage, say K_1 in (4.33), the right coprime factors, X_r, Y_r, the uncertainty weight W_1 and the performance weight W_p, it is possible to find an $\mathcal{H}_\infty$ controller K_2 by solving the optimization problem (4.28) in one step.

Solving the optimization problem (4.22) an $\mathcal{H}_\infty$ controller K_2 with 14 states is obtained. A balanced realization and an optimal Hankel norm approximation of order 10 on the state-space of K_2 provides an equivalent, reduced, controller K_2. Figure 4.11 shows, in solid line, the singular values Bode plot for the 14th state controller K_2 and its 10th states Hankel norm approximated controller in crosses. A state-space realization of the $\mathcal{H}_\infty$ controller $K_2(s) = C(sI - A)B^{-1} + D$ is given in Table C.2.

With the achieved $\mathcal{H}_\infty$ controller K_2, robust stability is guaranteed since $\bar{\sigma}(T_o(I + P_o^{-1}K_2N_rX_r)) < |W_1|^{-1}$. This condition is shown graphically in Figure 4.12 with solid line and it is seen to be satisfied for all frequencies.

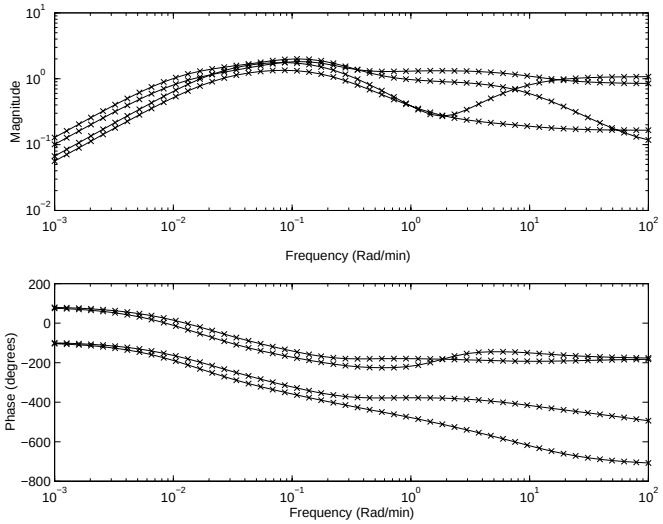

Figure 4.11: Frequency Bode plot for the $\mathcal{H}_\infty$ controller K_2 (solid) and its optimal Hankel norm approximation (crosses).

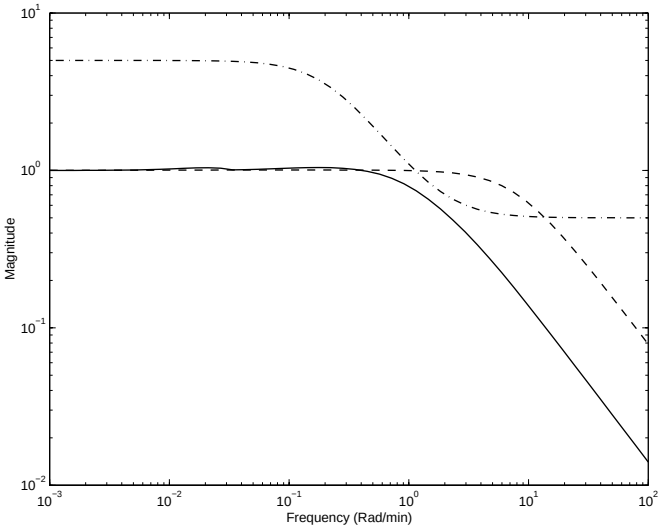

Figure 4.12: RS bound for K_1, $\bar{\sigma}(T_o)$, (dashed) and with the $\mathcal{H}_\infty$ controller K_2, $\bar{\sigma}(T_o(I + P_o^{-1}K_2N_rX_r))$, (solid). $|W_1|^{-1}$ (dash-dotted).

The dashed line reproduces the bound for Robust stability with the nominal controller K_1, which is $\bar{\sigma}(T_o) > |W_1|^{-1}$ for some frequencies.

The μ peak value for robust stability for K_1 is 1.6037 as it is shown, with dashed line, in Figure 4.13. The μ peak value for robust stability with the Robustness Enhancement Block with the $\mathcal{H}_\infty$ controller K_2 is 0.7796, as it is shown in solid line. Thus, the Robustness Enhancement Block with the $\mathcal{H}_\infty$ controller K_2 makes the condition for robust stability to be satisfied for all frequencies and this fact tells us that all the plants in the set $\mathcal{P}$ are stabilized.

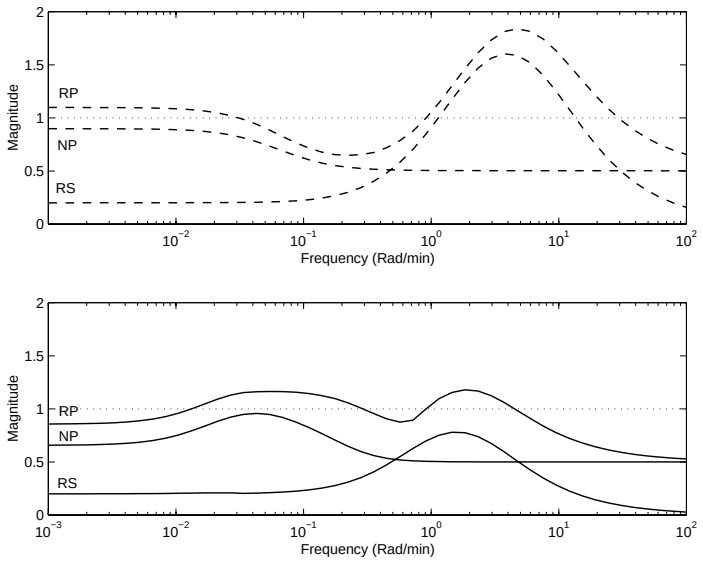

Figure 4.13: μ-plots for K_1 (dashed) and with the $\mathcal{H}_\infty$ controller K_2 (solid).

The addition of the Robustness Enhancement Block with the $\mathcal{H}_\infty$ controller K_2 has allowed to compensate the transfer matrix function form d_i to u' in order to fulfill robust stability. To make up for it, the nominal performance bound, i.e., the transfer matrix function from d_o to y', has also been modified. Figure 4.14 shows $\bar{\sigma}(S_o)$ in dashed line and $\bar{\sigma}(S_o(I - P_o K_1 K_2 (I - N_r Y_r)))$ in solid line. Note that the deterioration of the final output sensitivity is produced under the allowed bound, $|W_p|^{-1}$.

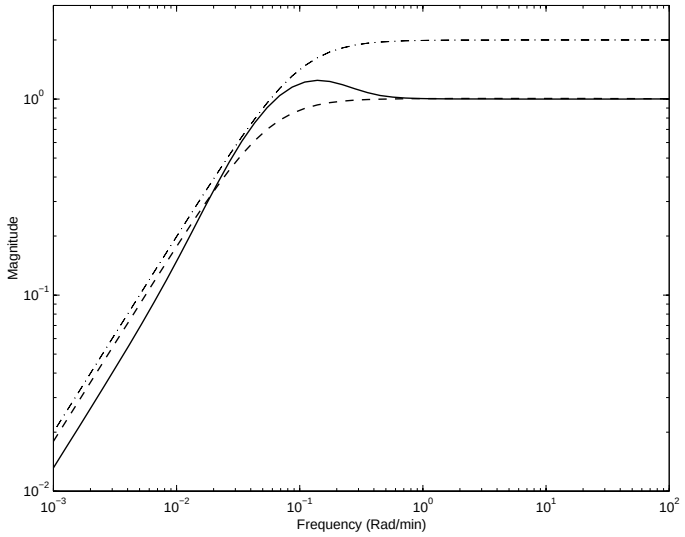

Figure 4.14: NP bound for K_1, $\bar{\sigma}(S_o)$, (dashed) and with the $\mathcal{H}_\infty$ controller K_2, $\bar{\sigma}(S_o(I - P_o K_1 K_2 (I - N_r Y_r)))$, (solid). $|W_p|^{-1}$ (dash-dotted).

The time responses of y_1 and y_2 to a filtered setpoint change in y_1, $r_1 = 1/(5s+1)$, are shown in Figure 4.15. The solid line represents the response with the nominal plant. Without uncertainty and without perturbations, the Robustness Enhancement Block is not working and the step response is that of the nominal controller K_1. The dashed lines represent the responses for the six perturbed plants $P_i(s)$, $i = 1, \ldots, 6$ with the Robustness Enhancement Block with the $\mathcal{H}_\infty$ controller K_2. Note that the nominal controller K_1, alone, can not stabilize the perturbed plants $P_i(s)$, $i = 5, \ldots, 6$. On the contrary, with the Robustness Enhancement Block, the closed-loop stability is guaranteed for all $P(s) \in \mathcal{P}$.

The Robustness Enhancement Block with the $\mathcal{H}_\infty$ controller K_2 assures robust stability while keeping the nominal step response unaltered. The step responses with the perturbed plants shown in Figure 4.15 are *similar* with that of the μ-"optimal" controller K_{opt} designed in Section 2.4 and shown in Figure 2.15.

Figure 4.16 shows the responses to a unitary step disturbance at the output with the $\mathcal{H}_\infty$ controller K_2. The response for the nominal plant P_o is illustrated in solid and the response for the uncertain plants $P_i = P_o E_{I_i}$,

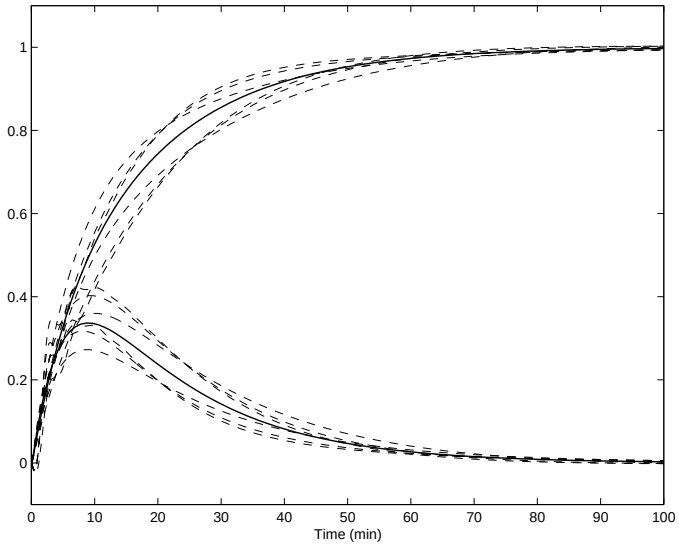

Figure 4.15: Closed-loop setpoint responses with the $\mathcal{H}_\infty$ controller K_2: Nominal plant (solid) and uncertain plants $P_i(s)$, $i = 1, \ldots, 6$ (dashed).

$i = 1, \ldots, 6$ are illustrated in dashed lines. It can be shown that the stability for the set of plant $P_i(s) \in \mathcal{P}$ is fulfilled since the $\mathcal{H}_\infty$ controller K_2 assures robust stability.

The disturbance rejection responses shown in Figure 4.16 are *similar* with that of the μ-"optimal" controller K_{opt} designed in Section 2.4 and shown in Figure 2.16.

The step responses provided by the proposed Observer-Controller configuration, i.e., K_1 with the $\mathcal{H}_\infty$ controller K_2, are more homogeneous — *similar* to the nominal responses — than the step responses for the μ-"optimal" controller K_{opt} designed in Section 2.4. This assertion is performed by comparing step responses in Figure 2.15 and that in Figure 4.15.

The disturbance rejection responses with the proposed Observer-Controller configuration for the uncertain plants $P_i(s)$, $i = 1, \ldots, 6$ are also closed to the disturbance response for the nominal plant P_o. Comparing simulation results in Figure 4.16 and Figure 2.16, we can observe the following: the proposed Observer-Controller configuration, with K_1 and the $\mathcal{H}_\infty$ controller K_2, presets a nominal disturbance rejection response slightly worst than the nominal disturbance rejection for the μ-"optimal" controller K_{opt}.

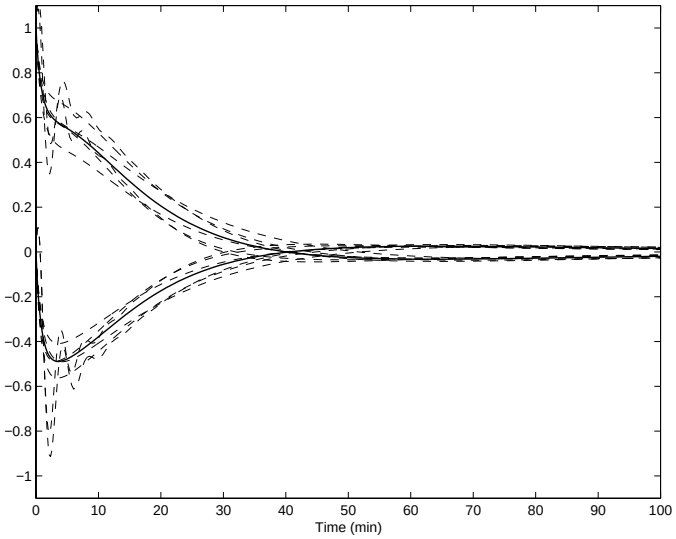

Figure 4.16: Closed-loop response to a disturbance at the output signal y_1 with the $\mathcal{H}_\infty$ controller K_2: response for the nominal plant P_o (solid) and for the uncertain plants $P_i = P_o E_{I_i}$, $i = 1, \ldots, 6$ (dashed).

In any case, within the structured singular value framework, we can design a μ-"optimal" controller K_2 for compensating this lost of performance is terms of disturbance rejections.

Design of K_2 as a μ-"optimal" controller

Given a right coprime factorization $P_o = N_r M_r^{-1}$, the nominal controller K_1 in (4.33), the right coprime factors, X_r, Y_r, the uncertainty weight W_1 and the performance weight W_p, is is possible to find a μ-"optimal" controller K_2 by solving the optimization problem (4.28).

The DK-iteration procedure, explained in detail in Section 2.4, with $D_\ell = D_r = I$ as initial scalings, provides a μ-"optimal" controller K_2 with 30 states. A balanced realization and an optimal Hankel norm approximation of order 10 on the state-space of K_2 provides an equivalent, reduced, controller K_2. Figure 4.17 shows, in solid line, the singular values Bode plot for the 30th state controller K_2 and its 10th states Hankel norm approximated controller in crosses.

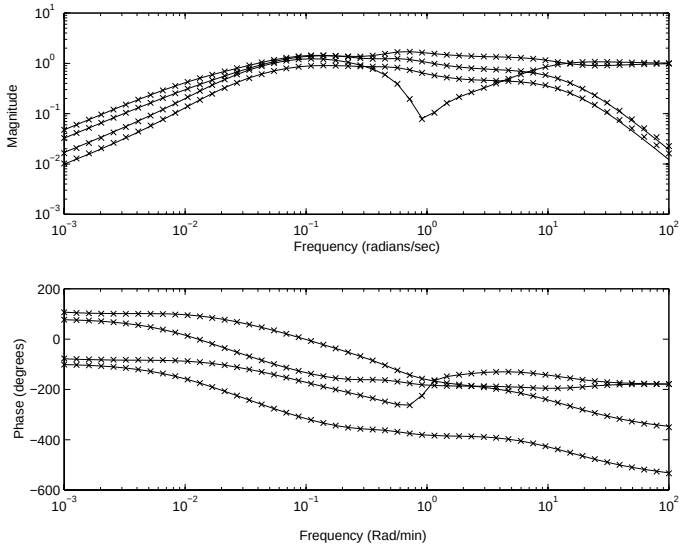

Figure 4.17: Frequency Bode plot for the *mu*-"optimal" controller K_2 (solid) and its optimal Hankel norm approximation (crosses).

The time responses of y_1 and y_2 to a filtered setpoint change in y_1, $r_1 = 1/(5s+1)$, is shown in Figure 4.18. The solid line represents the response with the nominal plant. Without uncertainty and without perturbations, the Robustness Enhancement Block is not working and the step response is that of the nominal controller K_1. The dashed lines represent the responses with the Robustness Enhancement Block with the μ-"optimal" controller K_2 for the six perturbed plants $P_i(s)$, $i = 1, \ldots, 6$.

Figure 4.19 shows the response to a unitary step disturbance at the output with the μ-"optimal" controller K_2. The response for the nominal plant P_o is illustrated in solid and the response for the uncertain plants $P_i = P_o E_{I_i}$, $i = 1, \ldots, 6$ in (B.15) are illustrated in dashed.

The Robustness Enhancement Block with the μ-"optimal" controller K_2 assures robust stability and *almost* robust performance. The term *almost* is used here to denote that the upper μ-bound has a peak value of $\mu = 1.0329$ and therefore, almost less than 1. This is the same value than the upper μ-bound for the μ-"optimal" K_{opt} in Section 2.4. This is observed by means of the μ curves for the Robustness Enhancement Block with the μ-"optimal" controller K_2, which are identical to that of the μ-"optimal" K_{opt}.

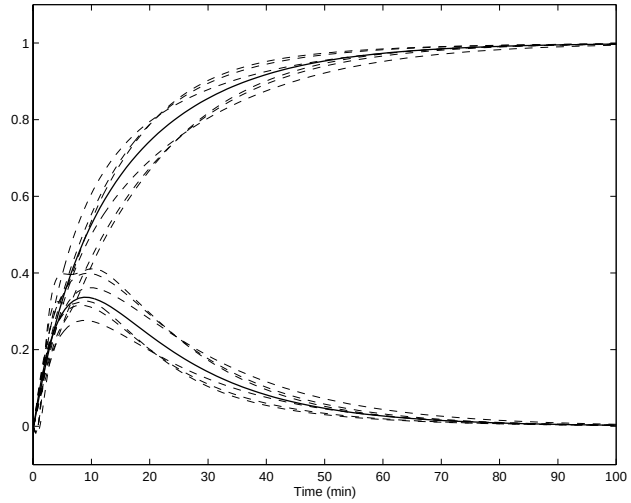

Figure 4.18: Closed-loop setpoint change with the μ-"optimal" controller K_2: response for the nominal plant P_o (solid) and for the uncertain plants $P_i = P_o E_{I_i}$, $i = 1, \ldots, 6$ (dashed).

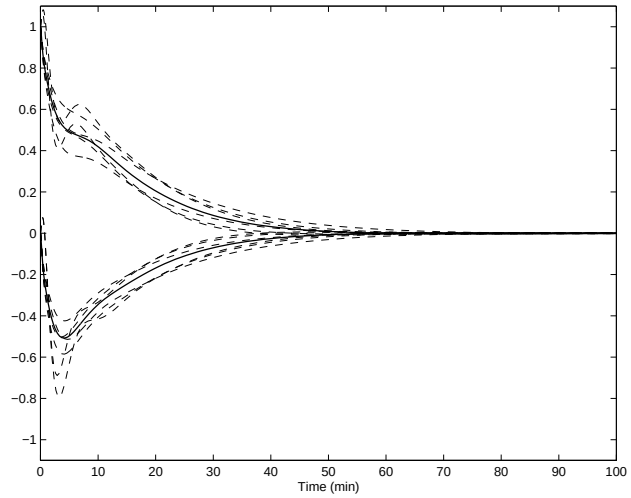

Figure 4.19: Closed-loop response to a disturbance at the output signal y_1 with the μ-"optimal" controller K_2: response for the nominal plant P_o (solid) and for the uncertain plants $P_i = P_o E_{I_i}$, $i = 1, \ldots, 6$ (dashed).

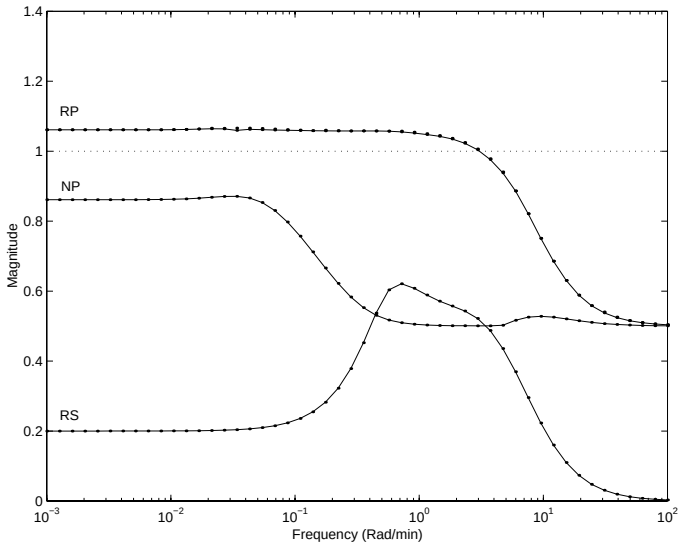

Figure 4.20: μ-plots: the μ-"optimal" controller K_{opt} (solid) and K_1 with the μ-"optimal" controller K_2 (dots).

△

4.6 Summary

This Chapter has shown how the Observer-Controller configuration can be used as a framework to enhance the robustness properties of a feedback control system. An initial controller is set for nominal specifications and the Robustness Enhancement Block is designed to cope with robustness without altering the nominal relations from the reference. By means of the application to the control of a high-purity distillation column, a process inherently difficult to control, we have illustrated how the Observer-Controller configuration for robustness enhancement can be used in a two design procedure. Such a procedure allows to cope, first, with nominal properties and, second, to cope with robustness.

The presented methodology represents the extension of the approach presented in (Vilanova *et al.*, 1999) and (Pedret *et al.*, 2001) to the general multivariable scenario. The design procedure is systematized by using the $\mathcal{H}_\infty$ / Structured Singular Value framework. With the resulting approach,

the enhancement of the robustness properties is completely general in the sense that it does not depend on the way the initial controller was designed nor his structure. The approach presented in this Chapter can also be found in (Pedret *et al.*, 2003).

Chapter 5

The 2-DOF Observer-Controller configuration

In this Chapter we present a new 2-DOF control configuration based on a right coprime factorization of the plant and the usage of the partial state as controlled variable. The presented approach makes use of an observer-based feedback control scheme which is designed first to guarantee some levels of stability robustness. This is done by solving a constrained $\mathcal{H}_\infty$ optimization problem using the right coprime factorization of the plant in an active way. Then, a prefilter controller is computed to guarantee robust open-loop processing of the reference commands. This is done by assuming a Reference Model and by solving a Model Matching Problem imposed on the prefilter controller.

5.1 Introduction

Standard feedback control is based on processing the difference between the reference inputs and the actual outputs. It is well known that, in such a case, the design problem has one degree of freedom (1-DOF) which may be described in terms of the stable Youla parameter (Vidyasagar, 1985). Two degrees-of-freedom (2-DOF) compensators are characterized by allowing a separate processing of the reference inputs and the controlled outputs and

may be stated by means of two stable Youla parameters. The 2-DOF compensators presents the advantage of a complete separations between feedback and reference tracking properties (Youla and Bongiorno, 1985): the feedback properties of the control system are assured by a feedback controller, i.e., the first degree of freedom; the reference tracking specifications are addressed by a prefilter controller, i.e., the second degree of freedom, which determines the open-loop processing of the reference commands.

As is is pointed out in (Vilanova and Serra, 1997), classical control approaches tend to stress the use of feedback to modify the systems' response to commands. A clear example, widely used in the literature of linear control, is the usage of Reference Models to specify the desired properties on a control system (Astrom and Wittenmark, 1984). What is specified through a Reference Model is the desired closed-loop system response. Therefore, as the system responds to commands is an open-loop property and robustness properties are associated with the feedback (Safonov *et al.*, 1981), no stability margins are necessarily guaranteed when achieving the desired closed-loop response behaviour.

A two degrees-of-freedom (2-DOF) control configuration may be used in order to achieve a control system with both a performance specification, e.g., through a Reference Model, and some guaranteed stability margins. Nevertheless, the lack of methodologies to design the two compensators may be the reason for the 2-DOF compensators not to be widely used. Since the best way of allocating the gain between the two controllers is not so clear, the approaches found in the literature are mainly based on optimization problems. Basically, these optimization problems procedures represent different ways of setting the Youla parameters to represent the controllers (Vidyasagar, 1985), (Youla and Bongiorno, 1985), (Grimble, 1988), (Limebeer *et al.*, 1993).

The approach presented in (Limebeer *et al.*, 1993) expands the role of $\mathcal{H}_\infty$ optimization tools in 2-DOF system design. The 1-DOF loop-shaping design procedure (McFarlane and Glover, 1992) is extended to a 2-DOF control configuration by means of a parametrization in terms of two stable, but otherwise free, Youla parameter (Vidyasagar, 1985), (Youla and Bongiorno, 1985). A feedback controller is designed to guarantee to meet robust stability and disturbance rejection requirements in a manner similar to the 1-DOF loop-shaping design procedure. A prefilter controller is then introduced to force the response of the closed- loop system to follow that of a specified Reference Model. The approach is carried out by assum-

ing uncertainty in the normalized coprime factors plant descriptions (Glover and McFarlane, 1989). Such uncertainty description allows a formulation of the $\mathcal{H}_\infty$ robust stabilization problem providing explicit formulas for the corresponding controller. Nevertheless, the translation of physical parameters uncertainty into normalized coprime factors plant uncertainty is not straightforward.

A frequency domain approach to Model Reference control with robustness considerations was presented in (Sun *et al.*, 1994). The design approach consist on a nominal design and a modeling error compensation component to compensate for the error due to uncertainty. However, since the approach is based on the Model Reference Adaptive Control theory, the minimum phase assumption for the plant to be controlled is inherited.

In this Chapter we present a new 2-DOF control configuration based a right coprime factorization of the plant. Within the factorization framework, the partial state is used as controlled variable. The presented approach is not based on setting the 2 controllers arbitrarily, with internal stability as the only restriction, and parameterize the controller in terms of the Youla parameter. Instead,

1) An observer-based feedback control scheme is designed to guarantee some levels of stability robustness. This is done by solving a constrained $\mathcal{H}_\infty$ optimization problem using partial state as controlled variable and the right coprime factorization of the plant in an *active* way.

2) A prefilter controller is computed to guarantee the robust open-loop processing of the reference commands. This is done by assuming a Reference Model with the desired relations from the reference signals and by solving a model matching problem imposed on the prefilter controller such that the response of the overall close-loop system match that of the reference model.

The presented approach is presented to provide good results for non-minimum phase systems because of the use of a special feedback control configuration.

The Chapter is organized as follows: Section 5.2 introduces the proposed 2-DOF control configuration and describes the two steps in which the design methodology is divided. Section 5.3 illustrates the design of the feedback

control structure for robust stability. In Section 5.4, a prefilter controller is designed to guarantee robust model reference responses. Finally, the proposed 2-DOF control configuration is evaluated on a high purity distillation column example, in Section 5.5.

5.2 Displaying the 2-DOF control configuration

This Section introduces a new 2-DOF control configuration based, as it is recurring in this work, on the fractional representation framework addressed in Chapter 3. Within that formulation, we know that a right coprime factorization of a matrix transfer function P_o reads as

$$P_o = N_r M_r^{-1} \tag{5.1}$$

where N_r and M_r^{-1} are said to be right coprime over $\mathcal{RH}_\infty$ if they have the same number of columns and if there exist stable matrices X_r and Y_r satisfying the Bezout identity

$$X_r M_r + Y_r N_r = I \tag{5.2}$$

Within this framework, the so-called partial state, ξ, is the fictitious signal that appears after the right factorization of P_o, as shown in Figure 5.1.

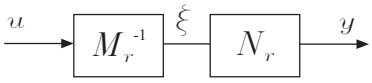

Figure 5.1: Right coprime factorization of P_o in (5.1).

In Chapter 4, we have considered how the partial state, ξ, may be used to complement a control system designed just for the nominal plant. The strategy is based on using the partial state to compute an estimation of the output signal. Such estimation is used to calculate how the estimated output differs form the real output and, in consequence, to take a suitable corrective control action. This give rise to a control configuration that allows the enhancement of the robustness properties of the nominal control system. For the control structure presented in this Chapter, the partial state is also taken into account but used in a different way. The particular manner in which

the proposed control configuration deals with the partial state is sketched in Figure 5.2.

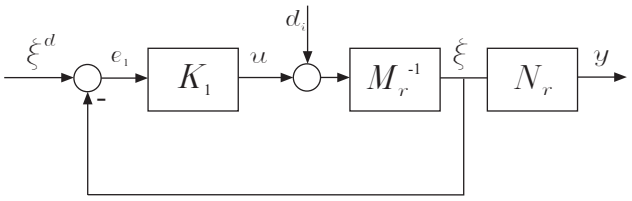

Figure 5.2: The basic structure for the proposed control configuration.

The new configuration results in a genuine way of building the error signal, e_1. Instead of comparing the output controlled signals with the reference signals, as it is usually done in standard feedback control, the error signal in the presented approach results form the difference between the *desired* partial state and the *actual* partial state, i.e., $e_1 = \xi^d - \xi$.

The controller K_1 in the scheme depicted by Figure 5.2 is designed to minimize the error signal e_1. In other words, to force the actual partial state, ξ, to match the desired partial states, ξ^d. The consequence of feeding the partial state back, instead of the output signals, is that disturbances entering at the output of the plant are not measured. For this reason, output disturbances can not be eliminated. Nevertheless, we saw in Section 3.4 that the final achieved controller K_1 feeding the partial state back presents the advantage of avoiding RHP-zeros to cause closed loop instability.

In a real scenario, the direct access to the partial state shown in Figure 5.2 is meaningless. Therefore, if we want to apply this control strategy to a real system, some estimation technique shall be used. To observe the partial state, the transfer matrix functions X_r and Y_r, satisfying the Bezout identity (5.2), are introduced to the control system. The resulting control scheme is depicted in Figure 5.3.

Within the coprime factorization framework, the two Bezout complements X_r and Y_r allow to recover the partial state, ξ^o. Recalling Section 3.4, we know that it is possible to write, from Figure 5.3,

$$y = N_r\xi, \;\; u = M_r\xi - d_i \tag{5.3}$$

Equations (5.2) and (5.3) show immediately how to recover the partial state:

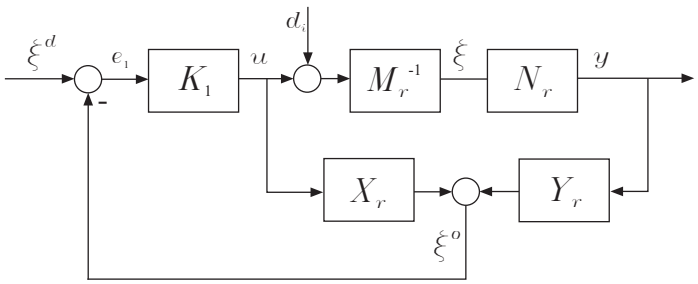

Figure 5.3: Observer-based control scheme.

$$\begin{aligned} \xi^o &= X_r u + Y_r y = && (5.4)\\ &= (X_r M_r + Y_r N_r)\xi - X_r d_i && (5.5) \end{aligned}$$

As long as the two observer transfer matrix functions X_r, Y_r, make the Bezout identity (5.2) to be satisfied, the scheme allows the reconstruction, i.e.,

$$\xi^o = \xi - X_r d_i \tag{5.6}$$

The reconstructed signal ξ^o in (5.6) incorporates a measure of the disturbances signal that can affect the input of the plant, P_o. Therefore, the error signal e_1 can be seen as a measure of how the *actual* partial state differs from the *desired* partial state due to the disturbances d_i, say

$$e_1 = \xi^d - \xi + X_r d_i \tag{5.7}$$

We will see how to design a suitable feedback controller K_1 and how to find a right coprime factorization, $P_o = M_r^{-1} N_r$, and the associated Bezout components, X_r and Y_r to minimize e_1.

When the feedback structure shown in Figure 5.3 is designed, a prefilter controller K_2 must be incorporated to allow building the desired value for the partial state, ξ^d, as it is shown in Figure 5.4. A static prefilter can be easily found to adapt the reference command signals, r, for steady-state accuracy. This reminds the constant prefilter controller that allows to include the reference signal to the one degree-of-freedom $\mathcal{H}_\infty$ loop-shaping control

configuration (McFarlane and Glover, 1992). However, for many tracking problems this will not be sufficient and a dynamic design for K_2 is required. The prefilter is designed to force the response of the closed-loop system to follow that of a specified Reference Model, T_{ref}. This is done in a manner similar to the dynamic two degrees-of-freedom control configuration proposed in (Limebeer *et al.*, 1993) as an extension to one degree-of-freedom $\mathcal{H}_\infty$ loop-shaping design procedure.

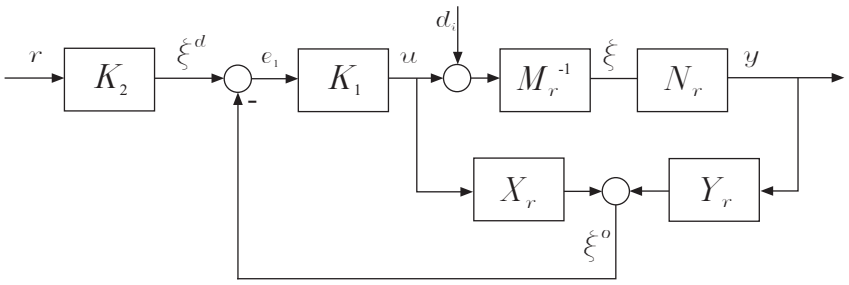

Figure 5.4: Overall 2-DOF control configuration.

The 2-DOF scheme shown in Figure 5.4 presents a concise, and well suited for design, separation between feedback and open-loop properties. Therefore, since robustness is, in fact a feedback property (Safonov *et al.*, 1981) we will setup the control problem as the design the robust feedback controller K_1 in order to give robustness to the control system and the reference controller K_2 in order to achieve Model Reference specifications.

Let us assume, without lost of generality, that multiplicative input uncertainty is considered. In such an uncertainty description, the plant P to be controlled is unknown but belonging to a set of plants, $\mathcal{P}$, built around a nominal model, P_o,

$$\mathcal{P} = \{P : P = P_o(I + W_2 \Delta W_1)\}, \;\; \bar{\sigma}(\Delta) \leq 1 \; \forall \omega \tag{5.8}$$

where $W_1 = w_I I$, $W_2 = I$.

Let us also assume that an input/output ideal response is specified by means of a Reference Model T_{ref}. Therefore, the control objective can be stated as follows:

Given a nominal system P_o, an uncertainty description that gives rise to the family of plants $\mathcal{P}$ in (5.8) and a Reference Model T_{ref}, design a control system so that the input/output relations for all possible plants $P \in \mathcal{P}$ behave as close as possible to T_{ref} and provides the desired stability margins.

This problem could be called the design of *Model Reference Robust Controller*. The way to the solution will comprise the application of the following steps to the control scheme depicted in Figure 5.4.

Step 1: Feedback controller design. Find a coprime factorization for the nominal model, $P_o = M_r^{-1} N_r$, the associated Bezout components, X_r and Y_r and design of the feedback controller K_1 so that the resulting closed-loop system remains stable for all $P \in \mathcal{P}$.

Step 2: Reference controller design. Design a prefilter controller K_2 so that relations from the references to the outputs for all $P \in \mathcal{P}$ behave as close as possible to that of the reference model T_{ref}. The design of the reference controller will depend upon the performance criterion chosen for the desired closeness to the reference model T_{ref}. We will address the problem to optimal Model Reference controller specifications in an ∞-norm sense. This way, the design of the reference controller turns out to be a Model Matching Problem.

Next Section deals with the design of the feedback structure for robust stability, i.e., the design of the feedback controller K_1, the right coprime factors M_r^{-1}, N_r, and the associated Bezout components, X_r, Y_r. Section 5.4 addresses the design of the prefilter controller K_2.

5.3 Feedback controller design

This Section presents the design of the feedback controller K_1 and also the finding of a coprime factorization for the nominal model, $P_o = M_r^{-1} N_r$, and the associated Bezout components, X_r and Y_r, for the proposed control configuration shown in Figure 5.3.

A right coprime factorization of the nominal model, $P_o = M_r^{-1} N_r$, with $N_r,\ M_r \in \mathcal{RH}_\infty$, is computed as we saw in Section 3.3. The only requirement will be to exist matrix transfer functions, $X_r,\ Y_r \in \mathcal{RH}_\infty$, such

that a Bezout identity holds. With right coprime factors N_r, M_r, X_r, Y_r and with a given uncertainty description (5.8), the feedback controller K_1 shown in Figure 5.3 may be designed by applying a robust control design methodology. The objective is that the resulting closed-loop system guarantees some stability margins. Obviously, the choice of the robust control design strategy will depend upon the uncertainty description. The only requirement will be to provide a Robust Stability test in order to check the stability margins that the resulting controller provides. Different approaches are (Vidyasagar, 1985), (Morari and Zafirou, 1989), (Grimble, 1994), (Green and Limebeer, 1995) and (Zhou and Doyle, 1998), among others.

One of the most distinctive features of the proposed approach is the usage of the partial state ξ as the control variable. It has been extensively commented and it is easily perceived from the control scheme in Figure 5.3. In this point we can reveal that this is not the only peculiarity in the proposed control scheme. Another distinguishing feature is that of giving the right coprime factors of the plant and its associated Bezout complements an *active* role in the overall control system.

Effectively, from Theorem 3.3.1 we know that a right coprime factorization of the nominal model, $P_o = M_r^{-1}N_r$, and the associated Bezout components, X_r and Y_r can be found by means of the state feedback gain, F, and the state observation gain, L. They are entirely free assignable matrices with the only restriction that $A + BF$ and $A + LC$ must be asymptotically stable. We can see, from equation (3.16), that the eigenvalues of $A + BF$ determine the resultant poles of M_r and N_r. Analogously from equation (3.17), the eigenvalues of $A + LC$ establish the poles of X_r and Y_r.

Obviously, for a right coprime factorization, $P_o = M_r^{-1}N_r$, the Bezout equation $X_rM_r + Y_rN_r = I$ must be fulfilled independently of the place that the eigenvalues of $A + BF$ and the eigenvalues of $A + LC$ are assigned. Nevertheless, depending on such a pole placement, each one of the involved factors, $M_r(s)$, $N_r(s)$, $X_r(s)$ and $Y_r(s)$, will have different poles and different zeros. As long as $M_r(s)$, $N_r(s)$, $X_r(s)$ and $Y_r(s)$ contribute individually in the relevant input/output transfer functions, the pole placement procedure can be seen, and used, to provide an extra degree of freedom. That is the key idea of the proposed design for the feedback control scheme.

To design the feedback structure shown in Figure 5.3, the control scheme with direct access to the partial state ξ is considered first (see Figure 5.2). Its input/output relations are developed and the properties of such an ideal

control configuration are analyzed. Next, the observer-based control scheme is considered since the structure with direct access to the partial state has not applicability to control a real system (see Figure 5.3). The resultant input/output relations are also developed. The final feedback controller K_1 and the coprime factors M_r, N_r, X_r and Y_r results from solving a constrained $\mathcal{H}_\infty$ optimization problem which, essentially, arises from enforcing the input/output relations of the observer-based control scheme in Figure 5.3 to match that of the direct access control scheme in Figure 5.2.

5.3.1 Direct access to the partial state

Let us assume that $P_o = M_r^{-1}N_r$ is a right coprime factorization for the nominal model of the plant. Let us also assume that partial state ξ is directly accessed. Both assumptions allow to consider the feedback control structure shown in Figure 5.2.

This situation is, in fact, unrealistic since the partial state is an artificial signal appearing in the context of coprime factorization and direct access to ξ is meaningless when one is faced with the real plant. Nevertheless, the structure in Figure 5.2 presents some advantages. In Section 3.3 we saw that it is possible to detect a remarkable difference between the standard output feedback control scheme and that shown in Figure 5.2: in the former, the feedback controller K_1 is in charge of the nominal plant $P_o = M_r^{-1}N_r$; in the later, the controller K_1 faces just one of the coprime transfer matrices in which the nominal plant is split up, that is M_r^{-1}. Within a right coprime factorization of the plant, the poles of P_o are absorbed into M_r^{-1} as poles; the zeros of P_o are absorbed into N_r as zeros. As it is stood out by remark 3.4.4, the final achieved controller K_1 in the ideal structure shown in Figure 5.2 avoids dealing with RHP-zeros of the plant. This is an important advantage since the possible RHP-zeros of the plant are prevented to cause closed-loop instability. Another important advantage is that the methodology used to design the controller K_1 does not have to be constrained with the requirement that the resulting controller be stable.

On the other hand, the scheme in Figure 5.2 does not allow output disturbances to be rejected. This is an obvious consequence of feeding the partial state back instead of feeding the output signal y back. Despite this serious drawback, we are primarily interested in exploiting the advantage pointed above and explained in Section 3.4.2.

From Figure 5.2 we can write, after some straightforward algebra, the relations between the input signals $[d_i\ \xi^d]^T$ and the output signals $[u\ y]^T$:

$$\begin{bmatrix} u \\ y \end{bmatrix} = \begin{bmatrix} -M_r R Y_r N_r M_r^{-1} & M_r R \\ N_r(I-R)M_r^{-1} & N_r R \end{bmatrix} \begin{bmatrix} d_i \\ \xi^d \end{bmatrix} \tag{5.9}$$

where

$$R \doteq (I + M_r^{-1} K_1)^{-1} M_r^{-1} K_1 \tag{5.10}$$

and

$$I - R = (I + M_r^{-1} K_1)^{-1} \tag{5.11}$$

Figure 5.5 illustrates typical frequency response shapes for R and $I - R$

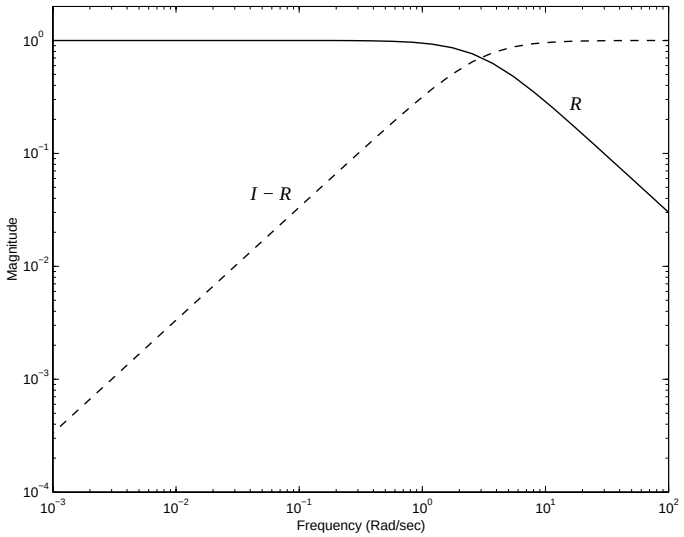

Figure 5.5: Typical frequency plots for R and $I - R$.

Assuming a nominal situation in which no disturbances d_i enter the control system, the scheme in Figure 5.2 can be represented as it is shown in Figure 5.6.

Figure 5.6 shows the ideal representation in which the input disturbances signal is zero, i.e., $d_i = 0$. In such a case, the feedback controller K_1 and the

right coprime transfer matrix M_r^{-1} can be grouped to form a new transfer function R defined in equation (5.10).

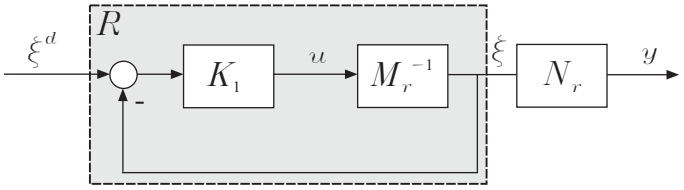

Figure 5.6: Ideal representation of the feedback scheme with $d_i = 0$.

Remark 5.3.1. *Assuming a nominal situation in which no disturbances d_i enter the control scheme in Figure 5.2, the relation from the desired partial state ξ^d and the output signal y, is just reduced to*

$$y = N_r R\, \xi^d \tag{5.12}$$

where N_r is the transfer matrix that contains the (possibly RHP) zeros of the plant and R is defined in equation (5.10).

The transfer matrix R is a function of the controller K_1 and the coprime factor M_r^{-1}. As long as R relates the desired partial state, ξ^d, and the actual partial state, ξ, it should have, ideally, an all pass shape with constant magnitude equal to one. Therefore, the feedback controller K_1 and the right coprime factors could be designed by minimizing the following weighted $\mathcal{H}_\infty$ norm:

$$\|W(I - R)\|_\infty \tag{5.13}$$

The optimization problem (5.13) represents the minimization of the maximum of the weighted difference between R and its ideal value, I. The weight W may be chosen to have a high-pass shape to enforce the optimization problem at low frequencies.

An alternative optimization problem could be to design the feedback controller K_1 and to find the right coprime factors by minimizing the following weighted $\mathcal{H}_\infty$ norm:

$$\left\|W N_r (I - R) M_r^{-1}\right\|_\infty \tag{5.14}$$

The optimization problem (5.14) represents the minimization of the maximum of the weighted transfer function from the disturbances d_i to the output y. Note that the effect of the disturbances d_i hinders the transfer function from y to ξ^d to be just $N_r R$, as it is stated by Remark 5.3.1.

5.3.2 Observer-based access to the partial state

Let us consider a more realistic case in which the partial state can not be directly accessed. So, the observer structure have to be used in order to recover ξ as shown in Figure 5.3.

The relations between the input signals $[d_i \ \xi^d]^T$ and the output signals $[u \ y]^T$ can be derived from Figure 5.3 after some straightforward algebra:

$$\begin{bmatrix} u \\ y \end{bmatrix} = \begin{bmatrix} -M_r R Y_r N_r M_r^{-1} & M_r R \\ N_r(I-R)M_r^{-1} + N_r R X_r & N_r R \end{bmatrix} \begin{bmatrix} d_i \\ \xi^d \end{bmatrix} \tag{5.15}$$

with R and $I - R$ defined in (5.10) and (5.11) respectively.

The resulting input/output relations (5.15) for the observer-based control scheme in Figure 5.3 are almost identical to the relations (5.9) for the direct access scheme in Figure 5.2. The only difference is the transfer matrix function from the disturbances d_i to the outputs y in which a new addend, $N_r R X_r$, appears due to the observer.

The optimization problem (5.13) proposed for the direct access case, may also be posed here. Alternatively, as it was performed in (5.14), the weighted transfer function from the disturbances d_i to the output y may be minimized,

$$\left\| W(N_r(I-R)M_r^{-1} + N_r R X_r) \right\|_\infty \tag{5.16}$$

Remark 5.3.2. *The transfer matrix function from the disturbances d_i to the outputs y is to be minimized by means of solving the optimization problem (5.16). This allows to design the feedback controller K_1 and to find coprime factors N_r, M_r, X_r and Y_r such that the observer-based structure in Figure 5.3 approximates as much as possible the ideal structure in Figure 5.6. In other words, the relation from the desired partial state ξ^d to the outputs y approximates as much as possible $N_r R$.*

5.3.3 Design procedure

The feedback control structure based on the direct access to the partial state (Figure 5.2) has been dealt and input/output relations have been developed in (5.9). As long as the the partial state can not be directly accessed dealing with the real plant, an observer-based control scheme has been used (Figure 5.3) and its input/output relations have been developed in (5.15). We have seen that the usage of the observer-based structure entails the appearance of an extra term in the transfer function from d_i to y, that is $N_r R X_r$.

As it has been pointed out in Remark 5.3.2, the design procedure could be based on minimizing the transfer matrix functions from the disturbances, d_i, to the output, y, in order to force the relations from the desired partial state, ξ^d, to the output, y, to match the ideal transfer function, i.e., $N_r R$.

Robust stability

In Section 2.3 we showed that a multiplicative input uncertainty description, as the one considered in (5.8), imposes a bound on the frequency response of the transfer matrix function from the input disturbances signal, d_i, to the control signal, u. This fact restricts the design of the feedback controller K_1 and the right coprime factors N_r, M_r, X_r and Y_r.

The uncertainty description assumed in (5.8) allows us to redraw the observer-based feedback control configuration. Figure 5.7 shows the resulting weighted observer-based feedback control scheme.

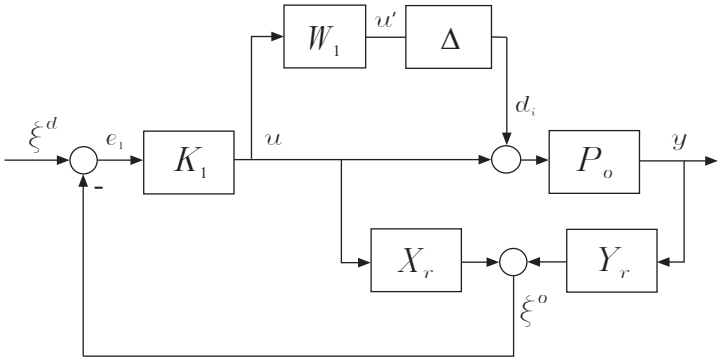

Figure 5.7: Observer-based feedback control scheme with the uncertain plant.

From the overall control scheme in Figure 5.7 we can compute the transfer matrix function, say $\mathcal{N}$, that relates the input signals $[d_i \ \xi^d]^T$ with the weighed control signals and the output signal, $[u' \ y]^T$,

$$\mathcal{N} = \begin{bmatrix} -W_1 M_r R Y_r N_r M_r^{-1} & W_1 M_r R \\ N_r(I-R)M_r^{-1} + N_r R X_r & N_r R \end{bmatrix} \tag{5.17}$$

where R and $I - R$ are defined in (5.10) and (5.11) respectively.

Considering unstructured uncertainty, e.g., Δ is a full complex matrix of appropriate dimensions, Theorem 2.3.1 imposes a condition on the ∞-norm of the transfer matrix function from the input disturbance, d_i, to the weighted control signal, u', i.e., $\mathcal{N}_{11} \doteq \mathcal{M}$, in order for robust stability to be guaranteed. From (5.17) we have that

$$\|\mathcal{M}\|_\infty = \left\|-W_1 M_r R Y_r N_r M_r^{-1}\right\|_\infty \tag{5.18}$$

Therefore, form (5.18) and condition (2.23) we have robust stability iff,

$$\left\|-W_1 M_r R Y_r N_r M_r^{-1}\right\|_\infty < 1 \tag{5.19}$$

Pole placement

It seems obvious that the problem is to find an optimal feedback controller K_1 by solving the optimization problem (5.16) subject to the constraint (5.19) for given coprime factors N_r, M_r, X_r and Y_r. Nevertheless, as we are mainly interested in making the most of the coprime factorization, the optimization problem is posed in a different way. It is considered next.

We showed by means of Theorem 3.3.1 that a proper choice of the state feedback gain matrix, F, and the state observation gain matrix, L, allows to fix, in an appropriate manner, the resultant poles of M_r and N_r — see equation (3.16) — and the poles for X_r and Y_r — equation (3.17). The state feedback gain, F, and the state observation gain, L, are free assignable matrices that provides an additional degree of freedom with the only restriction that $A + BF$ and $A + LC$ must be asymptotically stable. This degree of freedom is to be used in the optimization procedure.

The proposed design procedure does not consist on solving the optimization problem (5.16) subject to (5.19) for K_1 with given coprime factors N_r, M_r, X_r and Y_r. Instead, a *feasible* shape for $I - R$ is proposed, say

$$S^d \doteq I - R \tag{5.20}$$

and the following constrained optimization problem is solved being $I - R$ an initial fixed entry and the poles for N_r M_r, X_r and Y_r the unknowns:

$$\begin{aligned} &\min_{p_i} \left\| N_r(I-R)M_r^{-1} + N_r R X_r \right\|_\infty \\ &\text{subject to} \\ &\left\| -W_1 M_r R Y_r N_r M_r^{-1} \right\|_\infty < 1 \end{aligned} \tag{5.21}$$

Here, $p_i = [p_{F_i}\ p_{L_i}]^T \in \mathcal{C}^-$, being p_{F_i} the assigned eigenvalues of $A + BF$ and p_{L_i} the assigned eigenvalues of $A + LC$. In other words, p_{F_i} are the placed poles for N_r and M_r, and p_{L_i} the placed poles for X_r and Y_r.

Actually, N_r and also M_r are unknowns but they are not entirely free since the coprime factorization in equation (3.16) and (3.17) constrains them. The same happens with the Bezout complements Y_r and X_r, which are linked by means of the Bezout identity (3.12).

An asymptotic plot over the frequency of the *desired* Sensitivity function is illustrated in Figure 5.8.

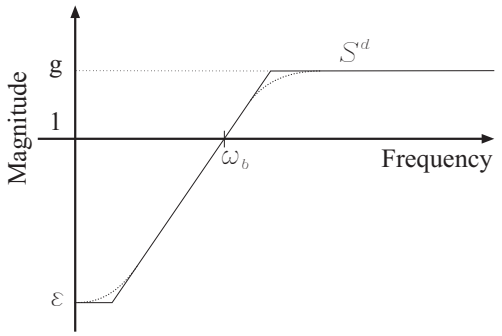

Figure 5.8: Exact and asymptotic plot of $S^d(j\omega)$.

A usual shape for S^d may be represented by

$$S^d = \frac{s + \omega_b \varepsilon}{s/\mathrm{g} + \omega_b} \tag{5.22}$$

It is observed that $|S^d(j\omega)|$ is equal to $\varepsilon \ll 1$ at low frequencies and it is equal to $\mathrm{g} \geq 1$ at high frequencies. The asymptote crosses 1 at ω_b, which is approximately the bandwidth requirement.

To finish the design procedure, the feedback controller K_1 must be recovered. Note that we have followed an *indirect* design approach: first a transfer matrix function S^d is set and then, the feedback controller K_1 that assures such transfer matrix function S^d is to be found by means of isolating it from equation (5.11). The design equation for K_1 is

$$K_1 = M_r R (I - R)^{-1} \tag{5.23}$$

For the design procedure, a *desired* shape for S^d must be provided. This shape will be the target for the optimization problem (5.21). Nevertheless, fixing the shape for S^d determines, indirectly, the shape for R i.e., the transfer matrix function from ξ^d to ξ. Then, as pointed out in Remark 5.3.1, the resulting shape for R and the achieved *optimal* coprime factor N_r determines the input/output dynamics for the nominal feedback controller structure.

Remark 5.3.3. *The minimization problem (5.21) has to find optimum coprime factors, N_r, M_r and X_r, to minimize $\left\| N_r(I-R)M_r^{-1} + N_r R X_r \right\|_\infty$ constrained with $\| -W_1 M_r R Y_r N_r M_{-1} \|_\infty < 1$. It should be noted that the high-pass shape S^d can not be chosen arbitrarily: if S^d was such that $\bar{\sigma}(R) > 1/\underline{\sigma}(W_1)$, the optimization problem would have to try very hard to fulfill the constraint $\| -W_1 M_r R Y_r N_r M_{-1} \|_\infty < 1$ and this fact would be in expenses of $\left\| N_r(I-R)M_r^{-1} + N_r R X_r \right\|_\infty$ which would not be, probably, minimized to a sufficient degree. Therefore, the high-pass shape S^d may be chosen such that*

$$\bar{\sigma}(R) \leq 1/\underline{\sigma}(W_1) \tag{5.24}$$

Design outline

The feedback controller design constitutes the first step for the proposed 2-DOF control configuration. Here, we briefly describe the important points in the design procedure.

1. **Uncertainty description:** Assume that the plant P to be controlled is unknown but belonging to a set of plants $\mathcal{P}$ build around the nominal model P_o, as in (5.8).

2. **Initial factorization:** Provide $p_{F_o} \in \mathcal{C}^-$ and $p_{L_o} \in \mathcal{C}^-$, i.e., initial stable eigenvalues for the right coprime factorization of the nominal model of the plant, $P_o = M_r^{-1}N_r$, and initial stable eigenvalues for the associated Bezout components X_r, Y_r, respectively.

3. **Desired sensitivity:** Impose the *desired* high-pass shape $S^d = I - R$ using equation (5.22).

4. **Constrained optimization problem:** Solve the constrained optimization problem (5.21) with S^d, p_{F_o} and p_{L_o} as initial guesses.

5. **Design of K_1:** Recover the feedback controller K_1 by means of the design equation (5.23), with S^d and the *optimum* solution M_r^{-1} .

6. **Implementation:** Implement the feedback controller scheme shown in Figure 5.3 with the recovered K_1 and the *optimum* right coprime solutions, i.e., N_r, M_r, X_r and Y_r.

We next present an example to illustrate the above procedure for the design of the feedback controller scheme shown in Figure 5.3.

Example 5.3.1. Consider that the feedback controller scheme in Figure 5.3 is used to control a system that is described by the following nominal model

$$P_o = \frac{5(s+1.3)}{(s+1)(s+2)} \tag{5.25}$$

The uncertainty in the model is parametrised by a multiplicative input uncertainty as in (5.8) with

$$W_1 = \frac{3(s+1)}{(s+20)} \tag{5.26}$$

To design the elements of the feedback controller scheme, a *desired* sensitivity function S^d is imposed from (5.22) with $\varepsilon = 0$, $g = 1$ and $\omega_b = 3$:

$$S^d = \frac{s}{s+3} \tag{5.27}$$

The shape (5.27) provides a first order response with time constant 1/3 seconds. The choice for S^d assures $|R(\omega)| < 1/|W_1(\omega)|$ as we pointed out in Remark 5.3.3.

To proceed with the example, it is necessary to initialize the optimization problem (5.21) with values for the pole placement. We try with $p_{F_o} = [-10 \ -10]^T$ and $p_{L_o} = [-20 \ -20]^T$.

The optimization procedure gives the following *optimal* right coprime factorization, $P_o = M_r^{-1} N_r$,

$$N_r = \frac{3(s+1.3)}{(s+100.0159)(s+100.0139)} \tag{5.28}$$

$$M_r^{-1} = \frac{(s+100.0159)(s+100.0139)}{(s+1)(s+2)} \tag{5.29}$$

and the corresponding Bezout transfer functions,

$$X_r = \frac{s(s+199.7791)}{(s+1.3746)^2} \tag{5.30}$$

$$Y_r = \frac{3317.8(s+1.4606)}{(s+1.3746)^2} \tag{5.31}$$

The desired sensitivity S^d selected in (5.27) and the optimum coprime factor M_r in (5.29) are substituted into equation (5.23) to obtain the final feedback controller K_1. Note that $S^d \doteq I - R$ as we pointed out in equation (5.20). Therefore,

$$K_1 = \frac{(s+1)(s+2)(s+30000)}{10000s(s+1.0002)^2} \tag{5.32}$$

The optimization problem (5.21) provides *optima* N_r, M_r, X_r and Y_r such that the maximum of the magnitude of $N_r(I-R)M_r^{-1} + N_r R X_r$ over all frequencies is minimized. The achieved frequency response for the resulting magnitude is shown in Figure 5.9, in solid line. It is also shown the frequency response of the magnitude of $N_r R X_r$, in dashed line, and the magnitude of the proposed shape, S^d, in dotted line. It should be noted that the optimization problem (5.21) tends to find solutions for X_r and N_r such that the addend $N_r R X_r$ is minimized with fixed R. At the same time, it tends to find solutions for N_r and M_r such that the addend $N_r(I-R)M_r^{-1}$ is minimized with fixed $I - R$.

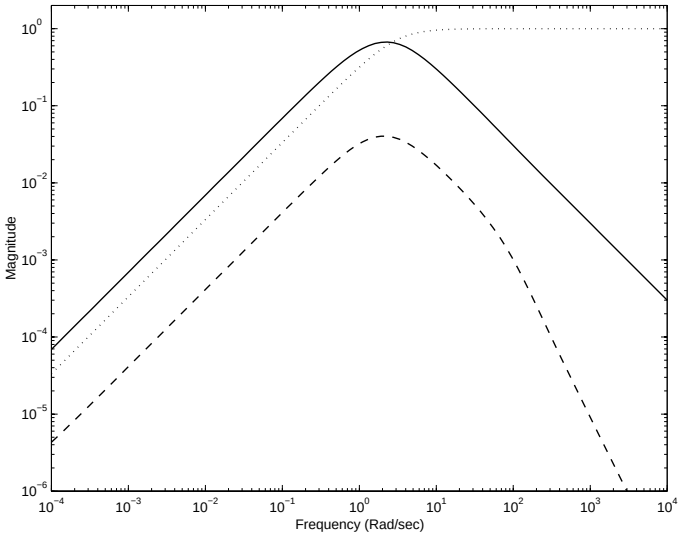

Figure 5.9: Magnitude plots after the optimization problem (5.21): $|N_r(I - R)M_r^{-1} + N_r R X_r|$ (solid) and $|N_r R X_r|$ (dashed). $|S^d|$ (dotted).

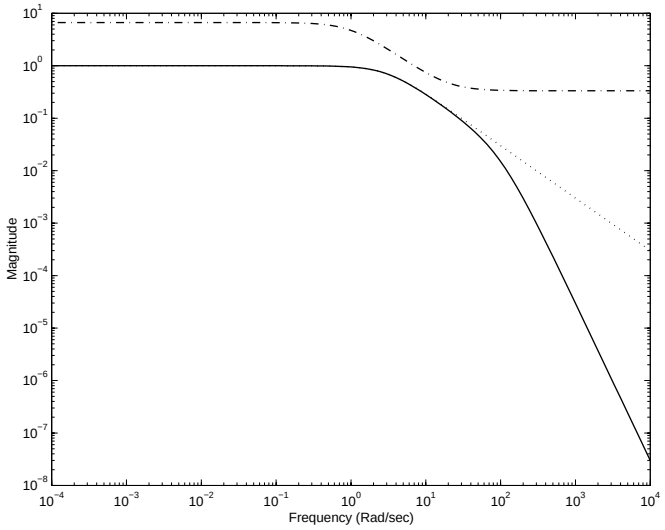

Figure 5.10: Bound for robust stability $|-W_1 M_r R Y_r N_r M_r^{-1}|$ (solid). $|R|$ (dotted) and $|W_1|^{-1}$ (dash-dotted)

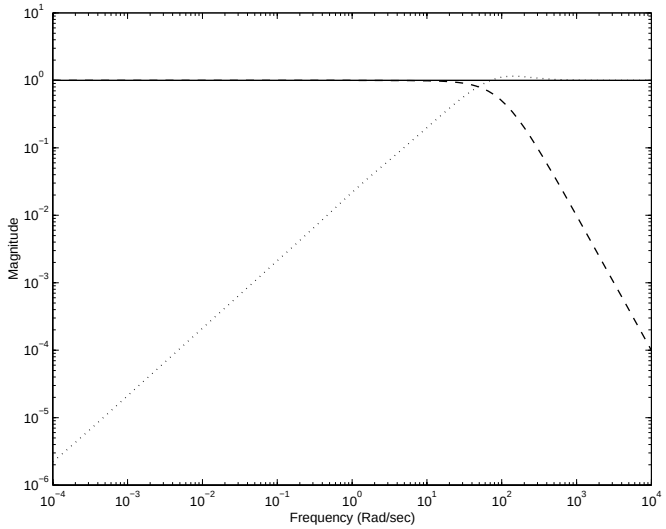

Figure 5.11: Bezout identity (5.2) (solid), $|N_r Y_r|$ (dashed) and $|M_r X_r|$ (dotted).

Figure 5.10 shows the bound for robust stability. The solid line illustrates that $|-M_r R Y_r N_r M_r^{-1}| < 1 \; \forall \omega$, i.e., the constraint on the optimization problem (5.21) is not failed. The dotted line shows the, indirectly fixed, magnitude of R. It is seen that the optimization problem (5.21) finds solutions for N_r, M_r, X_r and Y_r such that $|-M_r R Y_r N_r M_r^{-1}|$ approximates $|R|$. Since the plant is SISO, we have that $|-M_r R Y_r N_r M_r^{-1}| \equiv |R N_r Y_r|$. The term $N_r Y_r$, one of the addends of the Bezout identity (5.2), usually has a low-pass shape as it can be seen in Figure 5.11. This fact hinders $|-M_r R Y_r N_r M_r^{-1}|$ from matching $|R|$ for all frequencies.

The fulfillment of the Bezout identity (5.2) is shown in Figure 5.11 by means of solid line. The magnitude of $N_r Y_r$ and $M_r X_r$ are depicted in dashed and dotted lines, respectively.

△

5.4 Reference controller design

Once the feedback controller K_1 is obtained with the approach presented above, a prefilter controller K_2 has to be found. This controller is in charge

of adapting the reference signal r and providing the *desired* partial state ξ^d. The proposed 2-DOF control configuration is shown in Figure 5.4.

A simple constant prefilter K_2 allows for the commands, r, to enter the feedback control scheme keeping the steady-state accuracy. However, for many tracking problems this will not be sufficient and a dynamic design for the prefilter K_2 is required. Both the design for the static case and for the dynamic case is addressed next.

5.4.1 Static controller

A static inverse-based prefilter can be easily found to accommodate the reference signal r and to provide the *desired* partial state ξ^d. It can be implemented, as

$$K_2 \doteq [N_r(0)R(0)]^{-1} \tag{5.33}$$

This simple choice for the prefilter controller K_2 as scaling factor assures that the nominal closed-loop transfer matrix function from r to the controlled output signal y has unity steady-state gain. It is illustrated by means of an example.

Example 5.4.1. Consider the SISO feedback control system in Example 5.3.1 described by the nominal model P_o (5.25) and the multiplicative uncertainty description characterized by the weight W_1 (5.26). The feedback controller K_1 (5.32) was designed for robust stability together with *optima* right coprime factors N_r, M_r, X_r and Y_r in (5.28 – 5.31).

The inverse-based prefilter K_2 in equation (5.33) is just used to adapt the reference signal r and to guarantee unity steady-state gain. The *optimum* right coprime factor N_r (5.28) evaluated at $\omega = 0$ has a value of $N_r(0) = 3.8988 \cdot 10^{-4}$. The value of R from (5.27), being $R = 1 - S^d$, evaluated at $\omega = 0$ is $R(0) = 1$. Therefore,

$$K_2 = 2564.9 \tag{5.34}$$

Figure 5.12 shows the closed loop step responses for the nominal plant, P_o, and for the uncertain plant, $P \in \mathcal{P}$, with the static prefilter K_2 in (5.34). The step response dynamics are those given by the feedback controller scheme designed in Example 5.3.1.

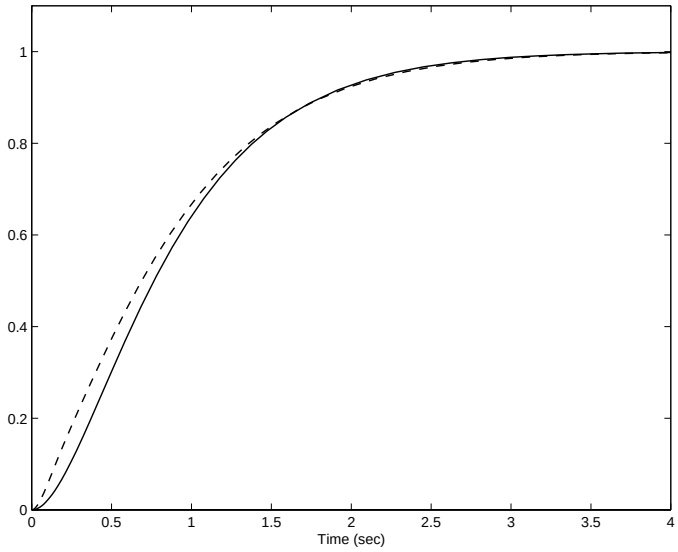

Figure 5.12: Closed loop step responses with the static prefilter K_2 (5.34): nominal plant (solid) and uncertain plant with $W_1\Delta = \text{diag}\{0.2,\ -0.2\}$ (dashed)

△

5.4.2 Dynamic controller

We have pointed out in Example 5.4.1 that a static prefilter controller K_2 allows for the reference signal r to be introduced into the feedback control scheme guaranteeing unity steady-state gain. The resultant step response dynamics are those fixed by the feedback controller structure. Note that in the nominal case, i.e., $P = P_o$, the prefilter controller K_2 sees just $N_r R$. Therefore, the relation from the references r to the outputs y reads as

$$y = N_r R K_2\, r \tag{5.35}$$

It should be noted that the right coprime factor N_r contains the zeros of P_o and the poles p_{F_i} achieved with the *optimum* pole placement; R has been fixed as a design parameter.

To include different and independent dynamics for the step response, we have to take advantage of the second degree of freedom that K_2 provides.

Therefore, the prefilter controller K_2 is designed to force the response of the closed-loop system for all plants $P \in \mathcal{P}$ described in (5.8) to follow that of a specified model, T_{ref}, often called the reference model. The overall design problem is shown in Figure 5.13.

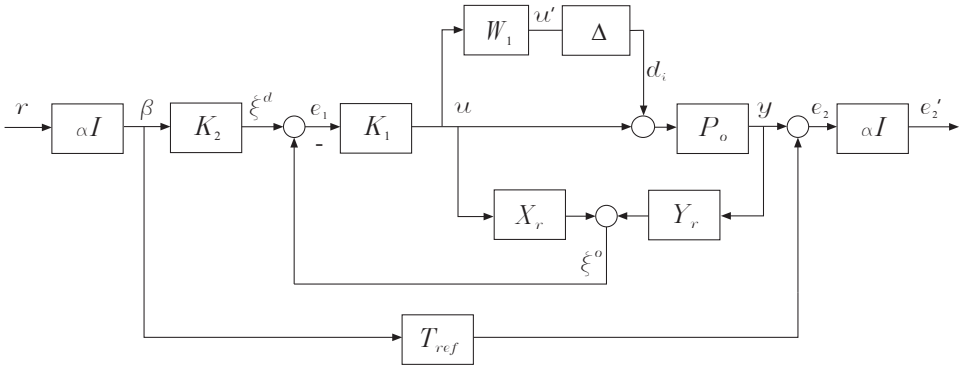

Figure 5.13: The two degrees-of-freedom design problem.

Let us assume that T_{ref} is the desired closed-loop transfer matrix function selected to introduce the desired step response characteristics into the design process (time-domain specifications). Then, the design problem is to find a reference controller K_2 so that the relation form the reference, r, to the output, y, behave as close as possible to that of the reference model, T_{ref}. The design of the reference controller will depend upon the performance criterion chosen for the desired closeness to the reference model T_{ref}. We address the problem to optimal Model Reference controller specifications in an ∞-norm sense. This way, the design of the reference controller turns out to be a Model Matching Problem.

From the overall scheme in Figure 5.13, we can compute the transfer matrix function $\tilde{\mathcal{N}}$ that relates the inputs $[d_i \ r]^T$, i.e., the disturbances d_i and the command signal r, with the outputs $[u' \ e_2']^T$, i.e., the weighted control signal u' and the weighted Model Matching error, e_2',

$$\tilde{\mathcal{N}} = \begin{bmatrix} -W_1 M_r R Y_r N_r M_r^{-1} & \alpha W_1 M_r R K_2 \\ N_r(I-R)M_r^{-1} + N_r R X_r & \alpha^2(N_r R K_2 - T_{ref}) \end{bmatrix} \tag{5.36}$$

Remark 5.4.1. *The relations from the disturbances signal, d_i, are not dependent on the prefilter controller K_2. Moreover, if $r = 0$ and $\alpha = 1$ we have that $e_2' = y$. Then, the relations from d_i are the same as those computed in the first step of the design, i.e. the feedback controller structure, as it can be seen in equation (5.17).*

The scaling parameter α is used to place more attention in model matching, i.e., the (2,2) block, rather than in transfer matrix function from r to u', i.e., the (1,2) block.

In view of Remark 5.4.1, the $\mathcal{H}_\infty$ norm of the complete transfer matrix function (5.36) is minimized to find K_2 without modifying the robust stability margins provided by the feedback controller scheme in the first step of the design, i.e., the (1,2) block.

The 2-DOF design problem shown in Figure 5.13 can be easily cast into the general control configuration shown in Figure 5.14(a).

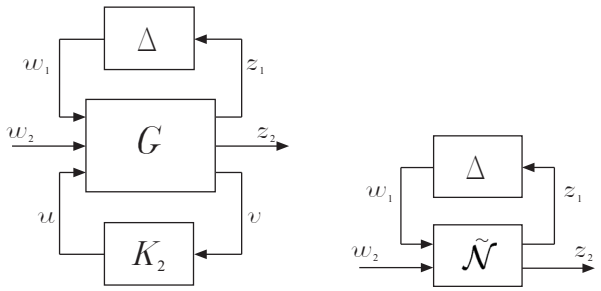

Figure 5.14: General interconnection of system with uncertainty.

The interconnection matrix G in Figure 5.14(a) contains the feedback control scheme with the *optimum* right coprime factors N_r, M_r^{-1}, X_r and Y_r; the controller K_1; the uncertainty weights W_1, W_2 and the scaling factors αI. Comparing Figure 5.13 with the scheme in Figure 5.14(a) we define $w_1 = d_i$, $w_2 = r$, $z_1 = u'$, $z_2 = e_2'$, $v = \beta$ and $u = \xi^d$. The augmented plant G and the controller K_2 are related by the following lower linear fractional transformation:

$$\mathcal{F}_\ell(G, K_2) \doteq G_{11} + G_{12}K_2(I - G_{22}K_2)^{-1}G_{21} \tag{5.37}$$

The lower LFT (5.37) is represented in Figure 5.14(b) by the matrix transfer function $\tilde{\mathcal{N}}$, calculated in (5.36).

The partitioned generalized plant G is:

$$\begin{bmatrix} u' \\ e_2' \\ \hline \beta \end{bmatrix} = \left[\begin{array}{c|c} G_{11} & G_{12} \\ \hline G_{21} & G_{22} \end{array}\right] \begin{bmatrix} d_i \\ r \\ \hline \xi^d \end{bmatrix} \tag{5.38}$$

$$= \left[\begin{array}{cc|c} -W_1M_rRY_rN_rM_r^{-1} & 0 & W_1M_rR \\ N_r(I-R)M_r^{-1} + N_rRX_r & -\alpha^2T_{ref} & \alpha N_rR \\ \hline 0 & \alpha I & 0 \end{array}\right] \begin{bmatrix} d_i \\ r \\ \hline \xi^d \end{bmatrix}$$

The generalized plant (5.38) is to be solved suboptimally for the prefilter controller K_2 using standard algorithms (Doyle *et al.*, 1989).

Remark 5.4.2. *The reference signals r must be scaled by a constant matrix W_r to make the closed-loop transfer function from r to the controlled output y match the desired reference model T_{ref} exactly at steady-state. This is not guaranteed by the optimization problem which aims to minimize the ∞-norm of the error, i.e., $\left\|\alpha^2(N_rRK_2 - T_{ref})\right\|_\infty$. The required scaling is given by*

$$W_r \doteq [K_2(0)N_r(0)R(0)]^{-1}T_{ref}(0) \tag{5.39}$$

Therefore, the resulting reference controller is K_2W_r.

We next present an example to illustrate the design procedure for the model reference robust controller K_2.

Example 5.4.2. To illustrate the design procedure for the dynamic prefilter K_2, let us use the feedback structure designed for the SISO system in Example 5.3.1. It was described by the nominal model P_o (5.25) and the multiplicative uncertainty description characterized by weight W_1 (5.26). The feedback controller K_1 (5.32) was designed for robust stability together with the *optima* right coprime factors N_r, M_r, X_r and Y_r in (5.28 – 5.31).

The following Reference Model is chosen:

$$T_{ref}(s) = \frac{7}{s+7} \tag{5.40}$$

Such Reference Model (5.40) provides first order responses with time constant 1/7 seconds.

To complete the design procedure, an appropriate value for the scalar parameter α have to be selected. A compromise between the relations from the command signal r, i.e., the (1,2) and (2,2) blocks in the transfer matrix (5.36), have to be found. Figure 5.15 represents the magnitude over the frequency of the product $M_r R K_2$, where K_2 has been computed for increasing values of α, i.e., $\alpha = 1, 2, 4, 6, 8 \text{and} 10$. Bottom line corresponds to $|M_r R K_2|$ for $\alpha = 1$; the top line corresponds to $|M_r R K_2|$ for $\alpha = 10$. We can observe that, for $\alpha = 10$ we have that $|M_r R K_2| > 1$. Since we are not interested in amplifying the control signal u, we will not chose values for α greater than 8.

Figure 5.16 illustrates the magnitude of the closed-loop relation from r to y, i.e., $N_r R K_2$, over the frequency, where K_2 has been computed for $\alpha = 1, 2, 4, 6, 8 \text{and} 10$. The curve with the largest peak at 2.85 corresponds to $\alpha = 1$. We see that the larger the value of α, the smaller the peak of the closed loop relation and the better the model matching. Therefore, we choose $\alpha = 8$ which assures a good model matching without amplification of the control signal.

The reference model T_{ref}, the *optimum* right coprime factorization M_r, N_r in (5.29 – 5.28), the corresponding Bezout components X_r, Y_r in (5.30 – 5.31) and the desired sensitivity S^d in (5.27) are used to build the generalized plant P as that in (5.38). The controller K_2 is designed by applying standard $\mathcal{H}_\infty$ algorithms to the generalized plant P (Balas *et al.*, 1998), (Chiang and Safonov, 1992).

The achieved prefilter controller K_2 has 11 states. A balanced realization and an optimal Hankel norm approximation on the state-space of K_2 provide a 4th order controller. The bode plots for the achieved controller and the reduced controller are shown in Figure 5.17. A state-space realization of the 4th order reduced controller is given in Table C.3.

Figure 5.18 illustrates the closed loop time responses to a unity setpoint change. The response for the nominal plant is shown in solid line and that for the uncertain system is in dashed line. The response for the target model (5.40) is shown in crosses.

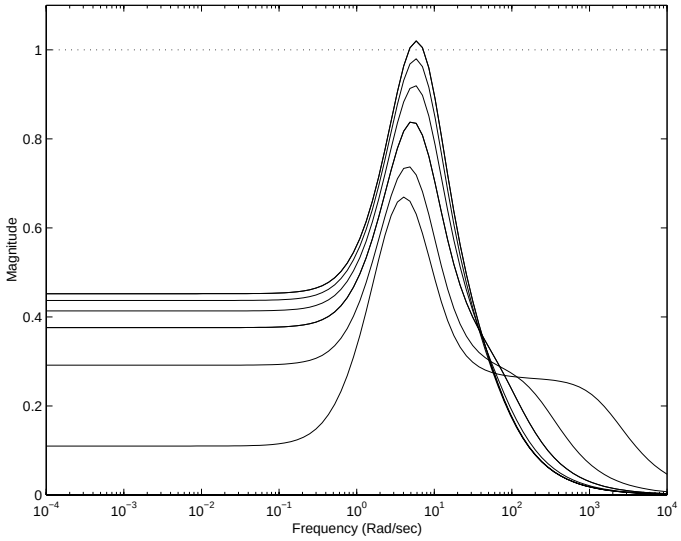

Figure 5.15: Relation from r to u: $|M_r R K_2|$ for $\alpha = 1,\ 2,\ 4,\ 6,\ 8$ and 10.

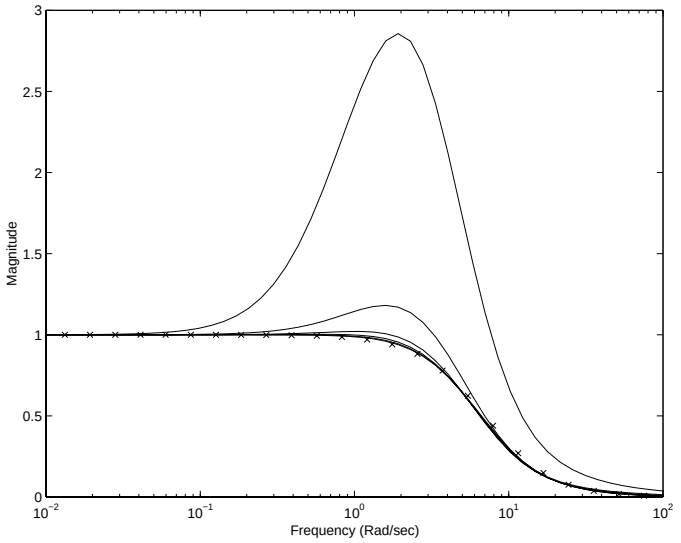

Figure 5.16: Relation from r to y: $|N_r R K_2|$ for $\alpha = 1,\ 2,\ 4,\ 6,\ 8$ and 10 (solid). Target model, (5.40) (croses).

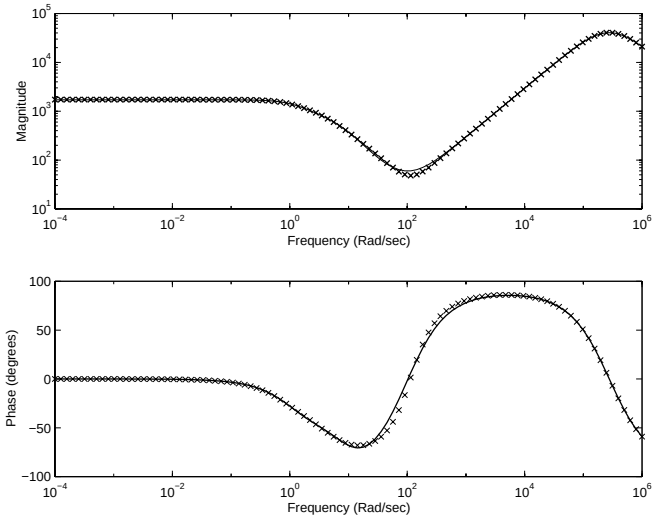

Figure 5.17: Frequency Bode plot for the 11th order prefilter controller K_2 (solid) and its 4th order optimal Hankel norm approximation (crosses).

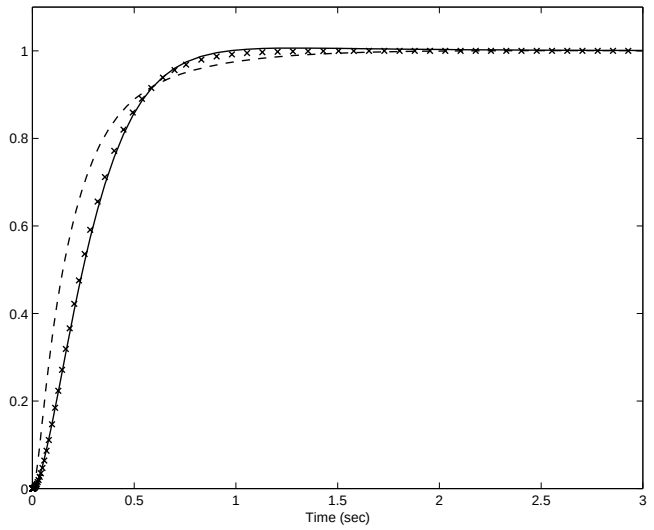

Figure 5.18: Closed loop step responses with the dynamic prefilter controller K_2 given in (C.3): nominal plant (solid) and the uncertain plant (dashed). Step response for of the target model (5.40) (crosses) $\triangle$.

In Example 5.3.1, we showed the design methodology for the feedback control scheme. A feedback controller K_1 was found by fixing a desired sensitivity transfer matrix function S^d and solving a $\mathcal{H}_\infty$ optimization problem for the poles of the right coprime factors N_r, M_r, X_r and Y_r to assure robust stability. In Example 5.4.1, we showed how a constant prefilter controller could be used to adapt the reference command, i.e., $\xi^d = K_2\, r$, providing input/output unity steady-state gain. The dynamics of such a 2-DOF control configuration were provided by the feedback control structure with $y = N_r R\, \xi^d$ for the nominal case. In Example 5.4.2, we showed how a prefilter controller could be designed to provide extra input/output dynamics to those given by the feedback control structure. In fact, this is the task of this prefilter controller and has been designed to provide robust model reference responses. Next Section evaluates the proposed design methodology to the control of the distillation column described in Appendix B.2.

5.5 Application Example

The proposed approach is applied to the control of a high purity distillation system to illustrate the design procedure. The original control problem was formulated by (Skogestad *et al.*, 1988) as a bound on the weighted sensitivity with frequency bounded input uncertainty. The optimal solution to this problem is provided by the one degree-of-freedom $\mu-$optimal controller discussed in Example 2.4.1.

The following is an idealized dynamic model of the distillation column described in detail in Appendix B.2,

$$P_o = \frac{1}{75s+1}\begin{bmatrix} 87.8 & -86.4 \\ 108.2 & -109.6 \end{bmatrix} \tag{5.41}$$

A relative uncertainty on each manipulated variable is considered with magnitude

$$w_I = 0.2\frac{5s+1}{0.5s+1} \tag{5.42}$$

The weight w_I in (5.42) may approximately represent a 20 % gain error and a neglected time delay of 0.9 min. $|w_I(j\omega)|$ levels off at 2 (200 % uncertainty) at high frequencies. This description of the uncertainty is the one

selected for our control system. This relative uncertainty can be written in terms of two scalar multiplicative perturbations Δ_L and Δ_V

$$\begin{array}{rcll} dL & = & (1 + w_I \Delta_L) dL_c, & |\Delta_L| \leq 1 \, \forall \omega \\ dV & = & (1 + w_I \Delta_V) dL_c, & |\Delta_V| \leq 1 \, \forall \omega \end{array} \tag{5.43}$$

where dL and dV are the actual inputs, while dL_c and dV_c are the desired values of the flow rates as computed by the controller K_1. Equation (5.43) can be approximated by an "unstructured" single perturbation,

$$\begin{pmatrix} dL \\ dV \end{pmatrix} = (I + W_2 \Delta W_1) \begin{pmatrix} dL_c \\ dV_c \end{pmatrix}, \;\; \bar{\sigma}(\Delta) \leq 1 \, \forall \omega \tag{5.44}$$

where Δ is a "full" 2×2 matrix, $W_1 = w_I I$ and $W_2 = I$.

Either the original control problem by (Skogestad *et al.*, 1988) and several similar formulations (Green and Limebeer, 1995), (Morari and Zafirou, 1989) among others, considered a bound on the weighted sensitivity, which allowed responses with closed-loop time constant of 20 min.

Our design procedure starts by choosing the following *desired* sensitivity function S^d:

$$S^d = \frac{s}{s + 1.5} I_2 \tag{5.45}$$

This corresponds to a first order response with time constant of approximately 1 minute. The choice for S^d satisfies $\bar{\sigma}(R) \leq 1/\underline{\sigma}(W_1)$ we pointed out in Remark 5.3.3.

To initialize the optimization problem (5.21) we choose $p_{F_o} = [-1 \;\; -1]^T$ and $p_{L_o} = [-10 \;\; -10]^T$ as values for the pole placement. State-space realizations of the *optimal* right coprime factors, M_r^{-1}, N_r, are given in (C.6) and (C.5); state-space realizations of the *optimal* associated Bezout complements, X_r, N_r, are given in (C.7) and (C.8).

The feedback controller K_1 is achieved by substituting the *optimal* solution M_r^{-1} (C.7) and S^d (5.45) in to equation (5.23), where $S^d = I - R$ as we pointed out in equation (5.20). A state-space realizations of K_1 is given in (C.9).

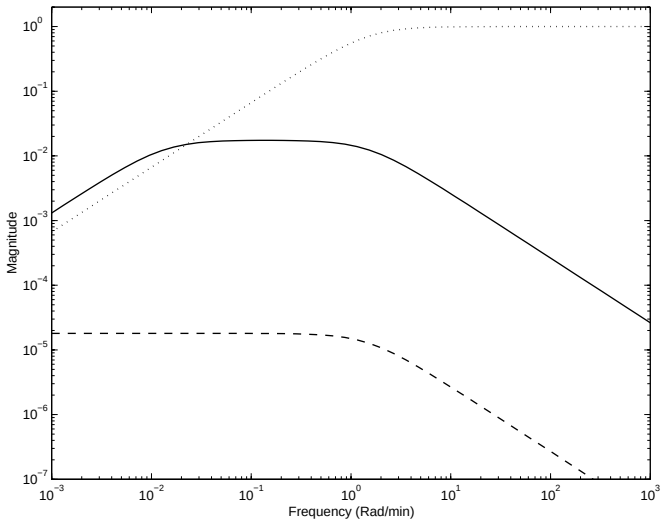

Figure 5.19: Largest singular values plot after the optimization problem (5.21): $\bar{\sigma}(N_r(I-R)M_r^{-1}+N_rRX_r)$ (solid) and $\bar{\sigma}(N_rRX_r)$ (dashed). $\bar{\sigma}(S^d)$ (dotted).

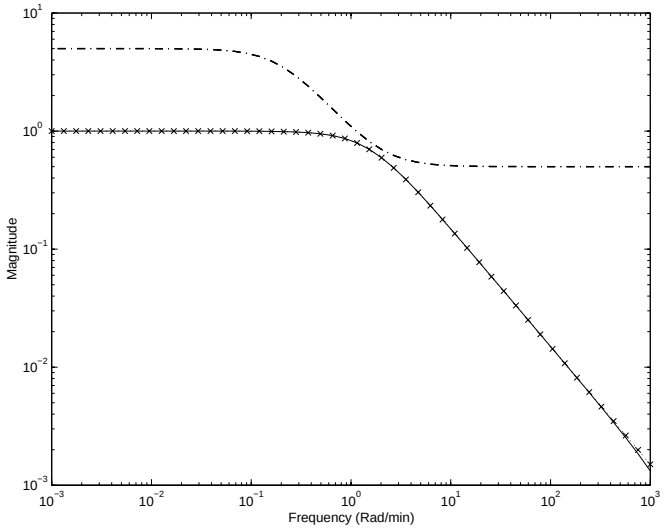

Figure 5.20: Robust stability bounds: $\bar{\sigma}(M_rRY_rN_rM_R^{-1})$ (solid) and $\bar{\sigma}(W_1^{-1})$ (dash-doted). $\bar{\sigma}(R)$ (crosses).

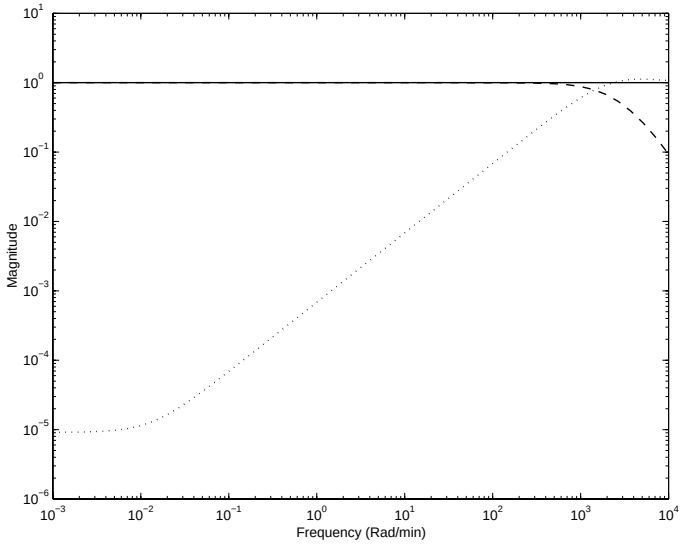

Figure 5.21: Bezout identity (5.2) (solid), $\bar{\sigma}(N_r Y_r)$ (dashed) and $\bar{\sigma}(M_r X_r)$ (dotted).

Figure 5.19 shows, in solid line, the achieved largest singular values plot of transfer matrix function between d_i and y, i.e., $\bar{\sigma}(N_r(I-R)M_r^{-1}+N_r R X_r)$. The resultant largest singular values plot of the addend $N_r R X_r$ is also plotted over the frequency in dashed line. The frequency response of the *desired* sensitivity in (5.45) is also shown in dotted line. Figure 5.20 illustrates, in solid line, the fulfillment of the robust stability condition, i.e., $\bar{\sigma}(M_r R Y_r N_r M_R^{-1}) < \bar{\sigma}(W_1^{-1})$. The curve in crosses illustrates the frequency response of $\bar{\sigma}(R)$ which is linked up with the desired sensitivity S^d by means of (5.20). Since S^d is chosen such that $\bar{\sigma}(R) < \bar{\sigma}(W_1^{-1})$, the optimization problem (5.21) has to compute N_r, M_r, X_r and Y_r such that $\bar{\sigma}(N_r(I-R)M_r^{-1}+N_r R X_r)$ is minimized and $\bar{\sigma}(M_r R Y_r N_r M_r^{-1}) < \bar{\sigma}(W_1^{-1})$. The Bezout identity is shown in Figure 5.21. Also, the largest singular values of $N_r Y_r$, e, and $M_r X_r$, in dashed line and in dotted line, respectively.

To proceed with the second step of our design methodology, the reference model for the step response is selected as

$$T_{ref} = \frac{0.12}{s+0.12} I_2 \tag{5.46}$$

which is the same chosen in (Limebeer *et al.*, 1993) and provides a first order response with a time constant of approximately 8 minutes. The design procedure is completed by choosing an appropriate value for the scalar α. We choose $\alpha = 10$.

The achieved prefilter controller K_2 has 14 states. A balanced realization and an optimal Hankel norm approximation of order 6 on the state-space of K_2 provides a controller with a state-space realization given in (C.10).

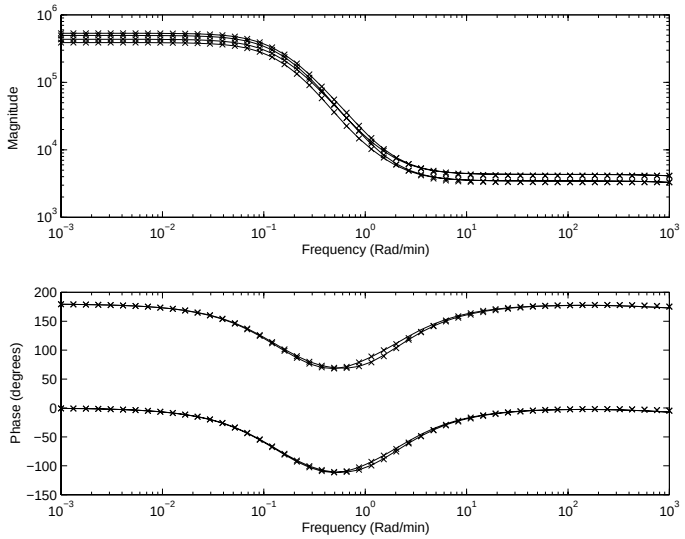

Figure 5.22: Frequency Bode plot for the 14th order prefilter controller K_2 (solid) and its 6th order optimal Hankel norm approximation (crosses).

Figure 5.22 shows, in solid line, the singular values Bode plot for the 14th states prefilter controller K_2 and the 6th states reduced controller in crosses.

As it is pointed out in Remark 5.4.2, it is necessary to scale the command signal r for steady-state accuracy. From equation (5.39) we chose the matrix W_r to be

$$W_r = \begin{bmatrix} 42.1863 & -32.1447 \\ -32.1437 & 27.7045 \end{bmatrix} \tag{5.47}$$

The time responses of y_1 and y_2 for setpoint change in y_1 is shown in Figure 2.15 for the nominal and the six perturbed plants $P(s) = P_o(s)E_{I_i}$

given in (B.11) and (B.12). The responses for the nominal plant are illustrated in solid lines and the time responses for the perturbed plants appear in dashed lines. The responses are not completely decoupled but show no strong sensitivity to the uncertainty. The step responses of the reference model T_{ref} are depicted with crosses.

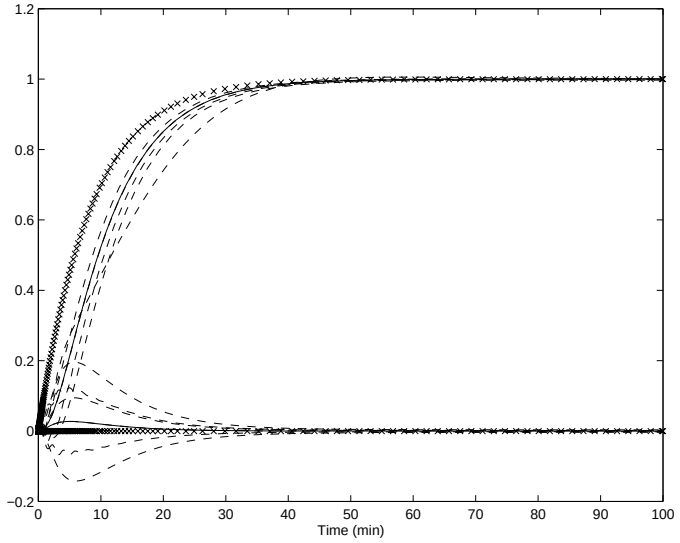

Figure 5.23: Closed-loop setpoint change: response for the nominal plant P_o (solid) and for the uncertain plants $P_i = P_o E_{I_i}$, $i = 1, \ldots, 6$ (dashed). Step response of the targed model T_{ref} (crosses).

5.6 Summary

A new 2-DOF control configuration based on a right coprime factorization of the model of the plant has been presented by using the partial state as controlled variable. The approach has been presented as an alternative to the commonly encountered strategy of setting the two controllers arbitrarily, with internal stability the only restriction, and parameterizing the controller in terms of the Youla parameter.

An observer-based feedback control scheme has been designed first to guarantee some levels of stability robustness. A feedback controller K_1 has been found by fixing a desired sensitivity transfer matrix function S^d and

solving a constrained $\mathcal{H}_\infty$ optimization problem for the poles of the right coprime factors N_r, M_r, X_r and Y_r.

Then, a prefilter controller has been computed. We have seen how to use a constant prefilter controller to adapt the reference command, i.e., $\xi^d = K_2 r$, providing input/output unity steady-state gain. In such a case, we have seen that the dynamics of the 2-DOF control configuration are provided by the feedback control structure with $y = N_r R\, \xi^d$ for the nominal case. We have shown how to design a prefilter controller to provide extra input/output dynamics to those given by the feedback control structure. Since this is the task of this prefilter controller it has been designed to provide robust model reference responses.

The proposed 2-DOF has been evaluated on a high purity distillation system. We have shown that our design procedure may be used to meet a demanding mixture of robust stability and robust performance specifications.

Chapter 6

Conclusions and Further Research

In this Chapter we recall the main conflicting objectives and the trade-offs that have to be done when a control system is to be designed and we summarize the main contributions presented in this work. In addition, some proposals for further research are introduced.

6.1 Conclusions

Control system analysis and design have to consider the existence of two different classes of properties, say *open-loop* and *feedback* properties. Whereas the former are concerned with the system responses to commands, the later are related to stability and disturbances rejection.

It is well-known that many design methodologies are focused on feedback control design. Nevertheless, what some approaches do is simply to design a feedback controller but not necessarily the feedback properties. For this reason, if we design for open-loop specifications, the final achieved feedback properties may not be satisfactory. Therefore, a trade-off have to be made in order to attain both kind of specifications.

Another point to consider in the analysis and design of a control system is the presence of some kind of uncertainty associated with the model of the plant. Effectively, such inherent uncertainty will affect both the open-loop and feedback properties. However, uncertain is usually considered as

affecting the feedback properties. The reason is obvious: a deterioration of feedback properties may cause more harmful operating conditions than an impairment of open-loop properties, i.e., instability is always undesirable while a deterioration of the command responses may be, in some cases, tolerated.

In this work we have presented two different approaches to figure out the above mentioned problems. We have referred them as the robustness enhancement and the 2-DOF approach.

6.1.1 The Robustness Enhancement approach

The Observer-Controller configuration for Robustness Enhancement allows a two-step design procedure: first, an initial feedback control system is set for *high performance* in terms of nominal command responses and second, the resulting *robustness* properties properties, which are associated with feedback properties, are conveniently enhanced while leaving unaltered the step responses provided by the initial controller.

Main points and contributions

The most important contributions with the robustness enhancement configuration are summarized next:

The presented approach is not based on reformulating a central controller in the Youla parametrisation of the stabilizing controllers from a nominal plant and then optimizing for the Youla parameter to get the final, *robustified*, controller.

Instead, an initial feedback control system is set for the nominal plant to satisfy some step response requirements. In the second stage of the design, the resulting robustness properties are conveniently enhanced while leaving unaltered the step responses provided by the initial controller. Therefore,

1.- *The Observer-Controller configuration for Robustness Enhancement allows to take profit of the well established feedback design methodologies for the nominal feedback controller.*

The resulting control configuration can be seen as a double feedback control configuration. The former stands for high performance nominal requirements in terms of step response; the later accounts for stability in presence of uncertainty.

We have pointed out that many standard design methodologies are mainly concentrated on the design of a one degree-of-freedom feedback control system. Such a control configuration cannot perform a separation between open-loop and feedback requirements. Nevertheless, classical control approaches tend to stress the use of feedback to modify open-loop properties. For such a reason,

2.- *The Observer-Controller configuration for robustness enhancement contributes in avoiding the conflicting objectives in standard 1-DOF feedback control configuration.*

The resulting two-step design control configuration can be seen as a two degrees-of-freedom control configuration. Strictly speaking, we have presented the 2-DOF control configurations as an structure that is able to perform a completely separation of properties in terms of a different processing for both the command signals and the output signals. Nevertheless, the separation principle can also be interpreted in a different direction, that is to say, a separation in terms of a different processing for the *nominal* high performance properties and the robustness properties.

For all this reasons,

3.- *The Robustness Enhancement approach is presented as an alternative to the design of a robust feedback control system.*

6.1.2 The 2-DOF approach

Two degrees-of-freedom controllers turns up to be a solution to avoid the dependence between open-loop and feedback properties, inherent in standard feedback control. It is known that 2-DOF control configurations have the attribute to deal separately with performance, in terms of command tracking, and robustness properties. Nevertheless, 2-DOF control configurations are not used as expected due to the lack of methodologies for an straightforward design of both compensators. Actually, the approaches found in the literature are mainly based on setting the two controllers arbitrarily, with internal stability the only restriction, and parameterizing the controller in terms of the Youla parameter.

In this work we have presented a new 2-DOF control configuration within the framework of fractional representation. By using the partial state as controlled variable, we have developed an observer-based feedback control scheme to guarantee some levels of stability in presence of uncertainty, i.e.,

robust stability. Since uncertainty also affects the command response performance, a prefilter controller has been designed to cope with the command responses for the uncertain system, i.e., robust performance.

Main points and contributions

Some important contributions can be drawn from the way to the solution:

The feedback controller has been found by fixing a desired sensitivity transfer (matrix) function and solving a constrained $\mathcal{H}_\infty$ optimization problem. The arguments of the optimization problem are the poles of the right coprime factors of the plant and the observer. Therefore,

1.- *The feedback control configuration is made up with an optimum right coprime factorization of the model of the plant and an optimum observer.*

The prefilter controller has been computed by means of a Model Reference problem. Therefore,

2.- *The prefilter controller is designed by solving a model matching problem such that the response of the overall close-loop system match that of the reference model.*

Finally,

3.- *The approach to design the 2-DOF control configuration can be seen as an alternative to the design methodologies mainly based on optimization problems in terms of a Youla parameterization.*

6.2 Further research

CDC benchmark problem[1]: The original high-purity distillation column benchmark problem has been used in the literature to test robust control approaches. Likewise, it has been employed through this work to experiment with the proposed design procedures. The original benchmark problem formulation is unrealistic since there is no bound on the input magnitudes and the bounds on the performance and uncertainty are given in the frequency domain (in terms of weighted $\mathcal{H}_\infty$ norm). A different formulation is that of the CDC benchmark problem, where the uncertainty is defined in terms of parametric gain and delay uncertainty and the control objectives are a

[1] (Limebeer, 1991)

mixture of time domain and frequency domain specifications. Such specifications cannot be directly transformed into frequency dependent weights and have to be approximated to fit into our design procedure. Imminent research is focused on evaluating our controller configurations with the CDC benchmark problem and comparing the results with that of similar approaches in the literature.

Parametrization of Linear Observers: The Bezout identity represents the basic equation for the reconstruction of the controlled signal, i.e., the partial state. We have pointed out that, by application of a Youla type parametrization, it is possible to characterize the set of linear observers (that gives the partial state) as the set of solutions to the Bezout identity. In broad terms, further research may be focused on analyzing in depth the characterization of the set of linear observers achieved through the pole placement procedure instead of the usual Youla parametrization.

Adaptive pole placement: The feedback control structure of the proposed 2-DOF control configuration is designed by solving a constrained $\mathcal{H}_\infty$ optimization problem over the poles of the right coprime factors of the plant and the observer. Then, it seems interesting to study the application of recent advances in adaptive control theory for the arguments, i.e., the poles, of the right coprime factors of the plant and the observer.

Adaptive reference controller: Application of adaptive control techniques could also be applied to the prefilter controller in order to enhance the robust tracking performance.

Appendix A

Background matrix theory

This Appendix reviews some basic topics of matrix theory and they are included as background material. A very extensive treatment of the issues dealt in this Appendix can be found, for example, in (Gantmakher, 1990).

A.1 Eigenvalues and eigenvectors

Let $A \in \mathcal{C}^{n\times n}$. Then the *eigenvalues* of A, i.e., $\lambda_i,\ i = 1, \ldots, n$, are the n solutions to the n'th order characteristic equation

$$\det(A - \lambda I) = 0 \tag{A.1}$$

A nonzero vector $x \in \mathcal{C}^n$ that satisfies

$$Ax = \lambda x \tag{A.2}$$

is referred to as *right eigenvector*, or simply *eigenvector*, of A. Dually, a nonzero vector y is called *left eigenvector* of A if

$$y^H A = \lambda y^H \tag{A.3}$$

The set of eigenvalues of A is called the *spectrum* of A. The magnitude of the largest eigenvalue of the matrix A is called *spectral radius*, denoted by $\rho(A) \doteq \max_i |\lambda_i(A)|$ (See Section A.2.5 for more).

A.2 Norms

Let V be al vector space over the field $\mathcal{C}$ of complex numbers and let $x \in V$ be a vector, matrix, signal or system. Then, a *norm* on V of x is a real number, denoted $\|x\|$, if and only if the the following properties are satisfied:

$$\|x\| > 0 \;\; \forall x \in V, \; x \neq 0 \quad \text{(Positivity)} \tag{A.4}$$

$$\|x\| = 0 \text{ iff } x = 0 \quad \text{(Positivedefiniteness)} \tag{A.5}$$

$$\|\alpha x\| = |\alpha| \, \|x\| \;\; \forall \alpha \in \mathcal{C}, \; \forall x \in V \quad \text{(Homogeneity)} \tag{A.6}$$

$$\|x + y\| \leq \|x\| + \|y\| \;\; \forall x, y \in V \quad \text{(Triangle inequality)} \tag{A.7}$$

Therefore, a norm is a single number that measures the "size" of an element of V. We will briefly deal with the norm on four different objects, i.e., norms on four different vector spaces: vectors x, constant matrices A, time dependent signals $x(t)$ and transfer functions $G(s)$.

A.2.1 Vector norms

Let us consider the vector space V over the field $\mathcal{C}^n$. A vector $x \in \mathcal{C}^n$ means that $x = [x_1 \; x_2 \; \ldots \; x_n]$ with $x_i \in \mathcal{C}, \forall i$. Then, the vector p-norm is:

$$\|x\|_p \doteq \left(\sum_{i=1}^{n} |x_i|^p \right)^{1/p} \quad \forall p \geq 1 \tag{A.8}$$

Three commonly used norms on $\mathcal{C}^n$ are:

Vector 1-norm:

$$\|x\|_1 \doteq \sum_{i=1}^{n} |x_i| \tag{A.9}$$

Vector 2-norm (Euclidean norm): This is the most common vector norm and corresponds to the shortest distance between two points.

$$\|x\|_2 \doteq \left(\sum_{i=1}^{n} |x_i|^2\right)^{1/2} \tag{A.10}$$

Vector ∞-norm: This is the largest element magnitude in the vector.

$$\|x\|_\infty \doteq \max_{1\le i\le n} |x_i| \tag{A.11}$$

A.2.2 Matrix norms

Let us consider the vector space V over the field $\mathcal{C}^{m\times n}$ be the set of all $m \times n$ matrices A with elements in $\mathcal{C}$. Then, a *norm* on V of a matrix A is a matrix norm if, in addition to the four properties, i.e., positivity, positive definiteness, homogeneity and triangle inequality, it also satisfies the multiplicative property,

$$\|AB\| \le \|A\| \cdot \|B\| \qquad \text{Multiplicative} \tag{A.12}$$

Four commonly used norms on $\mathcal{C}^{m\times n}$ are:

Sum matrix norm: This is the sum of the element magnitudes.

$$\|A\|_{\text{sum}} \doteq \sum_{i=1}^{m}\sum_{j=1}^{n} |a_{ij}| \tag{A.13}$$

Frobenius matrix norm (or Euclidean norm): This is the square root of the sum of the squared element magnitudes.

$$\|A\|_{\text{F}} \doteq \left(\sum_{i=1}^{m}\sum_{j=1}^{n} |a_{ij}|^2\right)^{1/2} = \sqrt{\text{tr}(A^H A)} \tag{A.14}$$

where $\text{tr}(\cdot)$ is the trace of a matrix i.e., the sum of the diagonal elements, and A^H denotes the complex conjugate transpose of A.

Max element norm: This is the largest element magnitude.

$$\|A\|_{\max} \doteq \max_{i,j} |a_{ij}| \tag{A.15}$$

This norm is not a matrix norm as it does not satisfy the multiplicative property A.12. It can be shown that $\sqrt{nm}\,\|A\|_{\max}$ is a matrix norm.

We have considered matrices as elements of a linear space. Next, we will consider matrices as representation of linear applications and will relate the matrix norms to the vector norms.

Let $\|\cdot\|$ be a norm on V_1 over $\mathcal{C}^n$ and a norm on V_2 over $\mathcal{C}^m$. Let A be a linear application from V_1 into V_2,

$$A : V_1 \mapsto V_2 \tag{A.16}$$

Then, the *induced norm* is defined as

$$\|A\|_{ip} \doteq \max_{x \neq 0} \frac{\|Ax\|_p}{\|x\|_p} \tag{A.17}$$

where $\|x\|_p$ is the vector p-norm defined in (A.8).

The vector x may be interpreted as a signal entering a linear system represented by the matrix A. The output signal may be represented by the vector $y = Ax$. The "gain" of the matrix A may be considered as the ratio $\|y\| \,/\, \|x\|$. Then, the maximum gain for all possible input directions is given by the induced norm in (A.17), i.e., the direction of the vector x such that the ratio $\|y\|_p \,/\, \|x\|_p$ is maximized. The induced norm in (A.17) can be equivalently represented as

$$\|A\|_{ip} = \max_{\|x\|_p = 1} \|Ax\|_p \tag{A.18}$$

A.2.3 Signal norms

A temporal norm on a time-varying (or frequency-varying) signal is computed by summing up the channels at a given time (or frequency) using a vector norm and, then summing up in time (or frequency) using a temporal norm. Usually, the same norm is employed for both the vector and the signal. A temporal p-norm may be defined as:

$$\ell_p \text{ norm}: \quad \|x(t)\|_p \doteq \left(\int_{-\infty}^{\infty} \sum_{i=1}^{n} |x_i(\tau)|^p \, d\tau \right)^{1/p} \quad \forall p \geq 1 \tag{A.19}$$

Three temporal norms of signals are commonly used:

ℓ_1 **norm:** Known as integral absolute error (IAE).

$$\|x(t)\|_1 \doteq \int_{-\infty}^{\infty} \sum_{i=1}^{n} |x_i(\tau)|^p \, d\tau \tag{A.20}$$

ℓ_2 **norm:** Known as quadratic norm or integral square error(ISE).

$$\|x(t)\|_2 \doteq \left(\int_{-\infty}^{\infty} \sum_{i=1}^{n} |x_i(\tau)|^p \, d\tau \right) \tag{A.21}$$

ℓ_∞ **norm:** This is the pack value in time.

$$\|x(t)\|_\infty \doteq \sup_{\tau} (\max_{1 \le i \le n} |x_i(\tau)|) \tag{A.22}$$

A.2.4 System norms

A frequency domain analysis of a scalar system, e.g., the study of the gain variation through the frequency, allows to determine its performance and stability characteristics. Such analysis procedures can be extended to multivariable systems through the concept of the matrix norm induced by a vector norm. As we saw above, the induced norm provides a "size" generalization of a liner application. This generalization is done by relating the "size" (norms) we have defined for the related vector spaces.

A matrix transfer function $F(s)$ can be seen as a linear application between two spaces, i.e.,

$$F(s) : \mathcal{U} \mapsto \mathcal{Y} \tag{A.23}$$

where $\mathcal{U}$ contains the set of input signals and $\mathcal{Y}$ contains the set of output signals. In fact, there is one linear application for each value of the frequency.

From a system theory point of view the spaces $\mathcal{U}$ and $\mathcal{Y}$ represents the sets of physical signals and the application $F(s)$ represents the system. In such case, relevant system norms are the $\mathcal{H}_2$ and $\mathcal{H}_\infty$.

$\mathcal{H}_2$ **norm:** Assuming a strictly proper system $F(s)$, the $\mathcal{H}_2$ norm is defined as

$$\|F(s)\|_2 \doteq \left(\frac{1}{2\pi}\int_{-\infty}^{\infty} \mathrm{tr}(G(j\omega)^H G(j\omega))\, d\omega\right)^{1/2} \tag{A.24}$$

For numerical computation of the $\mathcal{H}_2$ norm (A.24), the state-space realization of $F(s) = C(sI - A)^{-1}B$ is considered and then

$$\|F(s)\|_2 = \sqrt{tr(B^T Q B)} \tag{A.25}$$

where Q is the observability Gramian obtained as solution a Lyapunov equation (Doyle *et al.*, 1989).

The standard $\mathcal{H}_2$ optimal control problem is to find a stabilizing controller K for the plant P which minimizes $\|F(s)\|_2$ with $F \doteq \mathcal{F}_\ell(P, K)$. See for example, (Doyle *et al.*, 1992) or (Zhou *et al.*, 1996).

$\mathcal{H}_\infty$ norm: Assuming a proper system $F(s)$, the $\mathcal{H}_\infty$ norm is defined as

$$\|F(s)\|_\infty \doteq \max_\omega \bar{\sigma}(F(j\omega)) \tag{A.26}$$

where the singular value (induced 2-norm) is used spatially, i.e., for the matrix, and the resultant peak value, as a function of the frequency, is picked out.

For numerical computation of $\mathcal{H}_\infty$ norm (A.26), the state-space realization of $F(s) = C(sI - A)^{-1}B$ is considered. The smallest γ is found such that the Hamiltonian matrix H has no eigenvalues on the imaginary axis, where

$$H = \begin{bmatrix} A + B\hat{R}^{-1}D^T C & B\hat{R}^{-1}B^T \\ -C^T(I + D\hat{R}^{-1}D^T)C & -(A + B\hat{R}^{-1}D^T C)^T \end{bmatrix} \tag{A.27}$$

and $\hat{R} = \gamma^2 I - D^T D$. This is an iterative procedure in which a large value of γ is used to start and it is reduced until imaginary eigenvalues for H appear. This can be solved using standard algorithms (Doyle *et al.*, 1989).

The standard $\mathcal{H}_\infty$ optimal control problem is to find a stabilizing controller K for a plant P such that $\|F(s)\|_\infty < \gamma$ with $F \doteq \mathcal{F}_\ell(P, K)$. The $\mathcal{H}_\infty$ norm (A.26) is the peak of the maximum singular values of the transfer function. By introducing weights, the $\mathcal{H}_\infty$ norm can be interpreted as the magnitude of some close-loop transfer function relative to a specified upper bound. See for example, (Doyle *et al.*, 1992) or (Zhou *et al.*, 1996).

A.2.5 The spectral radius

The spectral radius $\rho(A)$ is the magnitude of the largest eigenvalue of the matrix A,

$$\rho(A) = \max_i |\lambda_i(A)| \tag{A.28}$$

The spectral radius is not a norm as it does not satisfy the properties (A.5) and (A.7). Nevertheless, it provides a lower bound on any matrix norm as it is stated by the following Theorem.

Theorem A.2.1. *Let $\|A\|$ represent either a matrix norm or an induced norm. Then,*

$$\rho(A) \leq \|A\| \tag{A.29}$$

Proof: *Let as assume that $\lambda_i(A)$ is an eigenvalue of A. Then, from equation (A.2) and the homogeneous property (A.6) we can write*

$$|\lambda_i| \cdot \|x_i\| = \|\lambda_i x_i\| = \|Ax_i\| \leq \|A\| \cdot \|x_i\| \tag{A.30}$$

The last inequality follows from the multiplicative property (A.12) in with we choose the matrix B to be a vector, i.e., $B = x_i$. Thus, for any matrix norm $|\lambda_i(A)| \leq \|A\|$ and as long as it holds for all eigenvalues, the result follows. □

A.3 Singular Value Decomposition

A very useful tool in matrix analysis is the *Singular Value Decomposition* (SVD). The singular values of a matrix are good measures of the "size" of the matrix and that the corresponding singular vectors are good indicators of strong/weak input or output directions.

Definition A.3.1. (SVD) Any complex $n \times m$ matrix A may be factorized into a singular value decomposition

$$A = U\Sigma V^H = \sum_{i=1}^{k} \sigma_i(A) u_i v_i^H \tag{A.31}$$

where U and V are unitary matrices, i.e., $U^H = U^{-1}$ and $V^H = V^{-1}$, with column vectors denoted by

$$U = [u_1\ u_2\ \ldots\ u_n] \tag{A.32}$$

$$V = [v_1\ v_2\ \ldots\ v_m] \tag{A.33}$$

and the $n \times m$ matrix Σ contains a diagonal matrix Σ_1 of real, non-negative singular values, σ_i, arranged in a descending order as in

$$\Sigma = \begin{bmatrix} \Sigma_1 \\ 0 \end{bmatrix}; \quad n \geq m \tag{A.34}$$

or

$$\Sigma = [\Sigma_1\ \ 0]; \quad n \leq m \tag{A.35}$$

where

$$\Sigma_1 = \text{diag}\{\sigma_1, \sigma_2, \ldots, \sigma_k\}; \quad k = \min(n, m) \tag{A.36}$$

and

$$\bar{\sigma} \doteq \sigma_1 \geq \sigma_2 \geq \ldots \geq \sigma_k \doteq \underline{\sigma} \tag{A.37}$$

$\diamond$

The column vectors of U (A.32), denoted u_i are called left or output singular vectors (output directions). It should be noted that this standard notation is unfortunate as it is also standard notation to use u to represent the input signals. By bearing this fact in mind, the column vectors of U are orthogonal and of unit length (orthonormal), that is

$$\|u_i\| = \sqrt{|u_{i1}|^2 + |u_{i2}|^2 + \ldots + |u_{in}|^2} = 1 \tag{A.38}$$

$$u_i^H u_i = 1, \quad u_i^H u_j = 0, \quad i \neq j \tag{A.39}$$

Likewise, the column vectors of V (A.33), denoted v_i are called right or input singular vectors (the input directions). This input and output directions are related through the singular values. Since V is unitary we have $V^H V = I$, so the SVD of A (A.31) may be written as $AV = U\Sigma$, which for column i becomes

$$Av_i = \sigma_i u_i \tag{A.40}$$

That is, if we consider an input in the direction v_i, then the output is in the direction u_i. Furthermore, since $\|v_i\|_2 = 1$ and $\|u_i\|_2 = 1$ it can be seen that the i'th singular value σ_i gives directly the gain of the matrix A in this direction, that is,

$$\sigma_i(A) = \|Av_i\|_2 = \frac{\|Av_i\|_2}{\|v_i\|_2} \tag{A.41}$$

The singular values are the positive square roots of the $k = \min(n, m)$ largest eigenvalues of both AA^H and A^HA. We have

$$\sigma_i(A) = \sqrt{\lambda_i(A^HA)} = \sqrt{\lambda_i(AA^H)} \tag{A.42}$$

The matrix of eigenvectors of AA^H is U and σ_i^2 are the corresponding eigenvalues. Similarly, the matrix of eigenvectors of A^HA is V.

The SSV presents some advantages over the eigenvalue decomposition for multivariable plants: the singular values provides better information about the gain of the plants; the plant directions obtained from a SVD are orthogonal and the SSV also applies directly to non-squared plants.

For squared, non-singular $m \times m$ matrices $A = U\Sigma V^H$, we can write

$$A^{-1} = V\Sigma^{-1}U^H \tag{A.43}$$

This is the SVD of A^{-1} but with the order of the singular values reversed. Let $j = m - i + 1$. Then, from (A.43) it follows that

$$\sigma_i(A^{-1}) = 1/\sigma_j(A), \quad u_i(A^{-1}) = v_j(A), \quad v_i(A^{-1}) = u_j(A) \tag{A.44}$$

In particular,

$$\bar{\sigma}(A^{-1}) = 1/\underline{\sigma}(A) \tag{A.45}$$

Finally, from (A.29) it follows that the singular values bound the magnitude of the eigenvalues, i.e.,

$$\underline{\sigma}(A) \leq |\lambda_i(A)| \leq \bar{\sigma}(A) \tag{A.46}$$

A.4 The condition number

The condition number of a matrix A can be defined as the ratio

$$\gamma(A) = \sigma_1(A)/\sigma_k(A) = \bar{\sigma}(A)/\underline{\sigma}(A) \tag{A.47}$$

where $k = \min(l, m)$. For a nonsingular (squared) matrix we have $\underline{\sigma}(A) = \bar{\sigma}(A^{-1})$, so

$$\gamma(A) = \bar{\sigma}(A)\bar{\sigma}(A^{-1}) \tag{A.48}$$

It can be seen that the condition number is large if both A and A^{-1} have large elements. A matrix with large condition number is said to be *ill-conditioned*.

The condition number has been used as an input-output controllability measure. It has been postulated (Skogestad and Morari, 1987*b*) that a large condition number indicates sensitivity to uncertainty. This is not true in general but the revere holds: if the condition number is small, then the multivariable effects of uncertainty are not likely to be serious (Skogestad and Morari, 1987*b*).

The condition number depends strongly on the scaling of the inputs and outputs. If D_1 and D_2 are diagonal scaling matrices, then the condition number or the matrices A and D_1AD_2 may be arbitrarily far apart. The *minimized* or *optimal condition number* is obtained by minimizing the condition number for all possible scalings. We have,

$$\gamma^*(A) \doteq \min_{D_1,\, D_2} \gamma(D_1AD_2) \tag{A.49}$$

A.5 Relative Gain Array

The Relative Gain Array (RGA) of a complex non-singular $m \times m$ matrix A, denoted RGA(A) or $\Lambda(A)$, is a complex $m \times m$ matrix defined by

$$\mathrm{RGA}(A) \equiv \Lambda(A) \doteq A \times (A^{-1})^T \tag{A.50}$$

where the operation $\times$ denotes element by element multiplication. For a 2×2 matrix with elements a_{ij} the RGA is

$$\mathrm{RGA}(A) = \begin{bmatrix} \lambda_{11} & \lambda_{12} \\ \lambda_{21} & \lambda_{22} \end{bmatrix} = \begin{bmatrix} \lambda_{11} & 1-\lambda_{11} \\ 1-\lambda_{11} & \lambda_{11} \end{bmatrix} \tag{A.51}$$

where

$$\lambda_{11} = \frac{1}{\frac{1-a_{12}a_{21}}{a_{11}a_{22}}} \tag{A.52}$$

Example A.5.1. Consider again the distillation process described in Appendix B.2 for which we have at steady-state

$$P_o = \begin{bmatrix} 87.8 & -86.4 \\ 108.2 & -109.6 \end{bmatrix}, \quad P_o^{-1} = \begin{bmatrix} 0.399 & -0.315 \\ 0.394 & -0.320 \end{bmatrix}, \tag{A.53}$$

Therefore

$$\Lambda(P_o) = \begin{bmatrix} 35.1 & -34.1 \\ -34.1 & 35.1 \end{bmatrix} \tag{A.54}$$

△

A.6 Useful matrix identities

Lemma A.6.1. Matrix inversion lemma *Let A_1, A_2 and A_3 and A_4 be matrices with compatible dimensions such that $A_2A_3A_4$ and $A_1 + A_2A_3A_4$ are defined. Also assume that the inverses given bellow exists. Then*

$$(A_1 + A_2A_3A_4)^{-1} = A_1^{-1} - A_1^{-1}A_2(A_4A_1^{-1}A_2 + A_3^{-1})^{-1}A_4A_1^{-1} \tag{A.55}$$

Proof: *The lemma is proved by pre-multiplying (or post-multiplying) the right hand side of (A.56) by $A_1 + A_2A_3A_4$.*

□

Lemma A.6.2. Matrix push-through lemma *Let A_1 and A_2 be matrices with compatible dimensions. Then*

$$A_1(I - A_2A_1)^{-1} = (I - A_1A_2)^{-1}A_1 \tag{A.56}$$

Proof: *The lemma is proved by pre-multiplying both sides by $(I - A_1A_2)$ and post-multiplying both sides by $(I - A_2A_1)$.*

□

Appendix B

Distillation Column

A high-purity distillation process has been used in the literature as a benchmark problem for comparing methods for robust controller design. This Appendix introduces a typical distillation column of the type described in (Morari and Zafirou, 1989), (Skogestad and Postlethwaite, 1997) and (Green and Limebeer, 1995), among others.

B.1 Introduction

The distillation process has been used as an illustrative example throughout this work and this Appendix gives a brief description of it. For a general discussion on distillation column control see, for example, (Skogestad and Morari, 1987*a*).

A typical scheme of a distillation column is depicted in Figure B.1. The objective of the distillation process is to separate the feed F into a distillate product D, which contains most of the light component of the feed product, and bottom product B, which contain most of the heavy component of the feed product. The flow compositions, z_F, y_D and x_B, refer to the mole fractions of the light component. Then, perfect separation would be obtained with $y_D = 1$ and $x_B = 0$. The difference in volatility between the light and the heavy components is used to produce the desired separation.

The overall control problem for the distillation column has five inputs,

L: reflux
V: boilup
D: distillate
B: bottom flow
V_T: overhead vapour

and five outputs,

y_D: top composition
x_B: bottom composition
M_d: condenser holdup
M_b: reboiler holdup
p: pressure

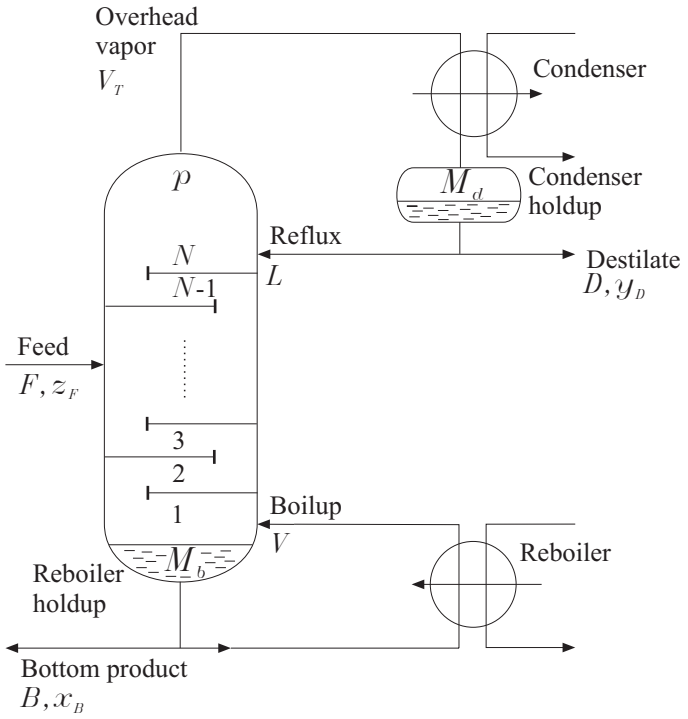

Figure B.1: The distillation column system.

This problem usually has no inherent control limitations caused by RHP-zeros, but the plant has poles in or close to the origin and needs to be stabilized. In addition, for high-purity separations the 5×5 RGA-matrix

may have some large elements. Another complication is that measurements are often expensive and unreliable.

The distillation column can be first stabilized by choosing three decentralized SISO loops for level and pressure, $y_2 = [M_d \; M_b \; p]^T$, and the remaining outputs, $y_1 = [y_D \; x_B]^T$. The SISO loops for controlling y_2 usually interact weakly and may be tuned independently of each other. Nevertheless, since the composition dynamics are usually much slower than the flow dynamics, the simplifying assumption of perfect control of holdup, i.e., M_d, M_b and p constant, is usually made. Also, instantaneous flow responses in the column are assumed.

Different control configurations are obtained by choosing different input pairs, i.e., $u_1 = [L \; V]^T$ or $u_1 = [D \; V]^T$, among others, for composition control y_1. The remaining three manipulated inputs are then determined by the requirement of keeping y_2 under perfect control. With the additional assumption of constant molar flows this implies that the following three relationships must hold:

$$dV = dV_T, \quad dD = -dB = dV - dL \tag{B.1}$$

The LV-configuration refers to a partially controlled system in which $u_1 = [L \; V]^T$ is used to control y_1. The above assumptions on y_2 are supposed to be hold by means of $u_2 = [D \; B \; V_T]^T$. With a LV-configuration the control of y_1 using u_1 is nearly independent of the control loop involving y_2 and u_2. Nevertheless, the problem of controlling y_1 with u_1 in such a configuration is often strongly interactive with large steady-state RGA-elements.

B.2 Idealized LV-configuration

The following idealized LV-model of the distillation process was originally presented by (Skogestad *et al.*, 1988):

$$P_o(s) = \frac{1}{75s+1} \begin{bmatrix} 87.8 & -86.4 \\ 108.2 & -109.6 \end{bmatrix} \tag{B.2}$$

The inputs are the reflux, L, and boilup, V, and the controlled outputs are the top product composition, y_D, and the bottom product composition, x_B. This is a very crude model of the distillation process but it is exhibited to

provide an excellent example of an ill-conditioned process where control is difficult, primarily due to the presence of input uncertainty. It is known that ill-conditioned plants may cause control problems

The singular value decomposition (SVD) of the steady-state gain matrix of the plant (B.2) is

$$P_o = U\Sigma V^H \tag{B.3}$$

where

$$\Sigma = \text{diag}\{\bar{\sigma}, \underline{\sigma}\} = \text{diag}\{197.2, 1.39\} \tag{B.4}$$

$$V = [\bar{v}\ \underline{v}] = \begin{bmatrix} -0.707 & 0.708 \\ 0.708 & 0.707 \end{bmatrix} \tag{B.5}$$

$$U = [\bar{u}\ \underline{u}] = \begin{bmatrix} -0.625 & 0.781 \\ -0.781 & -0.625 \end{bmatrix} \tag{B.6}$$

From the first input singular vector, $\bar{v} = [-0.707\ 0.708]^T$, we can see that the gain is 197.2 when one input is decreased and the other input is increased by a similar amount. On the other hand, from the second input singular vector, $\underline{v} = [0.708\ 0.707]^T$, we can see that the gain is only 1.39 if both input are increased by approximately the same amount. The reason for this is that the plant is such that the two inputs counteract each other. Thus the distillation process is ill-conditioned, at least at steady state, and the condition number is $\gamma = 197.2/1.39 = 141.7$.

The control of the distillation process was first formulated by (Skogestad *et al.*, 1988) in which the overhead composition is to be controlled at $y_D = 0.99$, output y_1, and the bottom composition at $x_B = 0.01$, output y_2, using the reflux L, input u_1, and boilup V, input u_2, as manipulated variables. The 1,1-element of the steady-state gain matrix in (B.2) is 87.8. This implies that an increase in the input u_1 by 1, holding u_2 constant, yields a large steady-state change in y_1 of 87.8. That is, the outputs are very sensitive to changes in u_1. Similarly, an increase in u_2 by 1, holding u_2 constant, yields a change in y_1 of -86.4. This is a very large change, now in the opposite direction of that for the increase in u_1. It is seen that changes in u_1 and u_2 counteract each other. If u_1 and u_2 are simultaneously increased by 1, the

overall steady-state change in y_1 is only $87.8 - 86.4 = 1.4$. The reason for this small change is seen from the smallest singular value, $\underline{\sigma}(P_o) = 1.39$. It is obtained for inputs in the direction $\underline{v} = [0.708\ 0.707]^T$. From the output singular vector $\underline{u} = [0.781\ -0.625]^T$ it can be seen that the effect is to move the output in different directions, that is to change $y_1 - y_2$. Therefore, it takes a large control action to move the compositions in different directions, i.e., to make both products pure simultaneously.

On the other hand, the distillation column is very sensitive to changes in external flows, i.e., increase $u_1 - u_2 = L - V$. This can be seen from the input singular vector $\bar{v} = [-0.707\ 0.708]^T$ associated with the largest singular value, and is a general property of the distillation processes where both products are of high purity.

B.3 Other configurations

Another configuration is the DV-configuration in which $u_1 = [D\ V]^T$ is used to control y_1 and, then y_2 is controlled by means of $u_2 = [L\ B\ V_T]^T$.

The following idealized DV-model of the distillation process was also originally presented by (Skogestad *et al.*, 1988):

$$P_o(s) = \frac{1}{75s+1} \begin{bmatrix} -87.8 & 1.4 \\ -108.2 & -1.4 \end{bmatrix} \tag{B.7}$$

In this configuration, the steady-state interactions from u_1 to y_1 are generally much less with smaller RGA-elements, about 0.5. The condition number $\gamma = 70.8$ is still large and the overall control configuration depends strongly on u_2.

There are also many other possible configurations. Nevertheless, the two mentioned above are the most popular for the control of a high-purity distillation column.

B.4 The benchmark problem

The benchmark problem introduced here corresponds to the control problem formulated originally by (Skogestad *et al.*, 1988). It considers the distillation column described in B.2 where the overhead composition is to be controlled

at $y_D = 0.99$ and the bottom composition at $x_B = 0.01$ using the reflux L and boliup V as manipulated variables. The linear model is

$$P_o(s) = \frac{1}{75s+1}\begin{bmatrix} 87.8 & -86.4 \\ 108.2 & -109.6 \end{bmatrix} \tag{B.8}$$

The uncertainty with respect to the manipulated inputs may be represented as multiplicative input uncertainty (See Figure 2.6) in which the set of possible plants $\mathcal{P}$ are

$$\mathcal{P} = \{P : P = P_o(I + \Delta W_1)\}, \;\; \bar{\sigma}(\Delta) \leq 1 \; \forall \omega \tag{B.9}$$

where $W_1 = w_I I_2$ gives the magnitude of the relative uncertainty on each manipulated input. The weight

$$w_I(s) = \frac{s+0.2}{0.5s+1} \tag{B.10}$$

represents an input error of up to 20 percent in the low frequency range, which increases at high frequencies, reaching a value of one (100 percent uncertainty) at about $\omega = 1$ Rad/min. This increase with frequency may take care of neglected flow dynamics. For example, it allows for a time delay of about 1 min in the responses between L and V and the outputs y_D and x_B. The magnitude of W_1 over frequency is shown in Figure B.2.

An unstructured uncertainty description may be assumed. That is, the perturbation Δ is a full 2×2 matrix. The off-diagonal terms allowed in Δ imply that a change in the one input may result in an undesirable change in the other one. This may be the case for some plants, for example, if the actuators are located very close toe each other. However, for the distillation column, it is more reasonable to assume that actuators are *independent*, that is, Δ diagonal. For mathematical convenience, Δ could be assumed to be a full matrix and this assumption does not make any difference for the LV-configuration (Skogestad *et al.*, 1988).

The following input gain perturbations are allowable (Skogestad and Postlethwaite, 1997):

$$E_{I_1} = \begin{bmatrix} 1.2 & 0 \\ 0 & 1.2 \end{bmatrix} \; E_{I_2} = \begin{bmatrix} 0.8 & 0 \\ 0 & 1.2 \end{bmatrix} \; E_{I_3} = \begin{bmatrix} 1.2 & 0 \\ 0 & 0.8 \end{bmatrix} \; E_{I_4} = \begin{bmatrix} 0.8 & 0 \\ 0 & 0.8 \end{bmatrix} \tag{B.11}$$

where $E_{I_i} = I + \Delta W_I$. The perturbations in (B.11) do not make use of the fact that $W_1(s)$ increases with frequency. Two allowed dynamic perturbations are:

$$E_{I_5} = \begin{bmatrix} f_1(s) & 0 \\ 0 & f_1(s) \end{bmatrix} \quad E_{I_6} = \begin{bmatrix} f_2(s) & 0 \\ 0 & f_1(s) \end{bmatrix} \tag{B.12}$$

with

$$f_1(s) = 1 - \frac{s - 0.2}{0.5s + 1} = 1.2\frac{-0.417s + 1}{0.5s + 1} \tag{B.13}$$

and

$$f_2(s) = 1 - \frac{s + 0.2}{0.5s + 1} = 0.8\frac{-0.633s + 1}{0.5s + 1} \tag{B.14}$$

Therefore, the six perturbed plants belonging to the set (B.9) can be considered:

$$P_i(s) = P_o(s)E_{I_i}(s) \tag{B.15}$$

for $i = 1, \ldots, 6$ and with nominal $E_{I_0} = I$.

The performance specification is simply

$$\bar{\sigma}(S_o) < |w_p|^{-1} \tag{B.16}$$

where $S_o = (I + P_oK)^{-1}$ and the weight is chosen as $W_p = w_pI_2$,

$$w_p(s) = 0.5\frac{10s + 1}{10s} \tag{B.17}$$

The performance weigh (B.17) means that integral action is required, i.e., $|w_p(0)|^{-1} = 0$, and that disturbances are amplified at high frequencies by a factor of 2 at most, i.e., $|w_p(j\infty)|^{-1} = 2$. The magnitude over frequency is shown in Figure B.2.

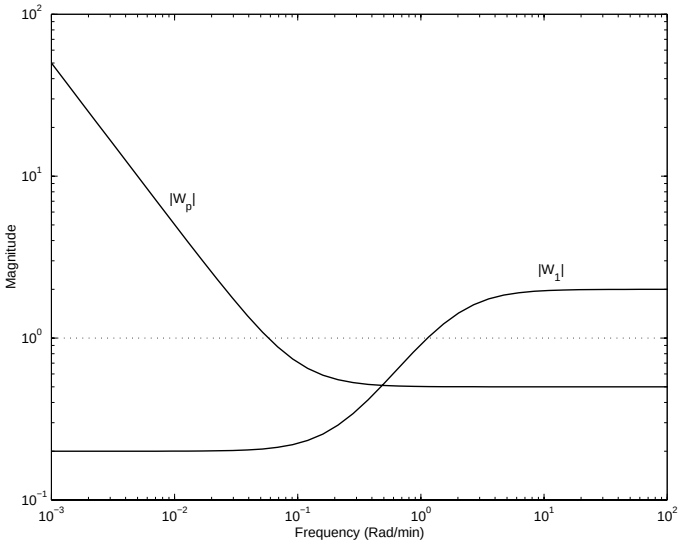

Figure B.2: Uncertainty and performance weights.

Appendix C

State-space solutions

This Appendix provides the solutions of several examples carried out along this work. The solution are given in state-space realizations, where any transfer function $K(s)$ is represented as $K(s) = C(sI - A)B^{-1} + D$.

$$A = \begin{bmatrix} -85.2341 & 0.0242 & -0.0001 & 31.4754 & 7.1400 & 0.0017 & -0.0001 & -0.0000 \\ 0 & -22.3525 & 21.9877 & -0.0029 & 0.0010 & -1.7958 & -0.0000 & 0.0000 \\ 0 & 0 & -6.3626 & -0.0001 & -0.0012 & 1.0870 & 0.0000 & -0.0000 \\ 0 & 0 & 0 & -3.0692 & -1.3699 & -0.0004 & 0.0000 & 0.0000 \\ 0 & 0 & 0 & 0 & -0.1994 & -0.0000 & -0.0000 & 0.0000 \\ 0 & 0 & 0 & 0 & 0 & -0.0554 & 0.0000 & -0.0000 \\ 0 & 0 & 0 & 0 & 0 & 0 & -0.0000 & -0.0000 \\ 0 & 0 & 0 & 0 & 0 & 0 & 0 & -0.0000 \end{bmatrix}$$

$$B = \begin{bmatrix} -8.7336 & 6.9804 \\ 2.5721 & 3.2176 \\ -0.9577 & -1.1997 \\ 1.2563 & -1.0041 \\ 0.5604 & -0.4482 \\ 0.1273 & 0.1592 \\ 0.1624 & -0.1301 \\ 0.0874 & 0.1088 \end{bmatrix} \qquad D = \begin{bmatrix} 0.0494 & -0.0395 \\ 0.0493 & -0.0394 \end{bmatrix}$$

$$C = \begin{bmatrix} 7.8116 & -2.5915 & 1.7037 & -1.6593 & -0.6243 & -0.2076 & -0.1472 & -0.0988 \\ 7.7972 & 2.5949 & -1.7079 & -1.6559 & -0.6234 & 0.2078 & -0.1471 & 0.0986 \end{bmatrix}$$

Table C.1: One degree-of-freedom μ-optimal controller K_{opt} found in Example 2.4.1.

$$A = \begin{bmatrix} -0.007 & 0.107 & -0.083 & 0.183 & -0.009 & 0.076 & -0.476 & 0.867 & -0.031 & 0.005 \\ -0.106 & -0.191 & 0.135 & -0.077 & 0.011 & -0.481 & 2.641 & -4.590 & 0.178 & -0.045 \\ 0.0776 & 0.329 & -0.376 & 0.836 & -0.167 & 1.481 & -7.712 & 3.238 & -0.425 & 0.045 \\ -0.178 & -1.140 & 1.565 & -4.255 & 0.950 & -6.161 & 0.746 & -2.223 & 1.547 & -0.051 \\ 0.011 & 0.032 & 0.049 & -0.492 & -0.096 & 2.554 & -0.913 & 6.322 & -0.371 & -0.014 \\ 0.102 & 0.677 & -1.093 & 3.843 & -2.469 & -7.112 & 2.051 & -2.287 & 3.736 & 0.015 \\ -0.408 & -1.873 & 1.861 & -3.661 & 1.361 & 7.786 & -6.579 & 0.523 & -6.105 & 0.007 \\ 0.505 & 1.305 & 0.625 & -8.806 & -7.174 & -1.239 & 4.442 & -5.305 & 4.583 & -0.014 \\ -0.013 & -0.013 & -0.076 & 0.513 & 0.430 & 1.871 & -4.178 & 7.678 & -2.532 & 0.089 \\ 0.007 & 0.040 & -0.055 & 0.166 & -0.058 & -0.862 & 5.960 & -1.520 & 0.550 & -0.176 \end{bmatrix}$$

$$B = \begin{bmatrix} 0.099 & -0.166 \\ 0.568 & -0.449 \\ -0.750 & 0.325 \\ 2.367 & -0.621 \\ 0.089 & 0.216 \\ -0.332 & 1.481 \\ -2.544 & -8.300 \\ 7.904 & 13.148 \\ -0.280 & -0.378 \\ -0.026 & 0.088 \end{bmatrix} \qquad D = \begin{bmatrix} -0.974 & 0.003 \\ 0.003 & -1.001 \end{bmatrix}$$

$$C = \begin{bmatrix} 0.003 & -0.228 & -0.252 & 1.600 & -0.209 & 1.006 & 9.3782 & -0.2042 & -0.0603 & -5.4225 \\ -0.193 & 0.688 & -0.778 & 1.852 & -0.105 & 1.137 & -6.779 & 12.140 & -0.424 & 0.070 \end{bmatrix}$$

Table C.2: $\mathcal{H}_\infty$ controller K_2 found in Example 4.5.

$$A = \begin{bmatrix} -304381.591 & -553369.047 & 548.413 & -347.007 \\ 0 & -251507.875 & 498.498 & -315.429 \\ 0 & 0 & -3.809 & 0.002 \\ 0 & 0 & 0 & -1.131 \end{bmatrix} \qquad B = \begin{bmatrix} -111386.744 \\ -101176.531 \\ 51.541 \\ -33.321 \end{bmatrix}$$

$$C = \begin{bmatrix} -111312.310 & -101258.416 & 51.652 & -33.437 \end{bmatrix} \qquad D = -12.972$$

Table C.3: Robust Model Reference Controller K_2 found in Example 5.4.2.

$$A = \begin{bmatrix} -0.01 & -0.28 & -0.46 & -0.01 & -0.03 & -0.03 & 0.32 & -0.03 & 0.05 & 0.00 \\ 0.25 & -0.62 & -0.62 & -0.12 & 0.04 & -0.43 & 3.44 & -0.35 & 0.61 & 0.050 \\ 0.34 & -2.15 & -3.65 & -0.34 & -0.59 & -1.11 & 9.12 & -0.70 & 1.09 & 0.082 \\ 0.01 & 0.03 & 0.18 & -0.01 & 0.02 & -0.15 & 0.77 & -0.08 & 0.14 & 0.011 \\ 0.05 & -0.56 & -1.13 & -0.07 & -0.45 & -0.88 & 4.99 & -0.03 & -0.23 & -0.02 \\ -0.03 & 0.28 & 0.60 & 0.14 & 1.02 & -0.32 & 5.98 & -0.41 & 0.82 & 0.07 \\ 0.17 & -3.47 & -9.24 & -0.39 & -6.96 & -1.37 & -27.28 & 4.54 & -9.22 & -0.77 \\ -0.03 & 0.28 & 0.60 & 0.07 & 0.51 & -0.47 & 3.40 & -1.06 & 2.84 & 0.29 \\ 0.08 & -0.43 & -0.78 & -0.15 & -0.86 & 1.09 & -6.46 & 2.77 & -8.72 & -1.11 \\ 0.00 & -0.03 & -0.07 & -0.01 & -0.07 & 0.09 & -0.69 & 0.30 & -1.10 & -0.22 \end{bmatrix}$$

$$B = \begin{bmatrix} 0.01 & 0.20 \\ 0.89 & -0.68 \\ 2.24 & -1.06 \\ -0.04 & -0.08 \\ 0.30 & -0.41 \\ 0.03 & 0.34 \\ 2.07 & -1.79 \\ -0.05 & 0.32 \\ -0.02 & -0.65 \\ 0.00 & -0.05 \end{bmatrix} \qquad D = \begin{bmatrix} -0.99 & 0.00 \\ -0.00 & -1.00 \end{bmatrix}$$

$$C = \begin{bmatrix} 0.130 & 0.46 & 1.97 & 0.03 & 0.50 & 0.19 & -1.52 & 0.03 & 0.039 & 0.00 \\ 0.16 & 1.03 & 1.50 & 0.09 & -0.10 & 0.29 & -2.27 & 0.32 & -0.65 & -0.05 \end{bmatrix}$$

Table C.4: μ-"optimal" controller K_2 found in Example 4.5.

$$A = \begin{bmatrix} -1340.660 & 0 \\ 0 & -1340.687 \end{bmatrix} \qquad B = \begin{bmatrix} 120.886\,10^{-3} & -107.331\,10^{-3} \\ -107.331\,10^{-3} & -120.886\,10^{-3} \end{bmatrix}$$

$$C = \begin{bmatrix} 101.465\,10^{-3} & 5.208\,10^{-3} \\ 126.752\,10^{-3} & 8.346\,10^{-3} \end{bmatrix} \qquad D = \begin{bmatrix} 0 & 0 \\ 0 & 0 \end{bmatrix}$$

Table C.5: *Optimum* Bezout factor N_r found in Section 5.5.

$$A = \begin{bmatrix} -0.013 & 0 \\ 0 & -0.013 \end{bmatrix} \qquad B = \begin{bmatrix} -120.886\,10^{-3} & 107.331\,10^{-3} \\ 107.331\,10^{-3} & 120.886\,10^{-3} \end{bmatrix}$$

$$C = \begin{bmatrix} -6201.462 & 5506.230 \\ 5506.120 & 6201.586 \end{bmatrix} \qquad D = \begin{bmatrix} 1 & 0 \\ 0 & 1 \end{bmatrix}$$

Table C.6: *Optimum* Bezout factor M_r^{-1} found in Section 5.5.

$$A = \begin{bmatrix} -2000.116 & 0 \\ 0 & -2000.156 \end{bmatrix} \qquad B = \begin{bmatrix} -0.121 & 0.107 \\ 0.107 & 0.121 \end{bmatrix}$$

$$C = \begin{bmatrix} -6201.462 & 5506.230 \\ 5506.120 & 6201.589 \end{bmatrix} \qquad D = \begin{bmatrix} 1 & 0 \\ 0 & 1 \end{bmatrix}$$

Table C.7: *Optimum* Bezout factor X_r found in Section 5.5.

$$A = \begin{bmatrix} -2000.116 & 0 \\ 0 & -2000.156 \end{bmatrix} \qquad B = \begin{bmatrix} -8.943\,10^{4} & 5.581\,10^{4} \\ 135.815\,10^{4} & -108.721\,10^{4} \end{bmatrix}$$

$$C = \begin{bmatrix} -6201.462 & 5506.230 \\ 5506.120 & 6201.586 \end{bmatrix} \qquad D = \begin{bmatrix} 0 & 0 \\ 0 & 0 \end{bmatrix}$$

Table C.8: *Optimum* Bezout factor Y_r found in Section 5.5.

$$A = \begin{bmatrix} 0 & 0 & 0 & 0 \\ 0 & 0 & 0 & 0 \\ -0.148 & 0.132 & -1340.660 & 0 \\ 0.132 & 0.148 & 0 & -1340.687 \end{bmatrix} \qquad B = \begin{bmatrix} -1.225 & 0 \\ 0 & -1.225 \\ 1.209\,10^{-5} & -1.073\,10^{-5} \\ -1.073\,10^{-5} & -1.209\,10^{-5} \end{bmatrix}$$

$$C = \begin{bmatrix} -1.225 & 0 & -6201.462 & 5506.230 \\ 0 & -1.225 & 5506.120 & 6201.586 \end{bmatrix} \qquad D = \begin{bmatrix} 10.001\,10^{-5} & 0 \\ 0 & 10.001\,10^{-5} \end{bmatrix}$$

Table C.9: Feedback controller K_1 found in Section 5.5.

$$A = \begin{bmatrix} -12074.802 & -0.001 & 0 & -42.965 & -28.213 & 0 \\ 0 & -4.237 & -2.127 & 0 & 0 & -0.374 \\ 0 & 0 & -1.035 & 0 & 0 & -0.413 \\ 0 & 0 & 0 & -0.206 & -0.196 & 0 \\ 0 & 0 & 0 & 0 - 0.121 & 0 & \\ 0 & 0 & 0 & 0 & 0 & -0.127 \end{bmatrix}$$

$$B = \begin{bmatrix} -7274.600 & 5818.278 \\ 15.676 & 19.601 \\ 32.730 & 40.922 \\ -16.440 & 13.149 \\ -239.044 & 191.189 \\ 46.843 & 58.569 \end{bmatrix} \quad D = \begin{bmatrix} 175.863 & -140.657 \\ 175.584 & -140.433 \end{bmatrix}$$

$$C = \begin{bmatrix} -6592.470 & 41.860 & -39.007 & 181.236 & -87.819 & 34.919 \\ -6582.147 & -41.928 & 39.068 & 180.952 & -87.681 & -34.974 \end{bmatrix}$$

Table C.10: Robust Model Reference Controller K_2 found in Section 5.5.

List of Acronyms

1-DOF	One degree-of-freedom
2-DOF	Two degrees-of-freedom
iff	if and only if
LCF	Left coprime factorization
LFT	Linear fractional transformation
MIMO	Multi-input multi-output
RCF	Right coprime factorization
RGA	Relative Gain Array
RHP	Right-Half Plane
SISO	Single-input single-output
SSV	Structured singular value

Notation and Symbols

$\mathbb{C}_-$	The open left-half plane
$\mathcal{RH}_\infty$	The set of all rational stable transfer functions
$\mathcal{F}_\ell(P,K)$	Lower LFT
$\mathcal{F}_u(P,K)$	Upper LFT
A^{-1}	Inverse of the matrix A
A^T	Transpose of the matrix A
A^H	Complex conjugate transpose of the matrix A
$\bar{\sigma}(A)$	Maximum singular value of A
$\underline{\sigma}(A)$	Minimum singular value of A
$\rho(A)$	Spectral radius of A
$\mathrm{tr}(A)$	Trace of A
$\deg(n)$	Degree of n
$\mathrm{Adj}(A)$	Adjoint of A
$\det(A)$	Determinant of A

$\in$	Belong to
$\doteq$	Defined as
$\approx$	Approximated to
$\equiv$	Equivalent to
$\triangle$	End of Example
$\square$	End of Proof
$\diamond$	End of Definition

List of Figures

1.1 Open-loop and closed-loop control configurations. 2
1.2 Standard one degree-of-freedom feedback control system. . . . 4
1.3 Standard two degrees-of-freedom control configuration. 5

2.1 General control problem formulation with no model uncertainty. 12
2.2 One degree-of-freedom control configuration. 13
2.3 General block diagram for analysis with no uncertainty. . . . 14
2.4 General control configuration with model uncertainty. 15
2.5 General block diagram for analysis with uncertainty. 16
2.6 Common uncertainty representations involving single perturbations 18
2.7 General $\mathcal{M}\Delta$ structure for robust stability analysis. 20
2.8 Block diagram for testing robust performance. 24
2.9 One degree-of-freedom control configuration with a multiplicative input uncertainty representation. 26
2.10 μ-plots for diagonal PI controller. 27
2.11 Closed loop response with diagonal PI controller to reference input 27
2.12 Upper μ-bound and scaled upper μ-bound 31
2.13 Frequency-dependent scaling $d_1(\omega)$ and the fitted transfer functions 32
2.14 μ-plots for K_{opt}. 33
2.15 Closed-loop setpoint change with μ-"optimal" controller K_{opt} 34
2.16 Closed-loop response with the μ-"optimal" controller K_{opt} to a disturbance in the output signal y_1 34

3.1 Classical unity feedback configuration. 39
3.2 Realization of P_o affected by state-variable feedback and the artificial signal ξ 45
3.3 Diagram block representation of *right coprime factorization* $P_o = N_r M_r^{-1}$. 46
3.4 Right coprime factorizations $P_o = N_r M_r^{-1}$ for two different p_F 47
3.5 Realization of P_o affected by state-variable observer and controller 48
3.6 Representation of partial state feedback from a right coprime factorization $P_o = N_r M_r^{-1}$. 50
3.7 Output feedback control configuration. 52
3.8 The Observer-Controller configuration. 54
3.9 The Observer-Controller configuration with external perturbations. 55

4.1 Nominal feedback control system. 60
4.2 Overall control configuration for robustness enhancement. . . 62
4.3 Detail of the Robustness Enhancement Block. 64
4.4 Overall control configuration for robustness enhancement. . . 66
4.5 General interconnection of system with uncertainty. 67
4.6 Block diagram for testing robust performance 70
4.7 Nominal Performance bound with K_1 74
4.8 Robust Stability bounds with K_1 75
4.9 Stable closed-loop responses for a reference change with K_1 . 75
4.10 Closed-loop response to output disturbance for K_1. Nominal plant (solid) and uncertain plants $P_i(s)$, $i = 1, \ldots, 4$ (dashed). 76
4.11 Frequency Bode plot for the $\mathcal{H}_\infty$ controller K_2 and its optimal Hankel norm approximation 78
4.12 RS bound for K_1 and with the $\mathcal{H}_\infty$ controller K_2 78
4.13 μ-plots for K_1 and with the $\mathcal{H}_\infty$ controller K_2 79
4.14 NP bounds for K_1 and with the $\mathcal{H}_\infty$ controller K_2 80
4.15 Closed-loop responses for a reference change with the $\mathcal{H}_\infty$ controller K_2 81

4.16 Closed-loop response to a disturbance at the output signal y_1 with the $\mathcal{H}_\infty$ controller K_2 82
4.17 Frequency Bode plot for the mu-"optimal" controller K_2 and its optimal Hankel norm approximation 83
4.18 Closed-loop setpoint change with μ-"optimal" controller K_2 . 84
4.19 Closed-loop response to a disturbance at the output signal y_1 with the μ-"optimal" controller K_2 84
4.20 Final μ-plots 85

5.1 Right coprime factorization of P_o 90
5.2 The basic structure for the proposed control configuration. . . 91
5.3 Observer-based control scheme. 92
5.4 Overall 2-DOF control configuration. 93
5.5 Typical frequency plots for R and $I - R$. 97
5.6 Ideal representation of the feedback scheme with $d_i = 0$. . . 98
5.7 Observer-based feedback control scheme with the uncertain plant. 100
5.8 Exact and asymptotic plot of $S^d(j\omega)$. 102
5.9 Magnitude plots after the optimization problem 106
5.10 Bound for robust stability 106
5.11 Bezout identity 107
5.12 Closed loop step responses with the static prefilter K_2 109
5.13 The two degrees-of-freedom design problem. 110
5.14 General interconnection of system with uncertainty. 111
5.15 Relation from r to u 114
5.16 Relation from r to y 114
5.17 Frequency Bode plot for the 11th order prefilter controller K_2 and its 4th order optimal Hankel norm approximation 115
5.18 Closed-loop step responses with the dynamic prefilter controller K_2 115
5.19 Largest singular values plot after the optimization problem . 118
5.20 Robust stability bounds 118
5.21 Bezout identity 119

5.22 Frequency Bode plot for the 14th order prefilter controller K_2 and its 6th order optimal Hankel norm approximation 120
5.23 Closed-loop setpoint change and step response of the targed model T_{ref} 121

B.1 The distillation column system. 142
B.2 Uncertainty and performance weights. 148

References

Ackerman, J. (1993). *Robust Control: Systems with uncertain physical parameters*. Apringer Verlag. Communication and Control Engineering Series.

Ansay, P. and V. Wertz (1997). Model uncertainties in gpc: A systematic two-step design. *Proc. of the 4th European Control Conference (ECC97)*.

Ansay, P., M. Gevers and V. Wertz (1998). Enhancing the robustness of a gpc via a simple choice of the youla parameter. *European Journal of Control* p. to appear.

Astrom, K.J. and B. Wittenmark (1984). *Computer Controlled Systems: Theory and Design*. Prentice-Hall.

Balas, G., J. C. Doyle, K. Glover, A. Packard and R. Smith (1998). μ-*Analysis and Synthesis Toolbox*. MUSYN Inc. and The MathWorks, Inc.

Boyd, S. P. and C. H. Barratt (1991). *Liner Controller Design. Limits of Performance*. system sciences series. Prentice-Hall International.

Braatz, R. D., P. M. Young, J. C. Doyle and M. Morari (1994). Computational compexity of μ calculation. *IEEE Trans. Automat. Contr.* **39**, 1000–1002.

Chen, J. (1995). Sensitivity integral relations and design trade-offs in linear multivariable feedback systems. *IEEE Trans. Automat. Contr.* **40**(10), 1700–1716.

Chiang, R. Y. and M. G. Safonov (1992). *Robust Control Toolbox Users's Guide*. The MathWorks, Inc.

Clarke, D. W., C. Mohtadi and P. S. Tuffs (1987). Generalized predictive control-part i. the basic algorithm. *Automatica* **23**(2), 137–148.

Desoer, C.A. and C.L. Gustafson (1984). Algebraic theory of linear multivariable systems. *IEEE Trans. Automat. Contr.* **29**, 909–917.

Desoer, C.A., R.W. Liu, J.Murray and R. Saeks (1980). Feedback system design: the fractional representation approach to analysis and synthesis. *IEEE Trans. Automat. Contr.* **25**, 399–412.

Ding, X., L. Guo and P.M. Frank (1994). Parameterization of linear observers and its application to observer design. *IEEE Trans. Automat. Contr.* **39**(8), 1648–1652.

Dorf, R. C. (1990). *Sistemas modernos de control*. Addison-Wesley.

Doyle, C. J., K. Glover, P.P. Khargonekar and B. A. Francis (1989). State-space solutions to standard H_2 and H_∞ control problems. *IEEE Trans. Automat. Contr.* **34**(8), 831–847.

Doyle, J.C. (1982). Analysis of feedback systems whith structured uncertainties. *IEE* **129**(6), 242–250.

Doyle, J.C. (1983). Synthesis of robust controllers and filters. *Proc. of the IEEE Conference on Decision and Control* pp. 109–124.

Doyle, J.C. and G. Stein (1981). Multivariable feedback design: Concepts for a classical/modern synthesis.. *IEEE Trans. Automat. Contr.* **26**(2), 4–16.

Doyle, J.C., B.A. Francis and A. Tanenbaum (1992). *Feedback Control Theory*. MacMillan Publishing Company.

Francis, B. A. (1987). *A course in $\mathcal{H}^\infty$ Control theory*. Springer-Verlag. Lecture Notes in Control and Information Sciences.

Gantmakher, F. R. (1990). *he Theory of matrices*. Vol. 1. 2nd ed.. Chelsea Publishing Company cop.. New York.

Glover, K. (1984). All optimal Hankel-norm approximations of linear multivariable systems and their L^∞-error bounds. *International Journal of Control.* **39**(6), 1115–1193.

Glover, K. and D. McFarlane (1989). Robust stabilization of normalized coprime factor plant descriptions with $\mathcal{H}_\infty$ bounded uncertainty. *IEEE Trans. Automat. Contr.* **34**(8), 821–830.

Green, M. and D. J. N. Limebeer (1995). *Linear Robust Control*. Prentice Hall Information and System Science Series.

Grimble, M. J. (1988). Two degrees of freedom feedback and feedforward optimal control of multivariable stochastic systems. *Automatica* **24**(6), 809–817.

Grimble, M. J. (1994). *Robust Industrial Control. Optimal design Approach for Polynomial Systems*. Prentice-Hall International.

Hold, B. R. and M. Morari (1985). Design of resilent processing plants VI: the effect of right plane zeros on dynamic resilience. *Chem. Eng. Sci.* **40**, 59–74.

Hrissagis, K. and O.D. Crisalle (1997). Mixed objective optimization for robust predictive controller synthesis. *Proc. of the 36th IEEE Conference on Decision and Control (CDC97).*

Hrissagis, K., O.D. Crisalle and M. Sznaier (1996). Robust unconstrained predictive control design with guaranteed nominal performance. *AIChE Journal* **42**(5), 1293–1303.

Kailath, T. (1980). *Linear Systems*. Prentice-Hall.

Kuo, B. C. (1982). *Automatic Control Systems*. fourth edition ed.. Prentice Hall, Englewood Cliffs, NJ.

Limebeer, D. J. N. (1991). The specification and purpose of a controller design case study. *Proc. of the IEEE Conference on Decision and Control* **29**, 1579–1580.

Limebeer, D. J. N., E. M. Kasenally and J. D. Perkins (1993). On the design of robust two degree of freedom controllers. *Automatica* **29**(1), 157–168.

Lundström (1994). Studies on Robust Multivariable Distillation Control. PhD thesis. Norwegian Uneversity of Science and Thechnology. Trondheim.

Maciejowski, J. M. (1989). *Multivariable Feedback Design*. Addison-Wesley Publishing.

McFarlane, D. C. and K. Glover (1992). A loop shaping design procedure using H_∞ synthesis. *IEEE Trans. Automat. Contr.* **37**(6), 759–769.

Morari, M. and E. Zafirou (1989). *Robust Process Control*. Prentice-Hall International.

Nett, C. N., C. A. Jacobson and N. J. Balas (1984). A connection between state-space and doubly coprime fractional representations. *IEEE Trans. Automat. Contr.* **29**, 831–832.

Ogata, K. (1990). *Modern Control Engineering*. 2nd ed.. Prentice-Hall.

Packard, A. and J. C. Doyle (1993). The complex structured singular value. *Automatica* **29**(1), 71–109.

Pedret, C. (2000). Controller robustification. an alternative approach to robust control design. Master's thesis. Universitat Autònoma de Barcelona.

Pedret, C., R. Vilanova, , I. Serra and R. Moreno (2001). Control configuration for robustness enhancement. *Proc. of the European Control Conference*.

Pedret, C., R. Vilanova, , I. Serra and R. Moreno (2003). Multivariable control configuration for robustness enhancement. *Proc. of the IEEE Multiconference on Computational Engineering in Systems Applications*.

Pedret, C., R. Vilanova and I. Serra (1999). Model reference robust control in frequency domain: Observer - controller configuration approach. *Proc. of the 12th International Conference on Control System and Computer Science (CSCS12)*.

Safonov, M. G. (1982). Stability margins of diagonally perturbed multivariable feedback systems. *IEE* **129**(6), 251–256.

Safonov, M.G., A.J. Laub and G.L. Hartmann (1981). Feedback properties of multivariable systems: The role and use of the return difference matrix.. *IEEE Trans. Automat. Contr.* **26**(2), 47–65.

Skogestad, S. and I. Postlethwaite (1997). *Multivariable Feedback Control*. Wiley.

Skogestad, S. and M. Morari (1987*a*). Control configuration selection for distillation columns. *AIChE Journal* **33**(10), 1620–1635.

Skogestad, S. and M. Morari (1987*b*). Effect of model uncertainty on dynamic resilence. *Chem. Eng. Sci.* **42**, 1765–1780.

Skogestad, S., M. Morari and J. C. Doyle (1988). Robust control of ill-conditioned plants. high-purity distillation. *IEEE Trans. Automat. Contr.* **33**(12), 1092–1105.

Stein, G. and M. Athans (1987). The LQG/LTR procedure for multivariable feedback control. *IEEE Trans. Automat. Contr.* **32**(2), 105–114.

Stoorvogel, A. (1992). *The $\mathcal{H}_\infty$ control problem. A state space approach*. Systems and control engineering. Prentice-Hall International.

Sun, J., A. W. Olbrot and M. P. Polis (1994). Robust satbilization and robust performance using model reference control and modelling error compensation. *IEEE Trans. Automat. Contr.* **39**(3), 630–634.

Tay, T., I. Marrels and J. B. Moore (1998). *High performance control*. Birkhäuser.

Vidyasagar, M. (1985). *Control System Synthesis. A factorization approach*. MIT Press. Cambridge, Massachusetts.

Vidyasagar, M., H. Schneider and B. A. Francis (1982). Algebraic and topological aspects of feedback stabilization. *IEEE Trans. Automat. Contr.* **27**(4), 880–894.

Vilanova, R. (1996). Design of 2-DOF Compensators: Independence of Properties and Design for Robust Tracking. PhD thesis. Universitat Autòmoma de Barcelona. Spain.

Vilanova, R. and I. Serra (1997). Realization of two degree-of-freedom compensators. *IEE Proceedings. Part D.* **144**(6), 589–596.

Vilanova, R. and I. Serra (1998). Model reference control in two-degrees-of-freedom control systems: Adaptive min-max approach. *IEE Proceedings. Part D.* p. to appear.

Vilanova, R., C. Pedret, I. Serra and F.Tadeo (1999). Observer-controller configuration approach to controller robustification. *Proc. of the IEEE Conference on Decision and Control*.

Youla, D. C. and J.J. Bongiorno (1985). A feedback theory of two degree-of-freedom optimal wiener-hopf design. *IEEE Trans. Automat. Contr.* **30**, 652–665.

Youla, D., H.A. Jabr and J. Bongiorno (1976*a*). Modern Wiener-Hopf design if optimal controllers, part II: The multivariable case. *IEEE Trans. Automat. Contr.* **21**(6), 319–338.

Youla, D., J. Bongiorno and H.A. Jabr (1976*b*). Modern Wiener-Hopf design if optimal controllers, part I: The single-input single-output case. *IEEE Trans. Automat. Contr.* **21**(2), 3–13.

Zhou, K. (2000). A new controller architecture for high performance, robust, and fault tolerant control. *Proc. of the IEEE Conference on Decision and Control* **4**, 4120 – 4125.

Zhou, K. and J. C. Doyle (1998). *Essentials of Robust Control*. Prentice Hall, Inc.. Upper Saddle River, New Jersey.

Zhou, K., J. C. Doyle and K. Glover (1996). *Robust and Optimal Control*. Prentice Hall, Inc.. Upper Saddle River, New Jersey.